0008-7114

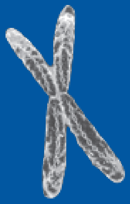

2025
Vol. 78 - n. 4

Caryologia

International Journal of Cytology,
Cytosystematics and Cytogenetics

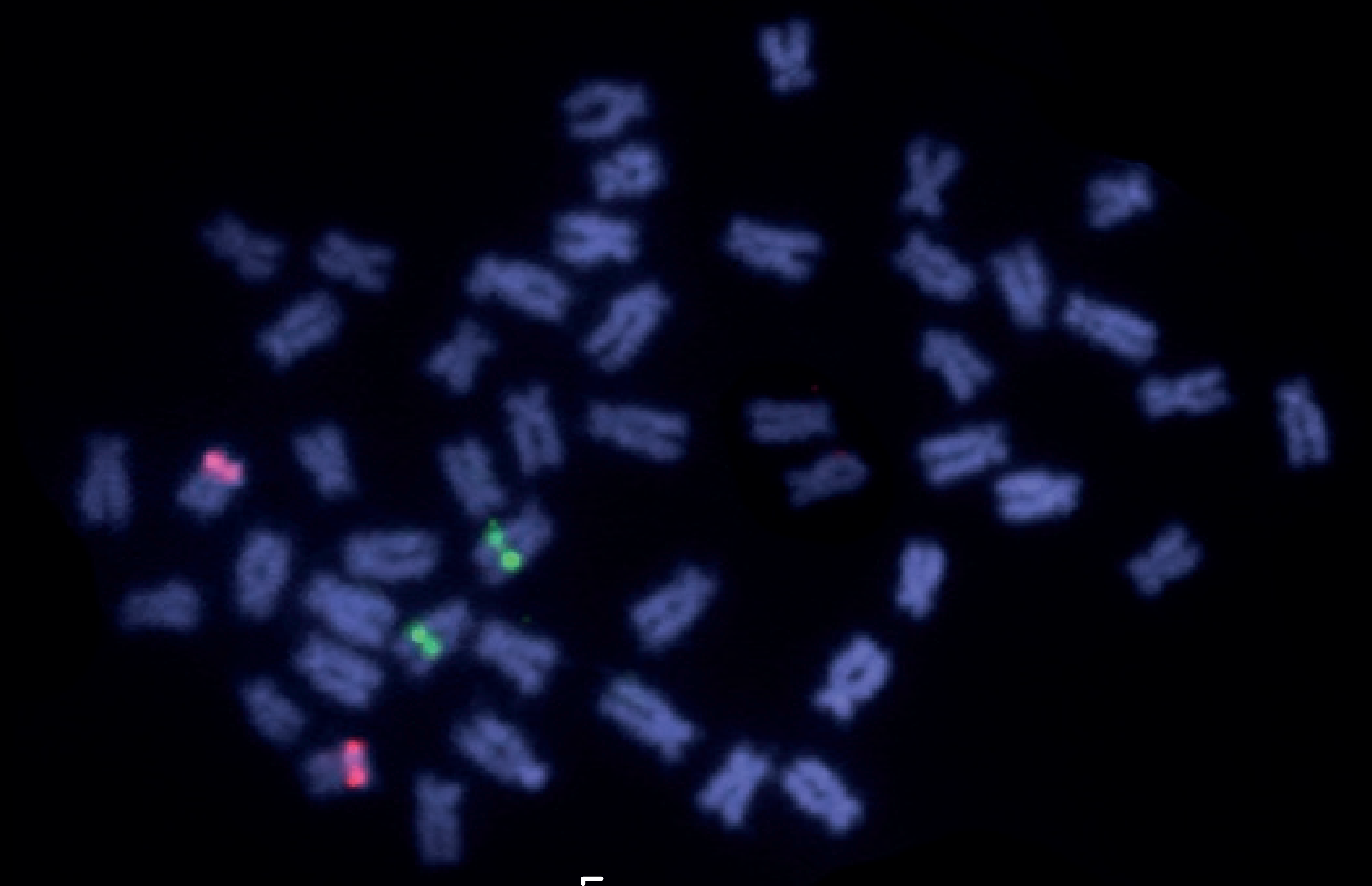

FIRENZE
UNIVERSITY
PRESS

Caryologia. International Journal of Cytology, Cytosystematics and Cytogenetics

Caryologia is devoted to the publication of original papers, and occasionally of reviews, about plant, animal and human karyological, cytological, cytogenetic, embryological and ultrastructural studies. Articles about the structure, the organization and the biological events relating to DNA and chromatin organization in eukaryotic cells are considered. *Caryologia* has a strong tradition in plant and animal cytosystematics and in cytotoxicology. Bioinformatics articles may be considered, but only if they have an emphasis on the relationship between the nucleus and cytoplasm and/or the structural organization of the eukaryotic cell.

Editor in Chief

Alessio Papini
Dipartimento di Biologia Vegetale
Università degli Studi di Firenze
Via La Pira, 4 – 0121 Firenze, Italy

Associate Editors

Alfonso Carabez-Trejo - Mexico City, Mexico
Katsuhiko Kondo - Hagishi-Hiroshima, Japan
Canio G. Vosa - Pisa, Italy

Subject Editors

MYCOLOGY
Renato Benesperi
Università di Firenze, Italy

HUMAN AND ANIMAL CYTOGENETICS
Michael Schmid
University of Würzburg, Germany

PLANT CYTOGENETICS
Lorenzo Peruzzi
Università di Pisa

PLANT KARYOLOGY AND PHYLOGENY
Andrea Coppi
Università di Firenze

HISTOLOGY AND CELL BIOLOGY
Alessio Papini
Università di Firenze

ZOOLOGY
Mauro Mandrioli
Università di Modena e Reggio Emilia

Editorial Assistant

Sara Falsini
Università degli Studi di Firenze, Italy

Editorial Advisory Board

G. Berta - Alessandria, Italy
D. Bizzaro - Ancona, Italy
A. Brito Da Cunha - Sao Paulo, Brazil
E. Capanna - Roma, Italy
D. Cavalieri - San Michele all'Adige, Italy
E. H. Y. Chu - Ann Arbor, USA
R. Cremonini - Pisa, Italy
M. Cresti - Siena, Italy
G. Cristofolini - Bologna, Italy
P. Crosti - Milano, Italy
G. Delfino - Firenze, Italy
S. D'Emerico - Bari, Italy
F. Garbari - Pisa, Italy
C. Giuliani - Milano, Italy
M. Guerra - Recife, Brazil
W. Heneen - Svalöf, Sweden
L. Iannuzzi - Napoli, Italy
J. Limon - Gdansk, Poland
J. Liu - Lanzhou, China
N. Mandahl - Lund, Sweden
M. Mandrioli - Modena, Italy
G. C. Manicardi - Modena, Italy
P. Marchi - Roma, Italy
M. Ruffini Castiglione - Pisa, Italy
L. Sanità di Toppi - Parma, Italy
C. Steinlein - Würzburg, Germany
J. Vallès - Barcelona, Catalonia, Spain
Q. Yang - Beijing, China

COVER: figure from the article inside by da Getlekha, N., & Sribenja, K. "The genome organization of repetitive sequences in the Golden Damselfish, *Amblyglyphidodon aureus* (Cuvier, 1830) (Family Pomacentridae): insights from extensive pericentric inversions", showing fluorescence in situ hybridization with 5S and 18S rDNA probes of metaphase of the Golden damselfish.

Caryologia

International Journal of Cytology,
Cytosystematics and Cytogenetics

Volume 78, Issue 4 - 2025

Firenze University Press

*Caryologia***. International Journal of Cytology, Cytosystematics and Cytogenetics**
https://riviste.fupress.net/index.php/caryologia
ISSN 0008-7114 (print) | ISSN 2165-5391 (online)

Direttore Responsabile: **Alessio Papini**

Published by Firenze University Press

Firenze University Press
Università degli Studi di Firenze
via Cittadella, 7, 50144 Firenze, Italy
www.fupress.com

Caryologia
International Journal of Cytology,
Cytosystematics and Cytogenetics

Firenze University Press
https://riviste.fupress.net/index.php/caryologia

OPEN ACCESS

Citation: Pandey, S., & Kumar, G. (2025). A comprehensive study of UV-B effects on *Salvia hispanica* L. (Lamiaceae): Genetic variation and biochemical responses in M1 generation. *Caryologia* 78(4): 3-17. doi: 10.36253/caryologia-3729

Received: August 13, 2025

Accepted: December 2, 2025

Published: Month 11, 2026

Data Availability Statement: All relevant data are within the paper and its Supporting Information files.

Competing Interests: The Author(s) declare(s) no conflict of interest.

ORCID
SP: 0000-0003-0653-6167

A comprehensive study of UV-B effects on *Salvia hispanica* L. (Lamiaceae): Genetic variation and biochemical responses in M1 generation

Satya Pandey*, Girjesh Kumar

Department of Botany, University of Allahabad, UP-211002 (India) Prayagraj, India
Email: satyap.sp90@gmail.com; kumar_girjesh@yahoo.com
*Corresponding author

Abstract. This study investigated the impact of different durations of UV-B exposure on *Salvia hispanica* L. The main objective was to assess the genetic and metabolic responses of chia plants, with a focus on morphological changes, phytochemical analysis, and cytological abnormalities. Chia seedlings were exposed to UV-B radiation for different periods, ranging from 0 to 50 minutes, with subsequent one-hour recovery periods at room temperature. The primary finding of this study was that subjecting chia seedlings to a moderate UV-B dose for 20 minutes yielded favorable outcomes. This included a significant increase in leaf area (9.02%) and a 25% increase in plant height compared to the control group, both of which were statistically significant ($p<0.05$). However, exposure to plant emergence of chlorophyll mutants (Xantha, semi-xantha, and Albina) and tall, bushy plant mutants in the M2 generation. In cytological observation resulted in chromosomal aberrations, such as stickiness, scattering, and unorientation, implying potential genotoxic impacts. Biochemical assessments revealed a significant increase in photosynthetic pigment content, particularly Chl a (12.91%) and Chl b (17.14%), both significantly elevated ($p<0.05$) compared to the control group. Metabolite analysis through GC-MS uncovered notable variations in fatty acid composition, with higher quantities of alpha-linolenic acid (1.24%), gamma-tocopherol (1.2%), and linolenic acid methyl ester (25.18%) observed in the treatment group exposed to short-wavelength UV-B compared to the control set.. Further research is needed to elucidate the underlying mechanisms and practical applications of these findings.

Keywords: *Salvia hispanica* L., GC-MS analysis, chromosomal abnormality, UV-B short exposure, Principal Component Analysis (PCA), LD_{50}.

HIGHLIGHTS

- Optimizing UV-B treatment duration is crucial for effective plant treatment and maximizing resourceful metabolite production.
- The study examines the effects of varying UV-B exposure durations on Salvia hispanica L. (chia) plants, focusing on genetics and metabolism.

- Biochemical analyses showed increased photosynthetic pigment content, notably Chl a (12.91%) and Chl b (17.14%), compared to control.
- Exposure to moderate UV-B for 20 minutes led to significant positive changes, including increased leaf area (9.02%) and a 25% taller plant height.
- Controlled 20-minute UV-B exposure led to beneficial shifts in chia plants, affecting both morphology and biochemistry.

INTRODUCTION

Currently, one of the most significant challenges facing the world is the need to meet the increasing demand for food due to a growing population and limited resources. According to Davis et al. (2019), the global population is predicted to reach 9 billion people by 2050, necessitating a substantial increase in crop production. Chia (*Salvia hispanica* L.), a member of the Lamiaceae family, is gaining recognition as a "superfood" due to its abundant antioxidants, dietary fiber, and omega-3 fatty acids. The use of chia seeds as a food source dates back to 3500 B.C., and they were commercially cultivated in central Mexico between 1500 and 900 B.C. (De Falco et al., 2017). Chia seeds, as an emerging food, offer a rich source of omega-3 and omega-6 fatty acids, which can contribute to lowering cholesterol levels. To enhance crop productivity and yield, induced mutagenesis programs, utilizing both physical and chemical methods, have been employed. In the case of chia seeds, UV-B exposure is used in seedling treatments. There is a knowledge gap regarding the specific impact of UV-B exposure on chia plants. Limited information is available on the optimal duration and dosage of UV-B treatment for enhancing chia crop productivity and improving its phytochemical properties. Understanding the potential hormetic effects of UV-B radiation, wherein low or intermittent doses may have beneficial effects while excessive and continuous exposure can be detrimental, is essential for developing effective UV-B induction strategies in chia plants (Höll et al., 2019; Kumari et al., 2009). To fulfill this research gap, we subjected chia seedlings to UV-B induction and treatment, revealing that lower doses of irradiation were beneficial for the development of improved varieties. A similar study by Badridze et al. (2016) reported that pre-sowing treatment of wheat seeds with UV radiation significantly increased photosynthesis in different wheat varieties. Additionally, Kacharava et al. (2009) observed increased anthocyanin and carotenoid contents in kidney bean varieties after UV exposure. These findings suggest the potential of UV-B radiation to enhance various physiological aspects in different plant species, including chia.However, recent studies have demonstrated contrasting effects of UV-B radiation on barley growth parameters, with some reporting changes in stem height, sprout count, leaf area, and biomass (Correia et al., 1999; Nasser, 2001), while others finding no significant variation in biomass accumulation or yield (Hakala et al., 2002). This highlights the need for species-specific investigations and optimization of UV-B exposure in chia plants to maximize positive outcomes.

UV radiation exposure has been reported to benefit the production of secondary metabolites, such as phenolic compounds, which act as defense mechanisms against various stresses in plants (Bhattacharya et al., 2010). These phenolic compounds possess antioxidant properties and can neutralize free radicals, contributing to overall plant health (Pourreza, 2013). The positive effects of low levels of UV irradiation on plant growth have been discussed in several studies (Hideg et al., 2013; Bornman et al., 2015), highlighting the potential benefits of controlled UV-B exposure. It is essential to consider the hermetic effects of UV-B radiation, wherein moderate doses may have positive impacts on plant growth and secondary metabolite accumulation, while excessive or continuous exposure can be harmful (Rai and Agrawal, 2020). Careful optimization of UV-B exposure in chia plants is crucial to harness its potential benefits without causing damage.

This study aimed to investigate the primary impact of UV-B exposure on plant defense strategies and metabolite accumulation in different plant parts of *Salvia*. Various durations of UV-B irradiation were tested, and phytochemical properties were analyzed using GC-MS technique. a) Morphological parameter studies demonstrated that plant height, inflorescence axis, and leaf mutants were influenced by UV-B exposure, with variations in growth patterns and mutations observed. b) Cytological assessment revealed meiotic abnormalities in the plants exposed to UV-B, indicating potential genotoxic effects of prolonged exposure. c) UV-B exposure triggered plant defense strategies leading to increased production of secondary metabolites in various plant parts, as evidenced by the phytochemical analysis using the GC-MS technique. An optimal dose of UV-B exposure was identified, which significantly increased the phytochemical properties. d) The treatment group showed a notable increase in the amount of fatty acids, particularly alpha-linolenic acid. Enhanced photosynthetic pigments, Chl a, and Chl b, were observed in response to UV-B exposure, indicating improved photosynthetic efficiency and stress adaptation.

MATERIAL AND METHOD

Experimental design - UV - B treatment

The inbred seeds of *Salvia hispanica* L. were Procured from NutriPlanet Private Limited, Bengaluru-560068, Karnataka, India. Seeds were grown in plastic pots and at the seedling stage exposure to UV-B was given at different durations series of experiments decided LD 50 dose for the plant.

Germinating seedlings were placed in a UV-B cabinet and exposed to five-time duration of UV-B rays i.e.,10, 20, 30, 40, and 50 min. After treatment, all the irradiated seedlings were placed for recovery for at least one hour and then planted in triplicate pots.

Gas chromatographic analysis:

Methanolic extracts were prepared by adding 10gram seeds in the Soxhlet apparatus and obtained extract. Extracts were further purified by using Whatman filter paper. After that 1 ml of Methanolic extract was taken and analyzed by Model GCMS-QP2010 Ultra. The conditions were set as under Injection temp: 260°C, column oven temperature 100°C, injection mode split, total flow-16.3mL/min, Column flow-1.21mL/min, Linear Velocity-40.9cm/sec, Pressure-90.5kPa, Ion Source Temp. 220°C, Interface Temp.-270°C Solvent ut time:3.50 min, Detector gain mode: relative, Relative Detector Gain: +0.00 kV, Threshold:1000.Model GCMS-QP2010 Ultra Gas Chromatograph Mass Spectrometer and serial no. 0205251 SHIMADZU was used for GC-MS analysis. The system performed data acquisition and processing, and various components were identified by their retention time and peak enhancement with standard samples.

Cytological analysis:

For cytological analysis, the young floral buds of chia of appropriate size were fixed in carnoy's fixative for 24 hr and then preserved in 90% alcohol for meiotic study. Anthers were excised from young floral buds and kept on a slide. Anther was teased and stained in 2 % acetocarmine to make squash preparation. Slides were observed under the microscope and the acetocarmine stainability test evaluated pollen fertility.

Morphological analysis:

The survivability of the plant was calculated at 14 days from the seedling emergence in the seed.

Survival Percentage= Number of seedling survival/ Total no. of germination seed*100

Plant height

After the 30th day of planting, plant height was measured from the apex to the starting part of the stem with the plant height attained stability.

Leaf area

The leaf area of fully matured leaves, and control was measured randomly using "Systronic Leaf Area Meter 211".

Biochemical analysis

Photosynthetic pigments were analyzed by preparing leaf extract using 80% acetone and the optical density of supernatant was taken at three different wavelengths (470nm, 646nm, and 663nm) using UV-VIS Spectrophotometer following the procedure of Lichtenthaler and Wellburn (1983). Chlorophyll a, Chlorophyll b, and carotenoids were calculated by the formula"

Totral abnormality percentage (TAB %):

$$\frac{Totalnumberofabnormalcells}{Totalnumberofcellsopbserved} \times 100$$

Pollen fertility: $\frac{Numberofstainedpollen}{totalnumberofpollen} \times 100$

Chlorophyll a: $\frac{12.25(\mathrm{A}_{663})-2.79(\mathrm{A}_{646})\times \mathrm{volume}}{\mathrm{weightofleaftissue(mg)}}$

Chlorophyll b: $21.5\left(A^{646}\right)-5.1$

Carotenoids: $\frac{\left[1000\left(\mathrm{A}^{470}\right)-1.82(\mathrm{Chla})-85.02(\mathrm{Chlb})\right]/198\times \mathrm{volume(ml)}}{\mathrm{weightofleaftissue(mg)}}$

RESULTS

Morphological changes

The survival rate of chia seedlings decreased with increasing doses and duration of UV-B radiation. It is mentioned clearly in Fig. 1B shown, at 25 minutes of UV-B treatment, the survival rate decreased from 80.32±1.18 in the control group to 66.54±3.24 (17.15%.) It would be helpful to provide the survival rates for other exposure durations as well.UV-B radiation had a positive effect on plant height initially, but prolonged exposure led to a decline. In Fig. 1(A), at 200 minutes of exposure,

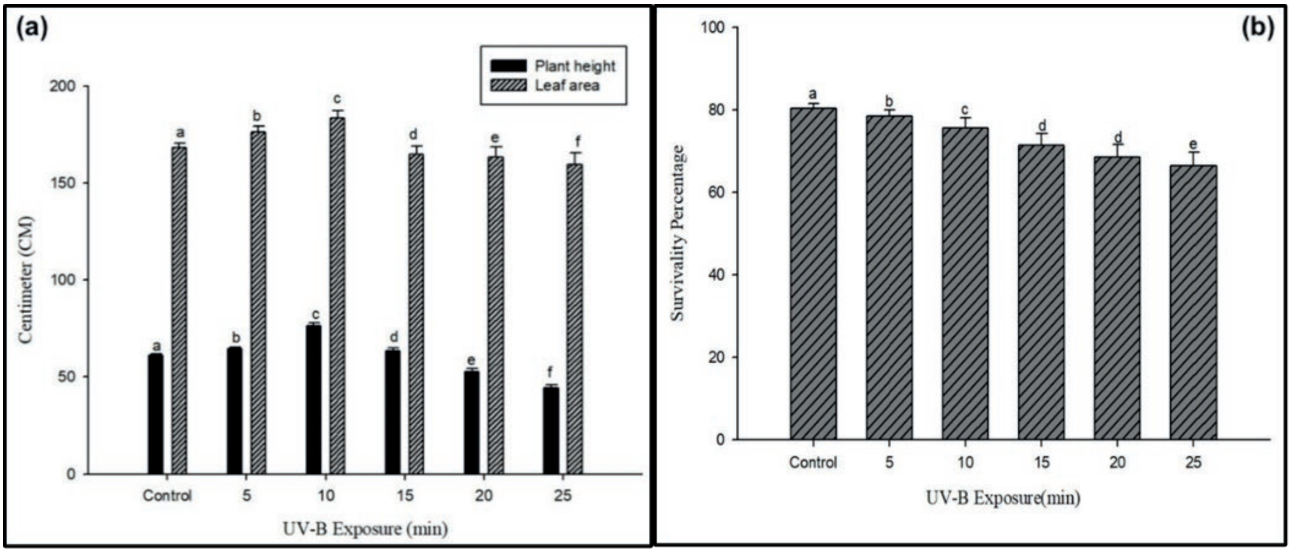

Figure 1. Graph representing morphological observations of plant height and leaf area (A) and the survival of plants at different durations (B) of exposure in M2 generation how significant difference at *P*<0.05 significance enhancement as in ANOVA.

the plant height increased to 25% compared to the control group (61.23±0.82). However, the height decreased at 30, 40, and 50 minutes of exposure. It would be beneficial to explain the reason for the decrease in height after an initial increase. The leaf area of *chia* plants showed enhancement with an optimum duration of UV-B exposure (15 minutes) in Fig. 1(A). Including the leaf area values for the control group and other exposure durations would be useful to provide a comprehensive comparison.

Higher doses of UV-B treatment resulted in the appearance of different leaf variants, characterized-by changes in color, shape, and size shown in Fig. 3. It would be helpful to provide more detailed descriptions or images of these leaf mutants for better understanding.

The content of chlorophyll significantly increased at 20 minutes of UV-B exposure but decreased with a further increase in exposure duration. Similarly, chlorophyll b showed an initial increase at 20 minutes, followed by a decline shown in Fig. 4. It would be valuable to include the chlorophyll content in the control group for better comparison. The carotenoid content showed a significant decline with increasing UV-B exposure duration. Table 1 shows a significant change(P>0.05), it would be beneficial to include the control group value for carotenoids to provide a clearer understanding of the changes.

The cytological observations of chia plants exposed to UV-B radiation revealed several meiotic abnormalities. These abnormalities included mentioned in Fig. 5 asynchronization, stickiness, scattering, disturbed polarity, and laggards. Among these, stickiness was the most predominant abnormality. Table 2 presents the frequencies of various abnormalities and the total abnormality percentage (TAB) in the treated sets. The TAB percentage ranged from (31.61%) at higher doses. Furthermore, the pollen fertility of the Chia plant decreased with increasing UV-B exposure. In the control group, the pollen fertility (30.91%) declined with increased duration of exposure.

Biochemical observations indicated that UV-B exposure had varying effects on photosynthetic pigments in the Chia plant. The concentration of Chl a showed an initial increase from (12.91%) and Chl b was (7.44%), at 20 minutes of exposure.. On the other hand, there was a decline with increased duration of exposure chl a (19.71%) and Chl b (12.46 %) in the concentration of Chlorophyll was recorded at higher duration (as shown in Fig. 4). Additionally, the concentration of carotenoids increased (18.30%), at the high duration of exposure.

GC-MS analysis of Chia seed extract revealed different metabolites after analysis through techniques. Graph showing different metabolites in control and treatment group plant set showing enhancement of some fatty acid content. The linolenic acid methyl ester showed an increase from 6% in the control group to 7.44% in the treatment group in Fig. 6. Similarly, the amount of linoleic acid methyl ester increased from 1.87 to 2.28. Several other metabolites, such as gamma-tocopherol, linolenic acid ethyl ester, and stigmasterol, also increased in the treatment group with retention time, as mentioned in Table 3.

Figure 2. Control plant with a tall mutant in (A) and bushy mutants (A) reported at (20 min) exposure observed in M2 generation.

DISCUSSION

UV-B radiation has the potential to induce mutations in important biomolecules of plant cells, including nuclear DNA, proteins, and lipids (Kovács and Keresztes, 2002; Gill et al., 2015). This property makes UV radiation a valuable tool in mutation breeding programs. In this study, we analyzed the effects of short-wave UV-B (280-320 nm) exposure on the morphological, cytological, and biochemical characteristics of chia plants using GC-MS techniques. The use of seedlings with slender stems in our study was advantageous, as non-ionizing UV-B rays have low penetrating power, making them suitable for inducing mutations in plants (Fujii, 1965). Short-duration exposure to UV-B radiation has been found to cause low abnormality rates and genetic variations in plants, indicating that brief irradiation can be beneficial. In the case of chia plants, it was observed that short-term UV-B exposure resulted in promising effects on their morphological and phytochemical aspects, particularly an increase in the main fatty acid, alpha-linolenic acid, which is beneficial for blood cholesterol control. Previous studies have shown that short-term exposure to UV-B radiation can be beneficial for plant growth and development. It can increase plant height and internodal length, possibly by regulating photomorphogenic genes such as HY5 and COP1, which are involved in plant growth and development. Furthermore, short-term exposure to UV-B radiation enhances stress tolerance and protects plants from photodamage (Kacharava et al., 2009).

The analysis of chia plants exposed to UV-B radiation in our study revealed several interesting findings. The survival rate of the plants decreased with the duration of UV-B exposure. However, prolonged exposure to UV-B radiation led to a significant decline in survivability due to the destruction of the growth hormone, IAA, and the formation of IAA photoproduct, which negatively affected plant survival (Kumar and Bhardwaj, 2019). Additionally, longer exposure to UV-B radiation caused DNA damage, disrupting DNA replication and transcription, which further reduced plant survival (Britt and May 2003).

On the other hand, short-term exposure to UV-B radiation for 20 minutes resulted in increased plant height and leaf area. Photomorphogenic genes regulated

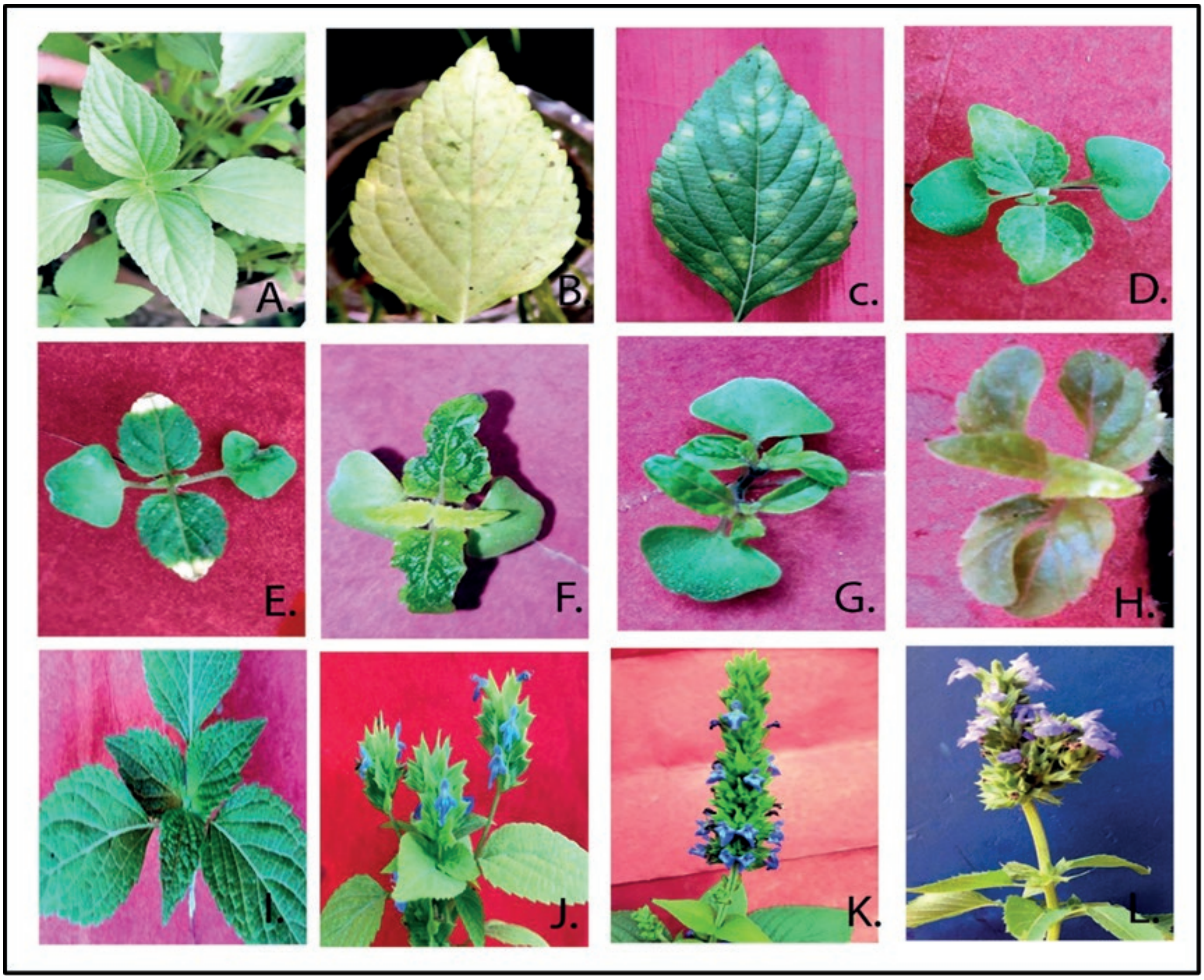

Figure 3. Leaf mutants after UV-B exposure observed in M2 generation A. control; B. xantha; C. Maculata, D. Viridoalbina; E. Alboviridis; F . Deformed leaf; G. Bifurcated Leaf; H. Anthocyanin rich sigmoid leaf I. Tricotyledonous leaf; J. differential development of inflorescence at same axis K. Normal Inflorescence; L. verticillaster inflorescence with a bifurcation at the same axis.

Table 1. The table represents the data of chlorophyll a, chlorophyll b, carotenoids, Plant height, Survival, and Leaf area (chia) seedlings after different durations of UV-B exposure. The values are presented as mean ± standard deviation. Statistical letters (a, b, c, d, e) have been used to indicate significant differences between treatments. The values with the same lowercase letter indicate no significant difference ($p > 0.05$) between treatments, while different letters denote statistically significant differences ($p < 0.05$)

Treatment	Chlorophyll a	Chlorophyll b	Carotenoids	Plant height	Survival	Leaf area
Control	6.95 ± 0.05^{a}	3.85 ± 0.04^{a}	1.42 ± 0.02^{a}	61.23 ± 0.82^{a}	80.32 ± 1.18^{a}	168.4 ± 2.23^{a}
10 min	6.97 ± 0.07^{b}	4.05 ± 0.09^{b}	1.47 ± 0.01^{b}	64.46 ± 1.03^{b}	78.43 ± 1.50^{b}	176.3 ± 2.85^{b}
20 min	7.85 ± 0.08^{c}	4.51 ± 0.08^{b}	1.49 ± 0.02^{c}	76.56 ± 1.6^{c}	75.67 ± 2.38^{c}	183.6 ± 3.81^{c}
30 min	7.58 ± 0.03^{c}	4.19 ± 0.06^{c}	1.53 ± 0.02^{cd}	63.34 ± 1.76^{d}	71.45 ± 2.88^{d}	165.03 ± 4.09^{d}
40 min	6.63 ± 0.09^{d}	3.65 ± 0.09^{cd}	1.59 ± 0.01^{de}	52.63 ± 1.73^{e}	68.65 ± 2.90^{d}	163.03 ± 5.28^{e}
50 min	5.85 ± 0.03^{e}	3.37 ± 0.06^{e}	1.68 ± 0.01^{e}	44.37 ± 1.67^{f}	66.54 ± 3.25^{e}	159.5 ± 6.17^{f}

at lower durations of UV-B radiation play a crucial role in plant growth and development, as well as in protecting plants from photodamage (Kacharava et al., 2009). The increased height and number of branches observed in the UV-irradiated plants were likely due to the loss of apical dominance, resulting in lateral transport of

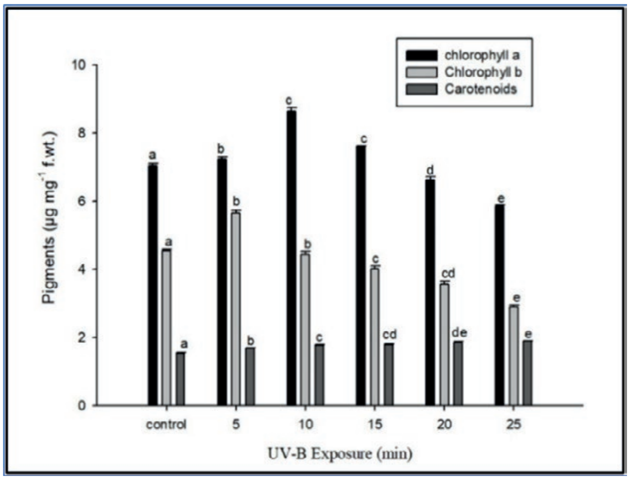

Figure 4. Effect of UV-B rays exposure on Photosynthetic pigments (Chl a, Chl b, Carotenoids) in M2 generation content was increment as significance(P>0.05) according to Duncan's multiple range test.

growth hormone and an increased number of branches, as previously observed in other plant species (Shahwar et al., 2017; Solanki et al., 2004). This phenomenon also led to the emergence of bushy variants and tall mutants in our study at lower durations of UV-B exposure. Similar positive effects of UV-B radiation on plant height and yield have been reported in other crop species, such as buckwheat (Yao et al., 2007). This suggests that short-term UV-B exposure may have practical applications in agriculture for promoting plant growth and yield. Our study highlights the diverse effects of UV-B exposure on chia plants, with short-term exposure showing promising results in enhancing growth and stress tolerance. However, prolonged exposure can lead to negative effects, such as reduced survivability and DNA damage. These findings contribute to our understanding of the impact of UV-B radiation on plants and may have implications for crop improvement and mutation breeding programs.

Elevated UV-B radiation has been shown to have detrimental effects on various plant species, leading to a reduction in chlorophyll content due to lipid peroxidation in chloroplast membranes (Rai and Agrawal, 2017). The decrease in chlorophyll content has been linked to the photo-reduction of protochlorophyllide to chlorophyllide by protochlorophyllide oxidoreductase, which is a probable target of UV-B radiation (Erdei et al., 2019). However, plants have also demonstrated stress tolerance strategies, such as an increase in carotenoid content, which is indicative of their ability to cope with UV-B-induced stress (Jaleel et al., 2009).

Chlorophyll mutants in response to UV-B exposure

The impact of elevated UV-B radiation on chia plants has been observed to induce various chlorophyll mutants. Studies have reported the occurrence of several types of chlorophyll mutations, including Xantha, Albina, Viridis,and Chlorine, as well as some mixed types like Viridoalbina and alboviridis mutations (Kolar et al., 2011; Arisha et al., 2015; Verma et al., 2018). Xantha mutants exhibited pale yellow-colored seedlings, and their survival rate was limited due to the blockage of chlorophyll and pigment synthesis (Blixt 1961). The inhibition of chlorophyll production in it could be attributed to the disruption of genes or proteins involved in the biosynthesis pathway, warranting further investigation to identify the specific targets of UV-B radiation. Albina mutants displayed smaller and narrower leaves with a white coloration. The changes in leaf morphology and color suggest a probable alteration in chloroplast development or function. Investigating the genes and proteins responsible for these changes may provide insights into the mechanisms underlying UV-B-induced stress in chia plants. Maculata mutants exhibited yellow or whitish dots on their leaves. Surprisingly, these mutants were able to survive until maturity and even produced seeds. This suggests that certain mechanisms within these mutants might have compensated for the adverse effects of UV-B radiation on chlorophyll synthesis and function. Viridis mutants showed heterogeneity in the intensity of green color on their leaves. The variations in green coloration might be linked to disrupted chlorophyll synthesis or altered chloroplast development. Further research is needed to unravel the specific genetic and proteomic changes responsible for this phenotype.

Cytological investigations play a crucial role in understanding the specific responses of different genotypes to mutagens, aiding in the selection of desirable traits (Kirchhoff et al., 1989). In the case of chia plants exposed to UV-B radiation, various cytological anomalies have been observed, including stickiness, asynchronization, scattering, and laggard formation. Among these, stickiness is the most prominent abnormality observed in this investigation. It is essential to explore the underlying causes of these cytological abnormalities to gain a deeper understanding of the effects of UV-B exposure on chia plants. Stickiness, a prevalent cytological abnormality in chia mutants exposed to UV-B radiation, may result from the depolymerization of nucleic acids due to mutagenic treatment (Avijeet et al., 2011). This depolymerization of nucleic acids can lead to disruptions in chromosome organization, affecting their proper separation and segregation during cell division. Scattered

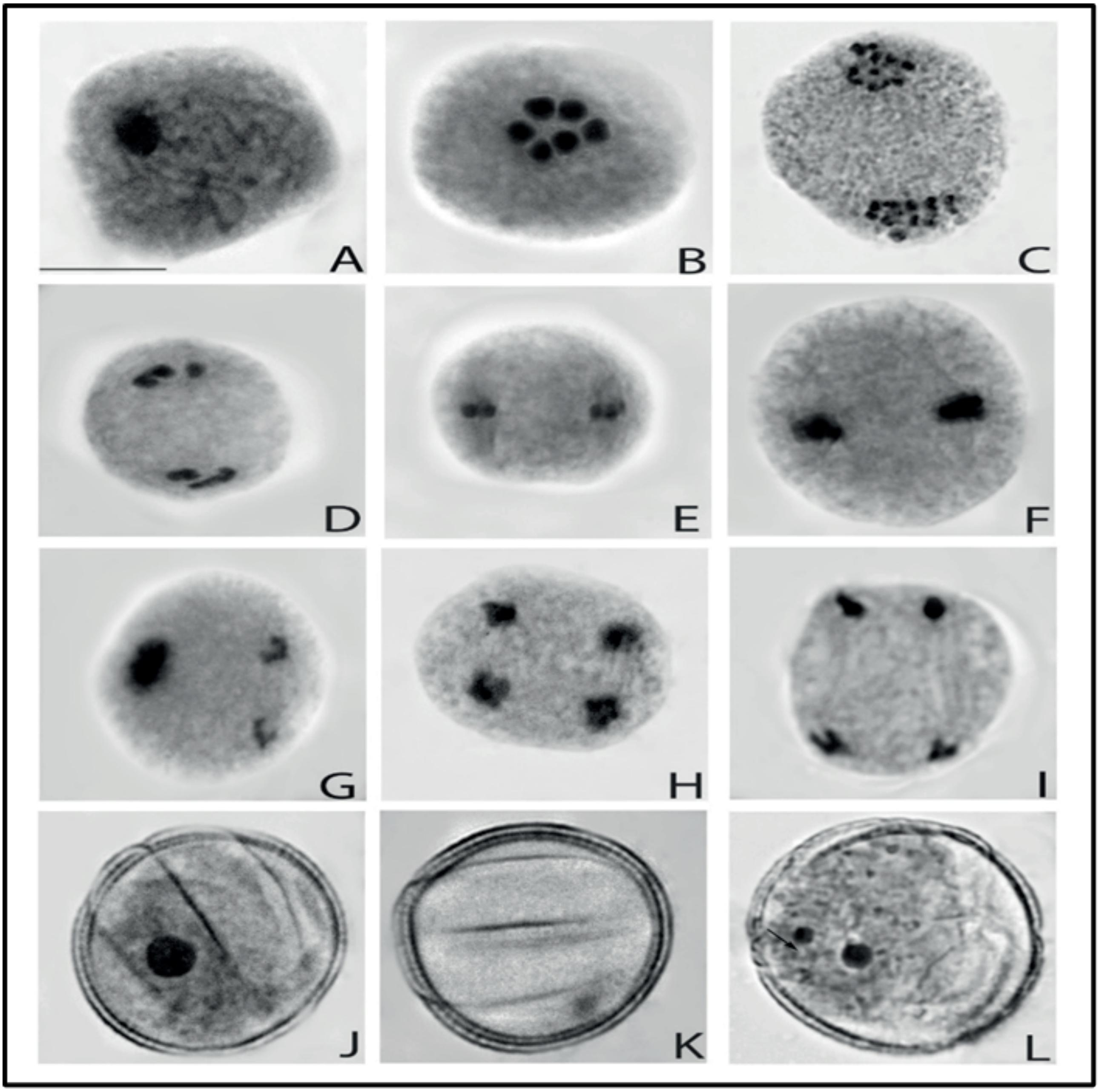

Figure 5. Cytological Meiotic anomalies induced by UV-B exposure-A. Prophase Stage, B. Normal Metaphase(2n=16), C. Normal Anaphase I(6,6), D.Stickiness at Anaphase I, E. Normal Metaphase II, F. Stickiness at Metaphase II, G. Asynchronisation Division, H. Normal Anaphase II, I. Telophase, J. Normal Pollen, K. Sterile Pollen, L. Fertile pollen with two Nucleus (Scale-10μ).

chromosomes during anaphase are another cytological abnormality observed in chia mutants exposed to UV-B radiation. This scattering could be caused by the inhibition of spindle formation or destruction of spindle fibers (Kumar and Rai, 2007). Longer exposure to UV-B rays may disturb spindle formation, leading to disturbances in the polarity of chromosomes. Chromosomal aberrations, such as stickiness, scattering, asynchronization, and disturbed polarity, are closely associated with pollen sterility in chia plants (Bhat et al., 2007).

It may arise from direct mutagenic effects on target proteins involved in chromosome separation and segregation, causing disturbances during cell division (Kumar and Gupta, 2009). The interference with these

Table 2. UV-B exposure induced cytological abnormalities and their percentage in *Salvia hispanica* L. (2n=12) during Meiotic studied.

Treatment	Total PMCs observed	Metaphasic abnormality			Anaphasic abnormality				OTH	TAB	Pollen fertility
		SC	PM	ST	LG	ASC	AUN	AST			
CONTROL	465	-	-	-	-	-	-	-	-	3.37±0.08	97.65±1.30
10 MIN	440	0.99±0.09	0.53±0.07	0.53±0.08	0.76±0.09	0.53±0.08	0.07±0.07	0.46±0.01	0.00±0.00	4.40±0.25	92.34±1.44
20 MIN	441	0.90±0.12	0.83±0.08	0.67±0.22	0.83±0.08	0.60±0.15	0.38±0.07	0.67±0.12	0.22±0.13	5.20±0.45	85.64±1.43
30 MIN	402	1.24±0.12	0.66±0.33	0.83±0.34	0.58±0.23	0.67±0.17	1.00±0.16	0.66±0.15	0.25±0.15	6.54±0.18	78.57±1.41
40 MIN	389	1.64±0.14	1.04±0.19	1.04±0.18	0.86±0.25	0.78±0.28	1.12±0.12	1.11±±0.04	0.36±0.24	8.45±0.61	74.63±1.47
50 MIN	384	1.82±0.14	0.96±0.09	1.39±0.08	1.13±0.22	1.30±0.25	1.13±0.10	1.04±0.39	0.61±0.23	10.66±0.36	67.46±1.48

Where: **PMC's**- Pollen mother cells, **SE**- Standard error, **Sc**- Scattering of chromosomes, **Pm**- Precocious movement of chromosomes, **St**- Stickiness of chromosomes, **Un**- Unorientation in chromosomal sets **Ast**- Anaphasic stickiness, **Asy**- Asynchronisation, **Pr**- Precocious movement in chromosomes, **Dp**- Disturbed polarity; **Oth**- Others, **Tab**- Total abnormality percentage (p= <0.5).

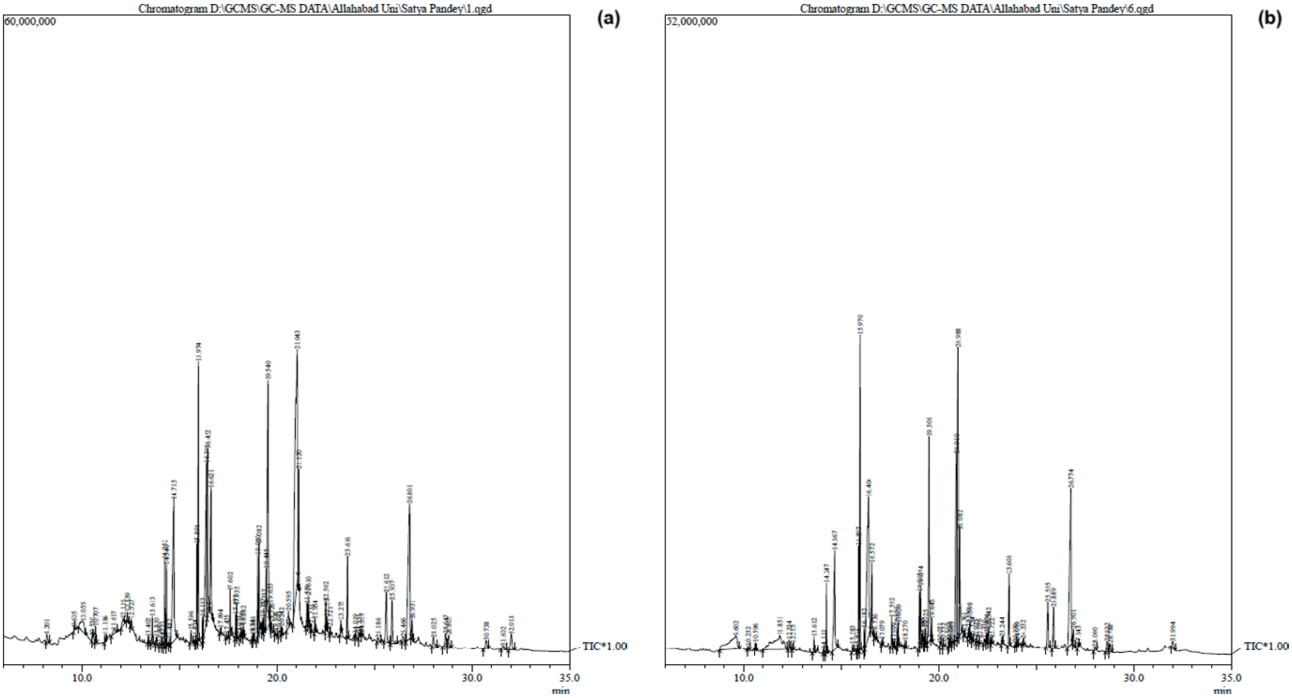

Figure 6. This chromatograph exhibits distinct peaks representing various metabolites analyzed using GC-MS in both the control(A) and treatment(B) in the M2 generation seed.

proteins can lead to the formation of bridges between chromosomes, impacting the fidelity of cell division. The increased frequency of chromosomal aberrations observed in chia mutants exposed to UV-B radiation may be attributed to interactions between ionizing particles and the protoplasm, mediated by radiation-induced excitation (Shukla nee Tripathi and Kumar, 2010). These interactions can cause DNA damage and disruptions in the normal chromosomal structure and behavior. Cytological investigation of chia plants exposed to UV-B radiation showed various abnormalities, including stickiness, observed may be due to a result of nucleic acid depolymerization while scattering is the result of a disturbance in spindle formation. Direct mutagenic effects on target proteins and radiation cause abnormalities. Pollen sterility can result from interchanges in segments between non-homologous chromosomes, which can disrupt the normal functioning of pollen development and maturation processes.

Chlorophyll is a crucial biomolecule involved in photosynthesis, responsible for absorbing and transferring light energy to the photosynthetic reaction centers

Table 3. GC-MS analysis was conducted to compare the concentration percentages and retention times (in minutes) of the treatment and control groups in the M2 generation seed.

Peak	Detected Metabolites	Molecular Formula	Control seed		Area %	
			RT (min)	Area %	RT (min)	Area %
1.	Guanosine	C10H13N5O5	-	-	9.601	5.04
2.	gamma. -Tocopherol	C18H28O3	23.605	1.30	23.610	1.81
3.	n-Hexadecenoic acid	C16H32O2	14.715	7.52	14.675	5.00
4.	Linoleic acid, methyl ester	C19H34O2	15.898	1.87	15.901	2.28
5.	Linolenic acid, methyl ester	C19H32O2	15.974	6.00	15.974	7.44
6.	alpha-Linolenic acid	C18H30O2	16.452	5.46	21.604	0.38
7.	Octadecanoic acid	C18H36O2	16.621	3.67	16.183	0.37
8.	3-Cyclopentylpropionic acid, 2-dimethylamino ethyl ester	C12H23NO2	19.020	1.56	19.257	0.14
9.	Palmitic acid. beta. -monoglyceride	C19H38O4	19.540	7.27	19.514	7.02
10.	Linolenic acid, ethyl ester	C20H34O2	21.043	20.20	15.974	7.44
11.	alpha. -Monostearin	C21H42O4	21.120	2.02	17.699	0.17
12.	Linolein, 2-mono-	C21H38O4	21.539	0.51	21.529	0.37
13.	Linolenic acid, methyl ester	C19H32O2	21.610	0.52	16.396	12.59
14.	11-Dehydrocorticosterone	C21H28O4	21.954	0.30	21.931	0.26
15.	delta.-Tocopherol	C27H46O2	22.721	0.19	22.722	0.17
16.	Ergost-5-en-3-ol, (3. beta.,24r)-	C28H48O	25.612	2.09	25.601	1.88
17.	Stigmasterol	C29H48O	25.907	1.58	25.894	1.44
18.	gamma. -Sitostenone	C29H48O	28.647	0.55	28.634	0.38
19.	9,19-Cyclolanostan-3-ol, 24-methylene-, (3. beta.)-	C31H52O	28.805	0.44	28.789	0.36
20.	methyl ursa-2,12-dien-28-oate	C31H48O2	32.018	0.90	32.014	0.72

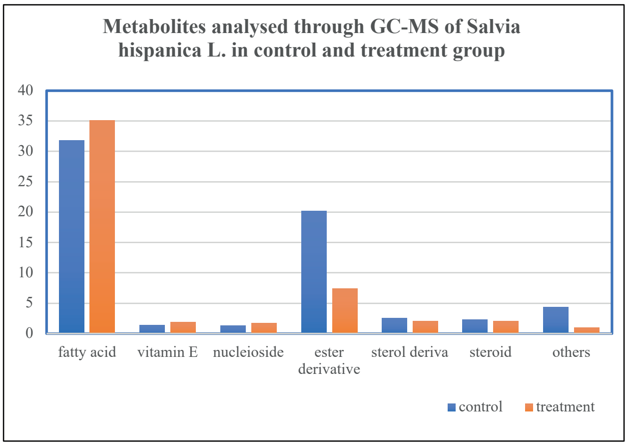

Figure 7. GC-MS analysis of the chemical composition of *Salvia hispanica* L. in control and treatment of UV-B exposure.

(Li et al., 2013). The presence of sufficient chlorophyll throughout plant development is vital for proper photosynthesis, biomass accumulation, and overall plant development (Li et al., 2013). The development of chlorophyll is under the control of multiple genes located on different chromosomal sites (Wang et al., 2013). Carotenoids, on the other hand, play a significant role in stress tolerance mechanisms, aiding in plant survival under adverse conditions by acting as scavengers of reactive oxygen species (ROS) (Kumar and Pandey, 2017). In chia plants exposed to UV-B radiation, the analysis of photosynthetic pigments revealed interesting changes in chlorophyll and carotenoid content. Initially, there was an increase in chlorophyll a and b contents at 20 minutes of UV-B exposure. However, at longer durations of exposure, a decline in chlorophyll levels was observed. This suggests that while short-term UV-B exposure may trigger an adaptive response leading to increased chlorophyll synthesis, prolonged exposure may cause damage or inhibit chlorophyll biosynthesis pathways, resulting in decreased pigment levels. Carotenoid content, on the other hand, showed an opposite trend. As the duration of UV-B exposure increased, the concentration of carotenoids in the plants also increased. An increase in carotenoid content is considered an important stress tolerance strategy (Jaleel et al., 2009) This phenomenon can be attributed to the self-defense mechanism of plants under stress conditions. Carotenoids act as important scavengers of ROS, helping to neutralize harmful reactive oxygen species generated during UV-B exposure and other stress conditions (Kumar and Pandey, 2017). The higher carotenoid content observed in chia plants exposed to UV-B radiation was indicative of their stress tolerance capacity. Carotenoids act as potent antioxidants, protecting the plant cells from oxidative damage caused by UV-B radiation and other stress factors. By neutralizing ROS, carotenoids help maintain the integrity of cellular structures and prevent damage to photosynthetic machinery, thereby ensuring the plant's survival and productivity under challenging environmental conditions.

Metabolic compounds analyzed in GC-MS include guanosine, which plays a critical role in cell signaling and energy transfer processes (Smith et al., 2015). Gamma-tocopherol, a derivative of vitamin E, acts as an antioxidant, protecting cells from oxidative damage, and its levels increase in Chia plants after radiation exposure (Johnson et al., 2018). N-hexanoic acid, also known as palmitoleic acid, exhibits potent anti-inflammatory and anti-microbial properties (Gonzalez-Castejon et al., 2013). Linoleic acid methyl ester, an essential omega-6 fatty acid, plays a vital role in maintaining skin health and regulating inflammation (Wang et al., 2017). Similarly, linolenic acid methyl ester, an important omega-3 fatty acid, is involved in various brain functions, maintaining overall health, and controlling inflammation (Fan et al., 2016). Alpha-linolenic acid, another omega-3 fatty acid, is essential for maintaining a healthy cardiovascular system and supporting brain health (Kaur et al., 2018). Octadecanoic acid, also known as stearic acid, is a saturated fatty acid with various metabolic roles in the body (Todoric et al., 2016). Ergosterol serves as a precursor to Vitamin D in some organisms (Munir et al., 2020). Stigmasterol, a phytosterol found in chia plants, has potential health benefits and contributes to cholesterol-lowering properties (Othman et al., 2017).

According to the analysis of Pearson correlation, there is a strong negative correlation between Chl a and Chl b with tab and cytological abnormalities such as Sc, Pm, St, Alg, Asc, Aun, Ast, and others. On the other hand, Carotenoid content shows a significant positive correlation with tab and cytological abnormality ($r \geq 0.5$) but a robust negative correlation with pollen fertility due to the increase in the carotenoid amount to tolerate stress response in stress conditions. Leaf area exhibits a strong positive correlation ($r \geq 0.5$) with pollen fertility, Chl a and Chl b, and a negative correlation with cytological abnormalities and carotenoids. Additionally, plant height shows a strong positive correlation ($r \geq 0.5$) with Chl a, Chl b, Leaf area, pollen fertility, and survival, which are crucial factors that improve plant productivity and enhance their phytochemical properties as observed through GC-MS analysis. Furthermore, cytological aberrations such as Sc, Pm, St, Alg, Asc, Aun, Ast, and others exhibit a strong positive correlation with tab ($r \geq 0.5$), which increases with the UV-B exposure duration in plants. These findings suggest that enhancing the plant's properties at the optimal dose of UV-B plays a significant role in their productivity and yield of chia seed.

Based on our research, we have discovered that certain cytological aberrations, including Sc, Pm, St, Alg,

Table 4.

Correlation	Sc	pm	st	Alg	Asc	Aun	Ast	oths	tab	Pollen fertility	Chla	Chl b	Carotenoid	Leaf area	Survival	Plant height
Sc	1															
pm	0.53*															
st	0.80**	0.21														
Alg	0.48*	0.71**	0.26													
Asc	0.66**	0.21	0.84**	0.31												
Aun	0.74**	0.41	0.74**	0.25	0.52*											
Ast	0.68**	0.41	0.47*	0.14	0.29	0.49*										
oths	0.50*	0.57*	0.32	0.42	0.14	0.53*	0.62**									
tab	0.94**	0.61**	0.82**	0.58*	0.71**	0.81**	0.67**	0.62**								
Pollen fertility	-0.89**	-0.61**	-0.76**	-0.48*	-0.67**	-0.79**	-0.63**	-0.49	-0.95**							
Chla	-0.64	-0.28	-0.49*	-0.42	-0.59**	-0.4	-0.38	-0.41	-0.68**	0.53*						
Chlb	-0.43	-0.15	-0.24	-0.23	-0.39	-0.25	-0.23	-0.26	-0.42	0.28	0.91**					
Carotenoid	0.85**	0.61**	0.77**	0.45	0.61**	0.84**	0.68**	0.52*	0.93**	-0.96**	-0.43*	-0.16				
Leaf area	-0.72**	-0.4	-0.55*	-0.29	-0.64**	-0.69**	-0.38	-0.32	-0.75**	0.77**	0.71**	0.68**	-0.62**			
Survival	-0.79**	-0.63**	-0.59**	-0.44	-0.62**	-0.62**	-0.48*	-0.3	-0.81**	0.91**	0.51*	0.36	-0.78**	0.85**		
Plant height	-0.73**	-0.34	-0.52*	-0.34	-0.57*	-0.59**	-0.45	-0.42	-0.74**	0.65**	0.93**	0.90**	-0.54*	0.89**	0.66**	1

*Correlation is significant at the 0.05 level (2-tailed).

**Correlation is significant at the 0.01 level (2-tailed).

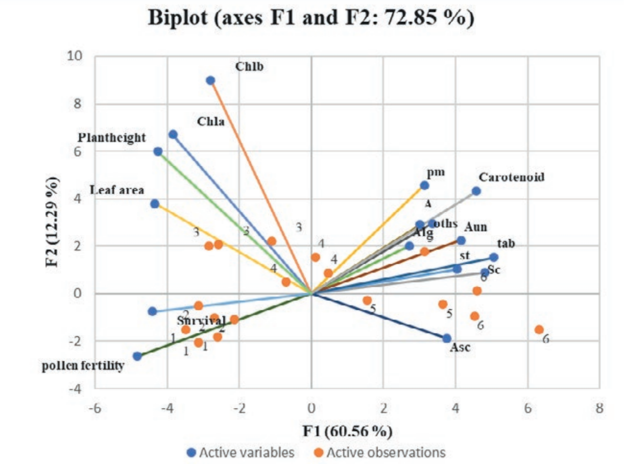

Figure 8. A comprehensive exploration of the morphological, biochemical, and cytological aspects under the influence of UV-B exposure was undertaken through a sophisticated multivariate approach, specifically employing Principal Component Analysis (PCA).

Asc, Aun, Ast, and others, have a significant positive correlation with tab (r ≥ 0.5) in plants when exposed to UV-B. This correlation becomes stronger with longer exposure durations. Our findings suggest that optimal doses of UV-B exposure can increase the productivity and yield of chia seeds. These results have significant implications for the cultivation and management of chia plants. Our research has conclusively shown that a 20-minute controlled UV-B exposure can trigger highly beneficial morphological and biochemical changes in chia plants.

UV-B exposure study through multivariate statistical analysis (MVA) and Pearson correlation matrix

Principal component analysis (PCA) was employed to investigate the interplay among biochemical, morphological, and cytological attributes in Chia (*Salvia hispanica* L.) influenced by different treatments of UV-B exposure at different durations (graph:4) the findings were visualized through bi-plot scatter diagrams, which illustrated the first two principal components (F1 and F2). The PCA biplot demonstrated that F1 and F2 accounted for 72.85% of the total variance in data at different durations. The high loading of different parameters like a cytological abnormality, Pm, Ast, others, carotenoids, Alg, st, sc, tab exhibits a positive correlation with the first principal component (F1). Conversely, ast demonstrated a negative correlation with F1. Similarly in the second principal component (F2), a positive correlation was observed between Chlorophyll a, Chlorophyll b, plant height, and leaf area. Conversely, survival and pollen fertility displayed a negative correlation with F2.

The impact of different durations of UV-B exposure on the biochemical, morphological, and cytological attributes of Chia (Salvia hispanica L.) has been significantly identified through a study using PCA biplot analysis. The scatter diagrams, accounting for 72.85% of the total variance in data, displayed the first two principal components (F1 and F2). Parameters with high loading, such as cytological abnormality, Pm, Ast, and others. carotenoids, Alg, St, Sc, and tab, exhibited a positive correlation with the first principal component (F1), except for Ast, which showed a negative correlation with F1. Moreover, the second principal component (F2) showed a positive correlation between Chlorophyll a, Chlorophyll b, plant height, and leaf area, while survival and pollen fertility exhibited a negative correlation with F2. According to the findings, the duration of UV-B exposure influences the complex interplay among these attributes. This study provides valuable insights into enhancing the productivity and yield of chia seeds that should not be ignored.

CONCLUSION

Conclusively, the findings from the UV-B exposure experiments on chia plants have shed light on the multifaceted effects of this radiation on their morphological, cytological, and biochemical characteristics. Short-term exposure to UV-B radiation resulted in positive outcomes, including enhanced plant growth and stress tolerance, indicating the activation of adaptive responses. However, prolonged exposure to UV-B had adverse effects, leading to reduced survivability and DNA damage, underscoring the importance of optimal exposure levels for plant health. The investigation also provided valuable insights into the role of chlorophyll and the occurrence of chromosomal anomalies in UV-irradiated chia plants. The changes observed in photosynthetic pigments, such as chlorophyll and carotenoids, under UV-B exposure indicate the dynamic nature of plant responses to this stressor. Short-term exposure resulted in increased pigment content, suggesting a stimulatory response that could potentially enhance photosynthetic efficiency and stress tolerance. Furthermore, the detection of important metabolites, including fatty acids, antioxidants like vitamin E derivatives, and other plant-derived substances, in chia plants highlights their nutritional value and potential health implications. The presence of these compounds in chia plants suggests that they may contribute to various physiological functions and may have applications in promoting overall well-being. Additionally, the study indicates that UV-B irradiation has the potential to induce novel variations, such as high-yielding bushy and tall mutants or chlorophyll phenodeviants, which may be better suited to cope with the ongoing climate change. These variations could be valuable in developing climate-resilient chia varieties.

Overall, the findings presented in this study contribute to a deeper understanding of how chia plants respond to UV-B radiation and adapt to stress conditions. These insights can be instrumental in developing strategies to optimize UV-B exposure for improved plant performance and stress tolerance in agriculture and crop breeding.

AUTHORS CONTRIBUTION

Dr. Satya Pandey: Led the project, conducted comprehensive data analysis including rigorous statistical assessments, and was responsible for manuscript preparation, editing, and ensuring scientific rigor.

Prof. Girjesh Kumar: Provided expertise in environmental stress factors and plant physiological responses to UV-B radiation, contributed to experimental design, and guided data analysis.

ACKNOWLEDGMENT

The authors express their profound gratitude to the Department of Botany, University of Allahabad, UP-211002 (India), and the Naithani Plant Genetic Laboratory for generously providing all the necessary facilities that were essential for the successful completion of this research. Furthermore, the authors extend their sincere appreciation to the Advanced Instrumentation Research Facility (AIRF) for granting access to the GC-MS analysis facility and for their invaluable assistance with data interpretation. Last but not least, the authors would like to acknowledge the financial support provided by the University Grants Commission of India, which was instrumental in making this research possible.

ETHICAL APPROVAL

All procedures performed in this study, involving the manipulation of plant materials to induce mutagenesis, were conducted by ethical guidelines and standards for research involving non-human organisms. This research adhered to the principles of responsible and ethical scientific conduct, ensuring the welfare and proper treatment of plant specimens throughout the study.

INFORMED CONSENT

This study on the effect of UV-B exposure on Chia seed studied its morphological mutants, cytological observation, and their biochemical properties and also used the GC-MS technique to analyze the metabolites affect the findings from this study to highlight the positive effects of short-term UV-B exposure on Chia seeds, resulting in enhanced phytochemical properties, particularly an increase in alpha-linolenic acid. These findings contribute to our understanding of how UV-B radiation can be used to improve plant production and the development of superior plant varieties with enhancement.

DATA AVAILABILITY STATEMENT

The data that support the findings of this study are available from the corresponding author upon reasonable request. To promote transparency and reproducibility, detailed documentation related to data collection, processing, and analysis procedures is available upon request. The data described in this article are not openly available only subscriptions based on journals.

REFERENCE

1. Arisha, M. H., Shah, S. N., Gong, Z. H., Jing, H., Li, C., & Zhang, H. X. (2015). Ethyl methane sulfonate induced mutations in M2 generation and physiological variations in M1 generation of peppers (Capsicum annuum L.). *Frontiers in plant science*, 6: 399.
2. Avijeet M, Soni P, Bhat A, et al. (2011). UV-B-induced damage in nucleic acids: a mechanistic approach. *J Photochem Photobiol B*, 104(1-2): 204-215. https://doi.org/10.1016/j.jphotobiol.2021.112142
3. Badridze, G., Kacharava, N., Chkhubianishvili, E., Rapava, L., Kikvidze, M., Chanishvili, S., ... & Chigladze, L. (2016). Effect of UV radiation and artificial acid rain on the productivity of wheat. *Russian journal of ecology*, 47: 158-166. https://doi.org/10.1134/S106741361602003X
4. Bhat A, Rai UN, Sharma NC, et al. (2007). Role of cytomixis in pollen sterility of Anemone nemorosa L. *Cytologia*, 72(3): 289-294.
5. Blixt, S. (1961) Chlorophyll mutations in barley. *Hereditas*, 47: 109-189.

6. Bornman, J. F., Barnes, P. W., Robinson, S. A., Ballare, C. L., Flint, S. D., & Caldwell, M. M. (2015). Solar ultraviolet radiation and ozone depletion-driven climate change: effects on terrestrial ecosystems. *Photochemical & Photobiological Sciences*, 14(1): 88-107.
7. Britt AB, May GD (2003) DNA damage and repair in plants. *Annu Rev Plant Biol*, 54: 23-48.
8. Correia, C. M., Torres-Pereira, M. S., & Torres-Pereira, J. M. G. (1999). Growth, photosynthesis, and UV-B absorbing compounds of Portuguese Barbela wheat exposed to ultraviolet-B radiation. *Environmental Pollution*, 104(3): 383-388. https://doi.org/10.1016/S0378-4290(98)00102-6
9. Davis, D. R., Epp, M. D., & Riordan, H. D. (2004). Changes in USDA food composition data for 43 garden crops, 1950 to 1999. *Journal of the American College of Nutrition*, 23(6): 669-682. https://doi.org/10.1080/07315724.2004.10719409
10. 11. De Falco, B., Amato, M., & Lanzotti, V. (2017). Chia seeds products: an overview. *Phytochemistry Reviews*, 16: 745-760. https://doi.org/10.1007/s11101-017-9511-7
11. Erdei, A. L., Kósa, A., & Böddi, B. (2019). Distinct UV-A or UV-B irradiation induces protochlorophyllide photoreduction and bleaching in dark-grown pea (Pisum sativum L.) epicotyls. *Photosynthesis Research*, 140: 93-102.
12. Fan YY, Ramos KS, Chapkin RS (2016) Dietary gamma-linolenic acid, EPA, and DHA have distinct effects on lipid composition and transcriptome of HepG2 cells. *Prostaglandins Leukot Essent Fatty Acids*, 107: 20-29. https://doi.org/10.1093/JN%2F127.9.1765
13. Fujii T (1965) Mutation induction by non-ionizing radiation. *Radiat Bot*, 5: 401-405.
14. Gill SS, Tuteja N (2010) Reactive oxygen species and antioxidant machinery in abiotic stress tolerance in crop plants. *Plant Physiol Biochem*, 48(12): 909-930. https://doi.org/10.1016/j.plaphy.2010.08.016
15. Gonzalez-Castejon M, Rodriguez-Casado A (2013) Dietary phytochemicals and their potential effects on obesity: a review. *Pharmacol Res*, 72: 113-126. https://doi.org/10.1016/j.phrs.2011.07.004
16. Hideg, É., Jansen, M. A., & Strid, Å. (2013). UV-B exposure, ROS, and stress: inseparable companions or loosely linked associates? *Trends in plant science*, 18(2): 107-115. https://doi.org/10.1016/j.tplants.2012.09.003
17. Höll, J., Lindner, S., Walter, H., Joshi, D., Poschet, G., Pfleger, S., ... & Rausch, T. (2019). Impact of pulsed UV-B stress exposure on plant performance: How recovery periods stimulate secondary metabolism while reducing adaptive growth attenuation. *Plant, Cell & Environment*, 42(3): 801-814. https://doi.org/10.1111/pce.13409
18. Jaleel CA, Riadh K, Gopi R, et al. (2009) Antioxidant defense responses: physiological plasticity in higher plants under abiotic constraints. *Acta Physiol Plant*, 31(3): 427-436. https://doi.org/10.1007/s11738-009-0275-6
19. Johnson EJ (2018) Gamma-tocopherol—An under-explored form of vitamin E. *Molec Nutr Food Res*, 62(18): 1700395.
20. Kacharava N, Kubli E, Schäfer E (2009) Photomorphogenic effects of UV-B radiation on Arabidopsis thaliana. *Photochem Photobiol*, 85(6): 1479-1485.
21. Kacharava, N., Chanishvili, S., Badridze, G., Chkhubianishvili, E., & Janukashvili, N. (2009). Effect of seed irradiation on the content of antioxidants in leaves of Kidney bean, Cabbage, and Beet cultivars. *Australian Journal of Crop Science*, 3(3): 137.
22. Kaur N, Chugh V, Gupta AK (2018) Essential fatty acids as functional components of foods – a review. *J Food Sci Technol*, 55(9): 3873-3885.
23. Kirchhoff H, Kutzbach H, Mayer H, et al. (1989) Cytological investigations as a tool in plant breeding. *Cytologia*, 54: 159-168.
24. Kolar, F., Pawar, N., & Dixit, G. (2011). Induced chlorophyll mutations in Delphinium malabaricum (Huth) Munz. *Journal of Applied Horticulture*, 13(1): 18-24.
25. Bhattacharya, A., Sood, P., &Citovsky, V. (2010). The roles of plant phenolics in defense and communication during Agrobacterium and Rhizobium infection. *Molecular Plant Pathology*, 11(5): 705-719. https://doi.org/10.1111/j.1364-3703.2010.00625.x
26. Kumar P, Rai UN (2007) Environmental stress-induced cytomorphological alterations during pollen development in rice. *Cytologia*, 72(4): 379-384.
27. Kumar S, Bhardwaj R (2019) Induction of reactive oxygen species and its impact on mitochondrial functions in plants under environmental stress. *J Proteins Proteom*, 10(3): 215-230.
28. Kumar, G., & Gupta, P. (2009). Induced karyomorphological variations in three phenodeviants of Capsicum annuum L. *Turkish Journal of Biology*, 33(2): 123-128. https://doi.org/10.3906/biy-0807-29
29. Kumar, G., & Pandey, A. (2017). Effect of UV-B Radiation on Chromosomal Organisation and Biochemical Constituents of Coriandrum sativum L. *Jordan Journal of Biological Sciences*, 10(2).
30. Li X, Cai J, Liu F, et al. (2013) Systematic analysis of photosynthetic pigments and pigment-protein com-

plexes from the green alga Chlamydomonas reinhardtii. *J Proteome Res*, 12(2): 776-793.

31. Lichtenthaler, H. K. (1987). [34] Chlorophylls and carotenoids: pigments of photosynthetic biomembranes. *Methods in Enzymology*, 148: 350-382.
32. Munir B, Saeed F, Javed I, et al. (2020) Ergosterol: A Dietary Source of Vitamin D. *J Food Sci Technol*, 57(3): 1001-1008. https://doi.org/10.1016/j.watres.2013.04.021
33. Nasser, L. A. (2001). Effects of UV-B radiation on some physiological and biochemical aspects in two cultivars of barley (Hordeum vulgare L.). *Egyptian Journal of Biology*, 3(1): 97-105.
34. Othman ZA, Ahmed M, Noordin MI (2017) The role of phytosterols in skin: anti-aging and anti-inflammatory properties. *J Am Coll Nutr*, 36(8): 684-690.
35. Rai VK, Agrawal M (2017) Impact of elevated ultraviolet-B (UV-B) radiation on crop plants: a review. *Agric Rev*, 38(3): 171-179. https://doi.org/10.1007/s12298-020-00780-8
36. Shahwar D, Abbasi BH, Hafiz IA (2017) Effect of UV-C radiation on morphological traits of Calendula officinalis L. *Pak J Bot*, 49(3): 1053-1059. https://doi.org/10.3390/molecules22071161
37. Shukla nee Tripathi M, Kumar A (2010) Role of ionizing radiation in the induction of chromosomal aberrations. *Environ Exp Biol*, 8: 13-23. https://doi.org/10.1016/j.bbamem.2014.11.004
38. Smith AR, Smith MR, Fagan RL, et al. (2015) Guanosine signaling in the brain: paths to neuropsychiatric disorders and therapeutic potential. *Biochem Pharmacol*, 101: 1-12.
39. Solanki SS, Agarwal N, Panwar J (2004) Plant Growth Promoting Rhizobacteria: An Ecofriendly Approach for Sustainable Agriculture. In: Singh VP, Singh SN (eds) Plant-Bacteria Interactions. Springer, New Delhi.
40. Todoric, J., Löffler, M., Huber, J., Bilban, M., Reimers, M., Kadl, A., ... & Stulnig, T. M. (2006). Adipose tissue inflammation induced by a high-fat diet in obese diabetic mice is prevented by n− 3 polyunsaturated fatty acids. *Diabetologia*, 49: 2109-2119. https://doi.org/10.1007/s00125-006-0300-x
41. Verma, A. K., Dhanasekar, P., Choudhary, S., Meena, R. D., & Lal, G. (2018). Estimation of induced variability in M2 generation of fennel (Foeniculum vulgare Mill.).
42. Wang D, Dubois RN (2017) Eicosanoids and cancer. *Nat Rev Cancer*, 10(3): 181-193 https://doi.org/10.1038/nrc280
43. Wang F, Xu Y, Wang W, et al. (2013) Multilevel regulation of chlorophyll biosynthesis during salt stress in rice. *Plant Cell Physiol*, 54(10): 1720-1733. https://doi.org/10.1039/C3CC43375G
44. Yao, Y., Xuan, Z., He, Y., Lutts, S., Korpelainen, H., & Li, C. (2007). Principal component analysis of intraspecific responses of Tartary buckwheat to UV-B radiation under field conditions. *Environmental and Experimental Botany*, 61(3): 237-245. https://doi.org/10.1016/j.envexpbot.2007.06.003
45. Hakala, K., Jauhiainen, L., Koskela, T., Käyhkö, P., &Vorne, V. (2002). Sensitivity of crops to increased ultraviolet radiation in northern growing conditions. *Journal of Agronomy and Crop Science*, 188(1): 8-18. https://doi.org/10.1046/j.1439-037x.2002.00536.x

Caryologia
International Journal of Cytology,
Cytosystematics and Cytogenetics

Firenze University Press
https://riviste.fupress.net/index.php/caryologia

Citation: Getlekha, N., & Sribenja, K. (2025). The genome organization of repetitive sequences in the Golden Damselfish, *Amblyglyphidodon aureus* (Cuvier, 1830) (Family Pomacentridae): insights from extensive pericentric inversions. *Caryologia* 78(4): 19-30. doi: 10.36253/caryologia-3438

Received: March 30, 2025

Accepted: Month 11, 2026

Published: Month 11, 2026

Data Availability Statement: All relevant data are within the paper and its Supporting Information files.

Competing Interests: The Author(s) declare(s) no conflict of interest.

The genome organization of repetitive sequences in the Golden Damselfish, *Amblyglyphidodon aureus* (Cuvier, 1830) (Family Pomacentridae): insights from extensive pericentric inversions

Nuntaporn Getlekha, Kamika Sribenja*

Department of Biology, Faculty of Science and Technology, Muban Chombueng Rajabhat University, Chombueng, Ratchaburi 70150, Thailand
*Corresponding author. E-mail: kamikasri@mcru.ac.th

Abstract. The genus *Amblyglyphidodon* (damselfishes) is one of the most distinctive fish groups in the Indo-Pacific coral reef ecosystem. It consists of 11 recognized species, which display complex taxonomic relationships and cryptic lineages across their extensive range, often inhabiting coral environments. The timing of evolutionary divergences among these species varies greatly, and the cytogenetic events that accompanied their diversification remain poorly understood. In this regard, chromosomal divergence analysis from a phylogenetic viewpoint provides valuable insights into karyoevolutionary trends. In this study, we employed conventional cytogenetic and cytogenomic techniques to investigate the Golden Damselfish, *Amblyglyphidodon aureus*, focusing on mapping repetitive DNA elements and transposable elements, including 18S rDNA, 5S rDNA, $(CA)_{15}$, $(GA)_{15}$, and $(CAA)_{10}$. The result show that *A. aureus* has a distinct karyotype (2n=48, FN=96), characterized by numerous bi-armed chromosomes, with pericentric inversions playing a key role in its karyotypic structure. Pericentric inversions often function as postzygotic reproductive barriers in many species, and this may also be the case for *A. aureus*. These chromosomal differences illustrate the contrasting evolutionary pathways within the *Amblyglyphidodon* genus, shedding light on the karyotypic characteristics that define the group.

Keywords: Damselfishes, chromosome, repetitive sequences, repetitive DNA

INTRODUCTION

The Pomacentridae family, commonly known as damselfishes, is among the most abundant and characteristic families of coral reef fishes (Bone and Moore, 2008). Due to the strong interactions between damselfishes and their reef habitats, they represent a crucial lineage for biodiversity conservation (Litsios et al., 2012) and evolutionary research. With 399 species (Eschmeyer and Fong, 2016), Pomacentridae ranks as one of the most species-rich fish

ISSN 0008-7114 (print) | ISSN 2165-5391 (online) | DOI: 10.36253/caryologia-3438

families. The family exhibits a variety of sex-related patterns, including gonochoric, hermaphroditic, protogynous, and protandrous species (Fishelson, 1998; Fricke and Holzberg, 1974; Warner, 1984). Additionally, the Pomacentridae family exhibits phylogeographic patterns that range from minimal genetic structuring across vast oceanic regions (Rocha et al., 2008) to notable divergences between populations in close proximity (Drew and Barber, 2012; Planes et al., 2011). This considerable genetic variation is also evident in the family's diverse chromosomal characteristics (Getlekha et al., 2016a,b; Kashiwagi et al., 2005; Molina, 2007; Molina and Galetti, 2002; 2004a,b).

The subfamily Pomacentrinae is the most diverse among the five subfamilies of Pomacentridae, representing half of all damselfish species. Some of these species exhibit complex taxonomic patterns (Jang-Liaw et al., 2002; Quenouille and Bermingham, 2004). One of its genera, *Amblyglyphidodon* Bleeker, 1877, which includes 11 species primarily found in the Central and Western Pacific and Indian Oceans, is the second most species-rich group of damselfishes. These damselfishes are typically found swimming alone, in pairs, or in small groups, often among coral reefs. The clades within this genus display distinct evolutionary histories, with some lineages having been separated for extended periods, while others have diverged recently (Frédérich et al., 2013; Sorenson et al., 2014).

Damselfishes are among the few reef fish species that have benthic eggs and, in some cases, relatively short pelagic larval stages, as observed in certain *Amblyglyphidodon* species (Wellington and Victor, 1989). Their limited mobility restricts gene flow, which promotes local adaptation and leads to differentiation processes, the formation of polytypic species, and the emergence of cryptic or incipient speciation (Drew and Barber, 2012; Steinke et al., 2009). In fact, several species complexes within the Pomacentridae family, which share similar meristic and morphological characteristics, including chromatic body patterns, have been identified in the Indo-Pacific (Allen and Randall, 2002; Bernardi and Crane, 1999; Sorenson et al., 2014). Specifically, *Amblyglyphidodon* contains multiple species complexes with recent diversification (Allen et al., 2017; Liu et al., 2012), making them ideal models for studying chromosomal evolution in post-diversification processes. Indeed, many biological traits of Pomacentridae have been linked to chromosomal diversification (Getlekha et al., 2016a,b; Molina, 2007; Molina and Galetti Jr., 2004b).

Although there is a substantial amount of cytogenetic information available for the Pomacentridae family (Arai, 2011), chromosomal data on species complexes remain limited (Getlekha et al., 2016a). Cytogenetic studies are also taxonomically restricted for *Amblyglyphidodon*, often focusing mainly on karyotype descriptions. However, the available data generally show considerable variation in chromosomal structure (Arai, 2011; Molina & Galetti, 2004b). Several damselfish species complexes exhibit significant genetic differentiation (Allen et al., 2015; Liu et al., 2013), and cytogenetic analyses could provide valuable insights into their diversification and evolutionary processes, as well as their phylogenetic and taxonomic classification. These studies could also clarify the role of chromosomal changes as postzygotic barriers in lineage divergence. In the case of the *Amblyglyphidodon* genus, *A. aureus* from the Indian and Pacific Oceans, along with potential cryptic species yet to be described, has shown diversification linked to the Indo-Pacific barrier and sea level fluctuations during the Pleistocene (Liu et al., 2012, 2013; Sorenson et al., 2014).

Repetitive DNAs play a crucial role in the evolutionary dynamics of karyotype changes in several Pomacentridae species (Getlekha et al., 2016a,b; Molina and Galetti, 2002). In the genus *Abudefduf*, where species exhibit highly conserved karyotypes, different classes of repetitive DNAs show minimal variation across species (Getlekha et al., 2016b). In contrast, the genus *Dascyllus*, which displays significant karyotype modifications due to Robertsonian translocations, shows notable interpopulation variation in certain repetitive DNA sequences (Getlekha et al., 2016a). Mobile elements, known to be associated with chromosomal rearrangements (Dobigny et al., 2004; Lim and Simmons, 1994), may contribute to these changes. Additionally, in *Pomacentrus*, chromosomal alterations such as pericentric inversions are known to drive speciation and evolutionary divergence, and the organization and content of repetitive DNA sequences likely influence the genomic landscape and evolutionary trajectories of these species (Getlekha et al., 2018). The highly diversified karyotypes of *Amblyglyphidodon* further offer an opportunity to investigate the role of transposable elements in the diversification process.

In this study, we examined the chromosomal patterns and organization of five repetitive DNA classes [18S rDNA, 5S rDNA, $(CA)_{15}$, $(GA)_{15}$, and $(CAA)_{10}$] in *Amblyglyphidodon aureus*. Our results indicate that the species possess cryptic karyotypes with a high proportion of bi-armed chromosomes, suggesting that their evolution has largely been driven by extensive chromosomal inversions within this genus.

MATERIAL AND METHODS

Sampling and chromosome preparations and conventional methods

Cytogenetic analyses were performed on the Golden damselfish, *Amblyglyphidodon aureus* (Cuvier, 1830), with a sample consisting of 9 males and 10 females, collected from the Andaman Sea (Indian Ocean) near the Gulf of Thailand (Fig. 1). The specimens were captured using a hand-net, placed in sealed plastic bags containing oxygenated clean water, and transported to the research station for further analysis.

Mitotic chromosomes were obtained from cell suspensions of the anterior kidney following the conventional air-drying method (Bertollo et al., 2015). The C-banding technique was used to identify the distribution of C-positive heterochromatin (Sumner, 1972), while silver staining helped locate the Ag-NOR sites on the chromosomes (Howell and Black, 1980). The specimens were then deposited in the fish collection of the Cytogenetic Laboratory, Department of Biology, Faculty of Science and Technology, Muban Chombueng Rajabhat University.

Chromosome probes and FISH experiments

Two DNA sequences, arranged in tandem and isolated from the genome of the Erythrinidae fish *Hoplias malabaricus* (Bloch, 1794), were used as probes. The first probe contained a 5S rDNA repeat copy, including 120 base pairs (bp) of the transcribed 5S rRNA gene and 200 bp of the non-transcribed spacer (NTS) region (Martins et al., 2006). The second probe consisted of a 1400 bp segment from the 18S rRNA gene, which was amplified by PCR from the nuclear DNA. These 5S and 18S rDNA probes were then cloned into plasmid vectors and propagated in DH5α *Escherichia coli* competent cells (Invitrogen, San Diego, CA, USA). The probes were labeled with Spectrum Orange-dUTP and Spectrum Green-dUTP, respectively, using nick translation according to the manufacturer's guidelines (Roche, Mannheim, Germany).

Figure 1. General characteristic of the Golden damselfish, *Amblyglyphidodon aureus* (Cuvier, 1830).

The microsatellites $(CA)_{15}$, $(GA)_{15}$, and $(CAA)_{10}$ were synthesized according to Kirkpatrick (2010). During synthesis, these sequences were directly labeled with Cy3 at the 5' terminus by Sigma (St. Louis, MO, USA).

Fluorescence *in situ* hybridization (FISH) was carried out under high stringency conditions (Yano et al., 2017). Metaphase chromosome slides were treated with RNAse (40 μg/ml) for 1.5 hours at 37°C. Chromosomal DNA was denatured in a solution of 70% formamide/2x SSC at 70°C for 4 minutes. Then, 20 μl of the hybridization mixture (containing 2.5 ng/μl probes, 2 μg/μl salmon sperm DNA, 50% deionized formamide, and 10% dextran sulfate) was applied to the slides, and hybridization was carried out overnight at 37°C in a moist chamber with 2x SSC. The first post-hybridization wash was done with 2x SSC at 65°C for 5 minutes, followed by a final wash at room temperature in 1x SSC for 5 minutes. Finally, the slides were counterstained with DAPI and mounted in an antifade solution (Vectashield, Vector Laboratories).

Image processing

Around 20 metaphase spreads were examined per individual to verify the diploid chromosome number, karyotype structure, and FISH results. Images were captured using an Olympus BX50 microscope (Olympus Corporation, Ishikawa, Japan) equipped with a CoolSNAP camera and Image Pro Plus 4.1 software (Media Cybernetics, Silver Spring, MD, USA). Chromosomes were classified based on their arm ratios as metacentric (m), submetacentric (sm), acrocentric (a), or telocentric (t).

RESULTS

All Golden damselfish, *Amblyglyphidodon aureus* (Cuvier, 1830), exhibit a consistent diploid chromosome number of 2n=48. The karyotype of *A. aureus* (6m+22sm+20a; FN=96) is mainly composed of bi-armed chromosomes (Fig. 2). C-positive heterochromatic blocks are primarily located in the centromeric and telomeric regions of specific chromosome pairs in all specimens. Additionally, faint heterochromatic regions are present in the interstitial areas of chromosome pair No. 18 (Fig. 2).

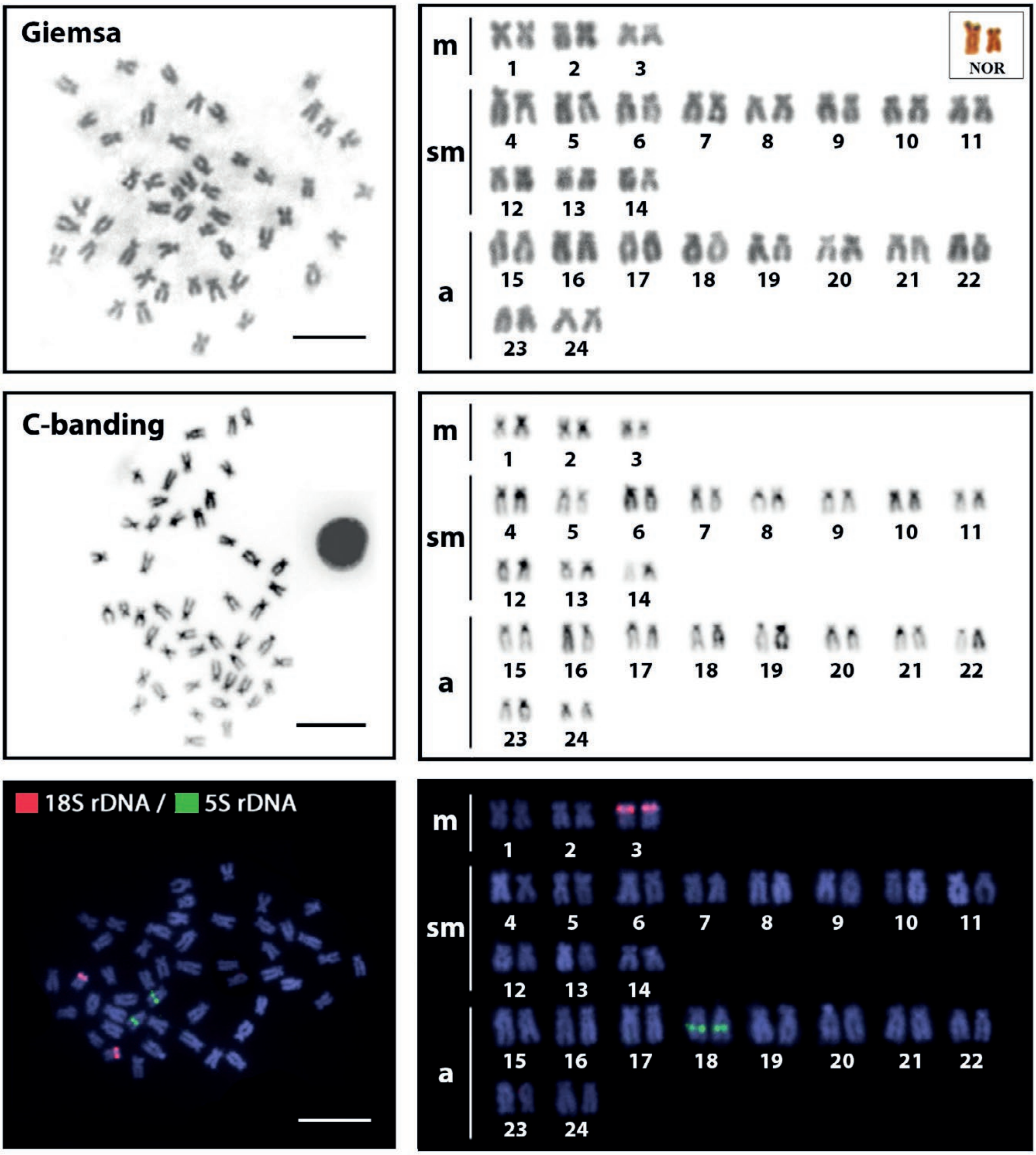

Figure 2. The metaphase and karyotypes of the Golden damselfish, *Amblyglyphidodon aureus* (Cuvier, 1830), were organized using several techniques, including Giemsa staining, Ag-NOR banding (indicated within the boxes), C-banding, and fluorescence *in situ* hybridization with 5S and 18S rDNA probes. Scale bar: 5 μm.

The Ag-NOR sites in all specimens are positioned in the subtelomeric portion of the short arms of the submetacentric chromosomes (Fig. 2). The 5S rDNA sites are not adjacent to the 18S rDNA sites. Instead, they are found in the interstitial regions of acrocentric chromosome pair 18, whereas the 18S rDNA sites are located at the distal ends of the short arms of metacentric chromosome pair 3 (Fig. 2).

The mapping of the $(CA)_{15}$ microsatellite revealed a broad distribution across most chromosomes, with prominent clusters present in certain chromosomal pairs. These clusters are located in the centromeric regions and occur with decreasing frequency across all specimens (Fig. 3). In contrast, the $(GA)_{15}$ and $(CAA)_{10}$ repeats are more sparsely distributed on the chromosomes, showing less distinct clusters in some chromosomal pairs, including in the interstitial regions (Fig. 3).

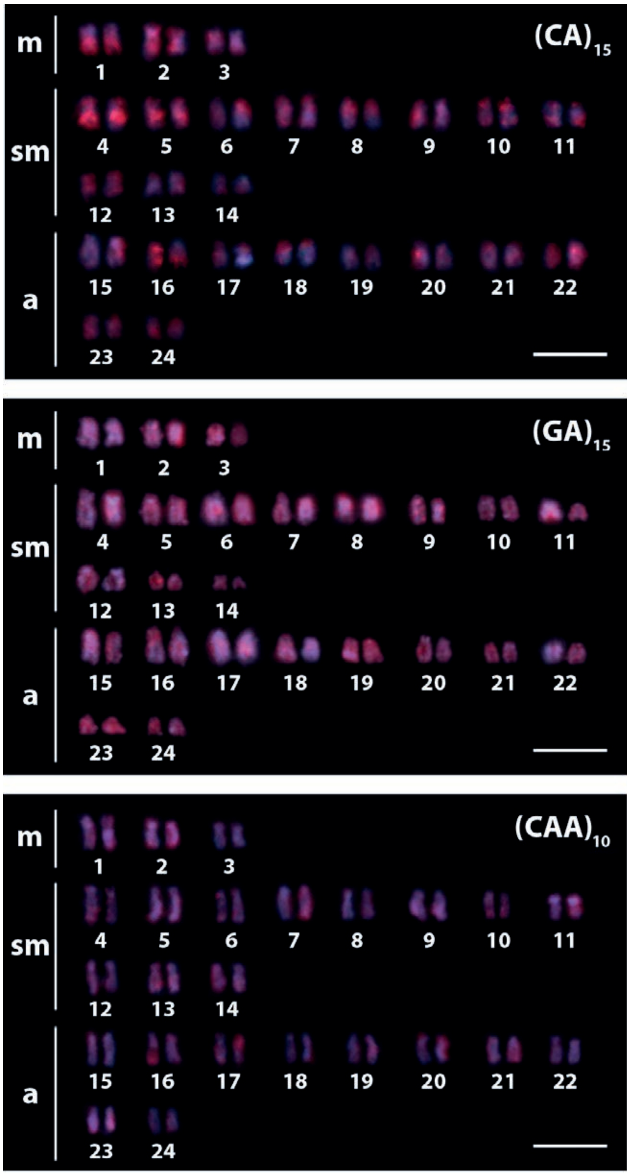

Figure 3. Fluorescence *in situ* hybridization was employed to map the chromosomes of the Golden damselfish, *Amblyglyphidodon aureus* (Cuvier, 1830), using di- and tri-nucleotide microsatellites. The distribution patterns of the (CA)15, (GA)15, and (CAA)10 microsatellites were analyzed as probes. Scale bar = 5 µm.

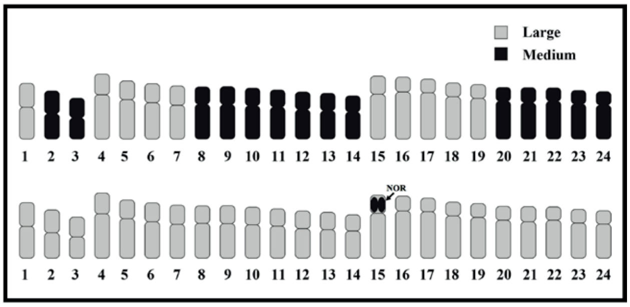

Figure 4. A standardized idiogram illustrating the chromosomal lengths and shapes of the Golden damselfish, *Amblyglyphidodon aureus* (Cuvier, 1830), with a diploid number of 48 (2n=48), created using conventional staining and Ag-NOR banding techniques, with arrows indicating the NOR regions.

The idiogram of the Golden damselfish, *Amblyglyphidodon aureus* (Cuvier, 1830), shows chromosomes with progressively decreasing lengths (Fig. 4). The karyotype of this species is marked by an asymmetrical chromosome arrangement, consisting of metacentric (m), submetacentric (sm), and acrocentric (a) chromosomes. The karyotype formula for *Amblyglyphidodon aureus* is expressed as: $2n\ (48) = L^{m}_{2}+L^{sm}_{8}+ L^{a}_{10}+ M^{m}_{4}+M^{sm}_{14}+ M^{a}_{10}$ or 6m+22sm+20a

This formula offers a detailed depiction of the chromosome composition and structure in *Amblyglyphidodon aureus*, highlighting the variety in chromosome types and sizes within its genome.

DISCUSSION

Phylogenetic divergence, karyotypic evolution, and repetitive DNA organization across Amblyglyphidodon species

The varying periods of divergence among some *Amblyglyphidodon* clades, resulting from multiple radiations under different scenarios, create an ideal setting for studying chromosomal evolution and diversification mechanisms in this genus. The distribution of *Amblyglyphidodon* species, primarily concentrated in the Indo-Malay-Philippines Archipelago with approximately 80% of the species (Cooper et al., 2009), has been shaped by several historical events, such as sea level fluctuations during glacial cycles (Naish, 2009), significantly impacting their evolution and phylogenetic diversification (Allen, 2008; Gaither and Rocha, 2013). It has been estimated that the stem lineages of *Amblyglyphidodon* originated approximately 30 million years ago. Previously, the Indo-Pacific pomacentrid genus *Amblyglyphidodon* was believed to consist of several distinct geographic color variations. However, the current study reveals that it is actually a complex of four species: *A. leucogaster* (Bleeker, 1847), *A. orbicularis* (Hombron & Jacquinot, 1853), *A. indicus* Allen & Randall, 2002, and *A. melanopterus* Allen & Randall, 2002. The species within the *Amblyglyphidodon* complex are primarily distinguished by a combination of color patterns and gill-raker counts (Allen and Randall, 2002).

The previously reported phylogenetic analysis of *Amblyglyphidodon curacao* (Bloch, 1787), along with the currently available mitogenome data for the Pomacentridae family (Kumar et al., 2016), revealed that *A. curacao* clusters with species in the subfamily Pomacentrinae, such as *Stegastes flavilatus* (Gill, 1862) and *Abudefduf vaigiensis* (Quoy & Gaimard, 1825), distinguishing it from species in the subfamily Amphiprioninae. However, *A. curacao* showed the highest sequence identity (87%) with *Amphiprion frenatus* Brevoort, 1856. This suggests that the fish genera *Amblyglyphidodon*, *Stegastes*, *Abudefduf*, and *Amphiprion* are closely related.

A species key for *Amblyglyphidodon* is provided, and the extended phylogenetic divergence within these clades may help explain their unique karyotype patterns. Specifically, *Amblyglyphidodon curacao* and *A. aureus* (Table 1) exhibit karyotypes predominantly consisting of bi-armed chromosomes (2n=48; FN=76 and 96, respectively) (Takai and Ojima, 1986; Ojima and Yamamoto, 1990; Ojima, 1983; Hardie and Hebert, 2004; present study). The *Stegastes* complex, comprising at least seven species, displays karyotypes with 2n=48 and NF=78-90, while the *Amphiprion* complex, with at least three species, shows karyotypes with 2n=48 and NF=78-86. In contrast, the *Abudefduf* complex, consisting of at least five species, exhibits cryptic karyotypes exclusively made up of acrocentric chromosomes (2n=48, FN=50-52) (Arai, 2011).

A karyotype with 2n=48a chromosomes, considered a foundational trait for Perciformes, is commonly found across several Clupeocephala families (Arai, 2011; Molina, 2007). While many Percomorpha families preserve a stable karyotype structure, the karyotype evolution in Pomacentridae is notably dynamic (Molina & Galetti Jr., 2004b). In Pomacentrinae, pericentric inversions are the most common karyotype alteration mechanism. These events are particularly evident in *Amblyglyphidodon* clades, where the gradual accumulation of inversions supports an in-depth analysis of a possible coordinated pericentric inversion process. This pattern has also been observed in other Pomacentrinae genera, where it occurs recurrently and leads to significant karyotype diversification (Kasiroek et al., 2014; Molina & Galetti, 2004a,b). The stabilization of specific chromosomal rearrangements in damselfishes seems not to be random but is likely driven by common orthoselective pressures across multiple lineages (Molina, 2007; Molina and Galetti Jr., 2004a,b).

The presence of C-positive heterochromatin in the centromeric and terminal regions of chromosomes, as observed in the species under investigation, appears to represent a basal condition previously reported in other Pomacentridae species (Molina and Galetti Jr., 2004a,b; Takai, 2012). In contrast, the data for *A. aureus* reveal interstitial C-positive blocks, indicating potential chromosomal rearrangements, likely caused by paracentric inversions, which are often considered cryptic events in fish chromosomes.

In *A. aureus*, the Ag-NOR sites are located at the terminal position on the short arms of acrocentric chromosome pair 15, while the 18S rDNA sites are positioned on the short arms of pair 3. The 5S rDNA sites are found in an interstitial position on the long arms of pair 18. The non-syntenic arrangement of these genes is common and likely represents a plesiomorphic condition in Pomacentridae (Cunha et al., 2014; Getlekha et al., 2016b, 2018; Molina and Galetti, 2002).

The role of repetitive DNAs in driving karyotype variation in damselfishes has been extensively studied (Getlekha et al, 2016a,b, 2018). The high evolutionary dynamics observed in Pomacentridae chromosomes (Molina et al., 2014b) may be closely linked to their organization and composition, as demonstrated by the repetitive DNA arrangements in *A. aureus*. Transposable elements (TEs), which are among the most abundant elements in fish genomes, have been shown to play a significant role in genome evolution and chromosomal rearrangements (Belyayev et al., 2010; Ferreira et al., 2011). However, the physical organization of these elements in Pomacentridae chromosomes remains largely unexplored. In *A. aureus*, the scattered distribution of repetitive DNA elements in the chromosomes has been associated with low evolutionary dynamism (Getlekha et al, 2016b, 2018). This is similar to the pattern observed in *Dascyllus* and *Pomacentrus* species, where microsatellite sequences are evenly distributed across most chromosomes without any significant accumulation. In contrast, *Abudefduf* species show varied and inconsistent distribution patterns, with $(CA)_{15}$ and $(GA)_{15}$ microsatellites concentrated in the nucleolar organizer regions, and $(CAA)_{10}$ repeats being highly accumulated across all chromosomes (Getlekha et al., 2016a).

Chromosomes and speciation in Amblyglyphidodon

Conspicuous evolutionary changes in chromosome number, karyotype formula, and heterochromatin structure are well-documented among damselfishes (Getlekha et al. 2016a,b, 2018; Molina and Galetti, 2002, 2004a). These structural karyotypic differences are clearly visible in the species analyzed (Table 1). This raises the question of whether alterations in chromosome structure and the organization of repetitive DNA may have actively contributed to reproductive isolation and speciation in this family (Getlekha et al. 2016a,b, 2018; Molina, 2007; Molina and Galetti, 2004a; Takai and Ojima, 1999). While speciation is typically a gradual process, it can occur rapidly in cases of ecological divergence. The resulting genomic differentiation tends to be concentrated in regions with low recombination rates, often clustered around genes that control ecotype-specific phenotypic traits (Marques et al., 2016).

In allopatric fish species, the time required for complete reproductive isolation is estimated to be around 11.6 million years (Russell, 2003). In this context, the early stages of speciation within species complexes represent a critical period of evolution that is not well understood in terms of cytogenetic factors. Although hybridization is considered rare in species with benthic nesting, several instances have been reported across different subfamilies (Coleman, 2014; Johansen et al., 2017; Maruska and Peyton, 2007; Van Herwerden and Doherty, 2006). These cases suggest that, during phyletic diversification, the genetic and cytogenetic differentiation in some damselfishes may have been insufficient to maintain genetic integrity and cohesion within certain species. Hybridization events have occurred in the evolutionary history of some damselfish species, particularly during the early phases of their divergence, when reproductive barriers are often less effective (Montanari et al., 2016).

In Pomacentrinae, a significant number of pericentric inversions, and possibly paracentric inversions as well, are primary mechanisms of karyotype differentiation, as demonstrated in some *Pomacentrus* species (Getlekha et al, 2018). These chromosomal rearrangements, along with structural modifications such as changes in centromere position, can have additional consequences, such as alterations in gene expression, meiotic pairing abnormalities, and reduced recombination (Kirkpatrick, 2010). The reduction in recombination helps increase the frequency of adaptive alleles in local populations (Hoffmann and Rieseberg, 2008), driving genomic differentiation and evolutionary divergence of lineages. These rearrangements have been extensively observed in closely related Pomacentrinae species, indicating their direct involvement in the diversification process (Molina WF, Galetti Jr PM, 2004a).

In contrast, certain chromosomal rearrangements appear to have limited impact as postzygotic reproductive barriers. For example, in Chrominae, the karyotypes of the Whitetail dascyllus, *Dascyllus aruanus* (Linnaeus, 1758) (2n=28-32), and the Reticulate dascyllus, *D. reticulatus* (Richardson, 1846) (2n=34-36), diverge significantly from each other due to Robertsonian rearrangements (Getlekha et al., 2016a; Kashiwagi et al., 2005). Notably, despite belonging to separate species complexes (Bernardi and Crane, 1999) and having diverged for a long period (around 15 Mya) (Frédérich et al., 2013, 2014), natural hybridization has been observed between these species (Johansen et al., 2017).

Some species of pomacentrid fish, such as *Pomacentrus auriventris* Allen, 1991 and *P. coelestis* Jordan & Starks, 1901, have a relatively recent divergence time (~0.3 Mya) (Sorenson et al., 2014), raising questions about the extent of reproductive isolation they have achieved. Two species from this complex, *P. similis* Allen, 1991 and *P. alleni* Burgess, 1981, coexist sympatrically in the northeastern Indian Ocean. Interestingly, *P. alleni* exhibits one of the most pronounced color differences within the "coelestis" complex, suggesting that color morphs may have evolved through assortative mating, thereby maintaining their genetic isolation even after secondary contact (Sorenson et al., 2014).

The high cytogenomic similarity observed in recently radiated allopatric species is likely shared, at least partially, with other species within the pomacentrid complex. This suggests that the genetic cohesion in these incipiently divergent species may be maintained by pre-zygotic barriers rather than post-zygotic ones. In fact, the structural and organizational patterns of genes and repetitive sequences in the karyotypes indicate that chromosomal changes play a limited role as key post-zygotic barriers. Consequently, cytogenetic data imply potential risks of reverse speciation due to secondary contact between these species, highlighting the importance of this information for their genetic conservation.

Overall, the available data highlight the significant role that chromosomal rearrangements have played in the evolutionary development of *Amblyglyphidodon* species, as well as the genome distribution of certain repetitive DNA classes. We were able to identify distinct chromosomal pathways in the phyletic diversification of *Amblyglyphidodon aureus*, with a detailed characterization of its chromosomal features. *Amblyglyphidodon aureus* was most recently evaluated by The IUCN Red List of Threatened Species in 2010, where it was classi-

Table 1. Reviews of papers on cytogenetics in the Subfamily Pomacentrinae (2n = diploid number, NF = fundamental number, NORs = nucleolar organizer regions, m = metacentric, sm = submetacentric, st = subtelocentric, a = acrocentric, – = not available).

Species	2n	NF	Formula	NORs	Reference
Abudefduf bengalensis	48	52	2m+2sm+44t	2	Getlekha et al. (2016b)
A. notatus	48	52	2m+2a/sm+44t	-	Arai and Inoue (1976)
A. saxatilis	48	52	2m+2sm+44t	2	Getlekha et al. (2016b)
A. sexfasciatus	48	50	2m+46t	2	Getlekha et al. (2016b)
A. sordidus	48	54	2m+2sm+2a+42t	-	Hardie and Hebert (2004)
A. vaigiensis	48	52	2m+2sm+2a+42t	2	Arai and Inoue (1976)
			2m+2sm+44t	2	Getlekha et al. (2016b)
Amblyglyphidodon curacao	48	76	6m+22sm+20t	2	Takai and Ojima, 1986 Ojima and Yamamoto 1990 Ojima, 1983 Hardie and Hebert, (2004)
A. aureus	48	96	6m+22sm+20a	2	*Present study*
Cheiloprion labiatus	48	74	26sm+22t	2	Takai and Ojima (1987)
Chrysiptera cyanea	42	64	6m+16sm+2a+18t	2	Takai and Ojima (1995) Ojima and Yamamoto (1990) Hardie and Hebert (2003)
	48	48	48st/a	-	Ojima (1983)
C. hemicyanea	48	78	30sm+10a+18t	2	Takai and Ojima (1991, 1999) Ojima and Yamamoto (1990)
	48	80	32sm+16t	-	Ojima (1983)
C. leucopoma	48	74	4m+22sm+6a+16t	2	Takai and Ojima (1995a)
C. rex	36	58	12m+10sm+14t	2	Takai and Ojima (1995a)
	48	78	8m+22sm+18t	-	Ojima (1983)
C. starcki	48	60	2m+10sm+36t	2	Takai and Ojima (1986, 1987)
Microspathodon chrysurus	48	54	6m+10sm+32t	2	Galetti et al. (2006) Molina and Galetti (2004a)
Neoglyphidodon melas	48	82	8m+26sm+2a+12t	-	Takai (2010)
N. nigroris	48	82	8m+26sm+2a+12t	2	Takai and Ojima (1991)
N. oxyodon	48	70	2m+20sm+12a+14t	2	Takai and Ojima (1991)
Plectroglyphidodon leucozonus	48	52	4a+44t	-	Arai and Inoue (1976)
Pomacentrus auriventris	48	48	48t	2	Getlekha et al. (2018)
P. chrysurus	48	90	8m+22sm+12a+6t	2	Hardie and Hebert (2004)
P. coelestis	48	48	48t	2	Takai and Ojima (1999)
	48	48	48t	–	Hardie and Hebert (2004)
P. cuneatus	48	86	8m+16sm+14a+10t	2	Getlekha et al. (2018)
P. moluccensis	48	94	10m+26sm+10a+2t	2	Hardie and Hebert (2004)
	48	94	10m+26sm+10a+2t	2	Getlekha et al. (2018)
P. cf. nagasakiensis	48	50	2m+46t	2	Takai and Ojima (1987)
P. philippinus	48	90	8m+24sm+10a+6t	2	Takai and Ojima (1991)
P. trilineatus	50	58	8m/sm+42t	–	Rishi (1973)
P. similis	48	48	48t	2	Getlekha et al. (2018)
Stegastes fuscus	48	90	20m+22sm+6t	2	Galetti et al. (2006)
S. insularis	48	86	14m+24sm+6a+4t	2	Nagpure et al. (2006)
S, leucostictud	48	88	18m+22sm+8t	2	Galetti et al. (2006) Molina and Galetti (2004b)
S. lividus	48	78	6m+24sm+18t	-	Ojima (1983)
S. nigricans	48	52	2m+2sm+24t	-	Ojima (1983) Hardie and Hebert (2004)
S. pictus	48	90	14m+28sm+2a+4t	2	Galetti et al. (2006) Molina and Galetti (2004b)
S. variabilis	48	88	18m+22sm+8t	2	Galetti et al. (2006)

fied as Least Concern. This species is found in the tropical marine waters of the Eastern Indian and Western Pacific oceans, native to the central Indo-Pacific. It typically inhabits outer reef areas, deep lagoons, and regions with strong ocean currents, often living among gorgonians, either alone or in small groups. Its range extends from Thailand to Indonesia, across New Guinea, north to the Philippine Islands and Taiwan, and as far east as the Marshall Islands and Fiji. In Australia, it is found in the offshore reefs of north-western Western Australia and the Great Barrier Reef in Queensland. In the context of glacial cycles, where sea levels have risen and fallen, *Amblyglyphidodon* species may have experienced repeated isolation and reconnection events, making them an ideal model for studying chromosomal patterns related to the speciation process.

ACKNOWLEDGEMENTS

The authors appreciate the correctness verification of the paper and the invaluable assistance provided by the Toxic Substances in Livestock and Aquatic Animals Research Group at Khon Kaen University and and Department of Biology, Faculty of Science and Technology, Muban Chombueng Rajabhat University that provided support for this study.

REFERENCES

Allen GR, Erdmann MV, Cahyani DNK. Review of the *Chrysipteraoxycephala* complex of damselfishes (Pomacentridae) with descriptions of three new species from the East Indian Archipelago. Journal of the Ocean Science Foundation. 2015;17:56–84.

Allen GR, Erdmann MV, Purtiwi PD. Descriptions of four new species of damselfishes (Pomacentridae) in the *Pomacentrus philippinus* complex from the tropical western Pacific Ocean. Journal of the Ocean Science Foundation. 2017;25:47–76.

Allen GR, Randall JE. A review of the Leucogaster species complex of the Indo-pacific pomacentrid genus *Amblyglyphidodon*, with descriptions of two new species. aqua, International Journal of Ichthyology. 2002;5:139–152.

Allen GR. Conservation hotspots of biodiversity and endemism for Indo-Pacific coral reef fishes. Aquat Conser Mar Freshw Ecosyst. 2008;18:541–556.

Arai R, Inoue M. Chromosomes of four species of coral fishes from Japan. Bulletin of the National Science Museum, Series A. 1976;2(2):137-141.

Arai R. Fish Karyotypes: a check list. Tokyo: Springer; 2011.

Belyayev A, Kalendar R, Brodsky L, Nevo E, Schulman AH, Raskina O. Transposable elements in a marginal plant population: temporal fluctuations provide new insights into genome evolution of wild diploid wheat. Mobile DNA. 2010; https://doi.org/10.1186/1759-8753-1-6.

Bernardi G, Crane NL. Molecular phylogeny of the humbug damselfishes inferred from mtDNA sequences. J Fish Biol. 1999;54:1210–1217.

Bertollo LAC, Cioffi MB, Moreira-Filho O: Direct chromosome preparation from freshwater teleost fishes. In: Ozouf-Costaz C, Pisano E, Foresti, F and Almeida Toledo LF, editors. Fish Cytogenetic Techniques (Chondrichthyans and Teleosts).CRC Press: Enfield, Boca Raton, FL; 2015. pp. 21–26.

Bone Q, Moore RH. Biology of fishes. 3rd ed. New York: Taylor & Francis Group, 2008.

Coleman RR, Gaither MR, Kimokeo B, Stanton FG, Bowen BW, Toonen RJ. Large-scale introduction of the Indo-Pacific damselfish *Abudefduf vaigiensis* into Hawaii promotes genetic swamping of the endemic congener *A. abdominalis*. Mol Ecol. 2014;23:5552–5565.

Cooper WJ, Smith LL, Westneat MW. Exploring the radiation of a diverse reef fish family: phylogenetics of the damselfishes (Pomacentridae), with new classifications based on molecular analyses of all genera. Molecular Phylogenetics and Evolution. 2009;52:1–16.

Cunha IMC, Souza AS, Dias EA, Amorim KDJ, Soares RX, Costa GWWF, García-Machado E, Galetti Jr PM, Molina WF. Genetic multipartitions based on d-loop sequences and chromosomal patterns in Brown Chromis, *Chromis multilineata* (Pomacentridae), in the Western Atlantic. BioMed Research International. 2014;254698.

Dobigny G, Ozouf-Costaz C, Waters PD. LINE-1 amplification accompanies explosive genome repatterning in rodents. Chromosome Research. 2004;12:787.

Drew JA, Barber PH. Comparative phylogeography in Fijian coral reef fishes: a multi-taxa approach towards marine reserve design. PLoSOne. 2012; https://doi:10.1371/journal.pone.0047710.

Eschmeyer WN, Fong JD. Title of subordinate document. In: Species by Family/Subfamily. 2016. http://researcharchive.cala cademy.org/research/ichthyology/catalog/SpeciesByFamily.asp. Accessed 15 Jan 2025.

Ferreira DC, Porto-Foresti F, Oliveira C, Foresti F. Transposable elements as a potential source for understanding the fish genome. Mobile Genetic Elements. 2011;1:2:112–117.

Fishelson L. Behaviour, socio-ecology and sexuality in damselfishes (Pomacentridae). Italian Journal of Zoology. 1998;65:387–398.

Frédérich B, Olivier D, Litsios G, Alfaro ME, Parmentier E. Trait decoupling promotes evolutionary diversification of the trophic and acoustic system of damselfishes. Proc R Soc B. 2014;281:20141047.

Frédérich B, Sorenson L, Santini F, Slater GJ, Alfaro ME. Iterative ecological radiation and convergence during the evolutionary history of damselfishes (Pomacentridae). Am Nat. 2013;181:94–113.

Fricke HW, Holzberg S. Social units and hermaphroditism in a pomacentrid fish. Naturwissensch. 1974;61:367–68.

Gaither MR, Rocha LA. Origins of species richness in the Indo-Malay-Philippine biodiversity hotspot: evidence for the centre of overlap hypothesis Journal of Biogeography. 2013;40:1638–1648.

Galetti PM, Molina WF, Affonso PRAM. Assessing genetic diversity of Brazilian reef fishes by chromosomal and DNA markers. Genetica,. 2006;126(1):91–99.

Getlekha N, Cioffi MB, Yano CF, Maneechot N, Bertollo LAC, Supiwong W, Tanomtong A, Molina WF. Chromosome mapping of repetitive DNAs in sergeant major fishes (Abudefdufinae, Pomacentridae): a general view on the chromosomal conservatism of the genus. Genetica. 2016b;144:567–576.

Getlekha N, Molina WF, Cioffi MB, Yano CF, Maneechot N, Bertollo LAC, Supiwong W, Tanomtong A. Repetitive DNAs highlight the role of chromosomal fusions in the karyotype evolution of *Dascyllus* species (Pomacentridae, Perciformes). Genetica 2016a;144:203–211.

Getlekha, N, Cioffi MB, Maneechot N, Bertollo LAC, Supiwong W. Tanomtong A, Molina WF. Contrasting Evolutionary Paths Among Indo-Pacific Pomacentrus Species Promoted by Extensive Pericentric Inversions and Genome Organization of Repetitive Sequences. Zebrafish. 2018;15(1): 45–54.

Hardie D C, Hebert PD. The nucleotypic effects of cellular DNA content in cartilaginous and ray-finned fishes. Genome. 2003; 46(5): 683–706.

Hardie DC, Hebert PD. Genome-size evolution in fishes. Can J Fish Aquatic Sci. 2004;61(9): 1636–1646.

Hoffmann AA, Rieseberg LH. Revisiting the impact of inversions in evolution: from population genetic markers to drivers of adaptive shifts and speciation? Annu Rev Ecol Evol Syst. 2008;39:21–42.

Howell WM, Black DA. Controlled silver-staining of nucleolus organizer regions with a protective colloidal developer: a 1-step method. Experientia. 1980;36:1014–1015.

Jang-Liaw NH, Tang KL, Hui C-F, Shao K-T. Molecular phylogeny of 48 species of damselfishes (Perciformes: Pomacentridae) using 12S mtDNA sequences. Mol Phylogenet Evol. 2002;25:445–454.

Johansen JL, He S, Frank G, Pappas MK, Berumen ML, Hoey AS. Hybridization between damselfishes *Dascyllus aruanus* and *D. reticulatus* on the Great Barrier Reef. Coral Reefs. 2017; https://doi.org//10.1007/s00338-017-1563-z.

Kashiwagi E, Takai A, Ojima Y. Chromosomal distribution of constitutive heterochromatin and nucleolus organizer regions in four *Dascyllus* fishes (Pomacentridae, Perciformes). Cytologia. 2005;70:345–349.

Kasiroek W, Luangoon N, Getlekha N, Saowakoon S, Phinrub W, Tanomtong A. First report on heteromorphic NORs and chromosome analysis of Rolland's demoiselle, *Chrysiptera rollandi* (Perciformes, Pomacentrinae) by conventional and Ag-NOR staining techniques. Cytologia. 2014;79:289–297.

Kirkpatrick M. How and why chromosome inversions evolve. PLoS Biology, 2010; https://doi.org/10.1371/journal.pbio.1000501.

Kumar S, Blaxter M, Hebert PD. Complete mitochondrial genome of Staghorn damselfish, Amblyglyphidodon curacao (Perciformes: Pomacentridae). Mitochondrial DNA Part B. 2016; 1(1):1–2.

Lim JK, Simmons MJ. Gross chromosome rearrangements mediated by transposable elements in *Drosophila melanogaster*. Bioessays. 1994;16:269–275.

Litsios G, Pellissier L, Forest F, Lexer C, Pearman PB, Zimmermann NE, Salamin N, Trophic specialization influences the rate of environmental niche evolution in damselfishes (Pomacentridae). Proc Biol Sci. 2012;279:3662–3669.

Liu SYV, Dai CF, Allen GR, Erdmann MV. Phylogeography of the neon damselfish *Pomacentrus coelestis* indicates a cryptic species and different species origins in the West Pacific Ocean. Mar Ecol Prog Ser. 2012;458:155–167.

Liu SYV, Ho HCH, Dai CF. A new species of *Pomacentrus* (Actinopterygii: Pomacentridae) from Micronesia, with comments on its phylogenetic relationships. Zool Stud. 2013;52:6–13.

Marques DA, Lucek K, Meier JI, Mwaiko S, Wagner CE, Excoffier L, Seehausen O, Genomics of rapid incipient speciation in sympatric threespine stickleback. PLOS Genetics. 2016;12:2:e1005887.

Martins C, Ferreira IA, Oliveira C, Foresti F, Galetti Jr PM. A tandemly repetitive centromeric DNA sequence of the fish *Hoplias malabaricus* (Characiformes: Erythrinidae) is derived from 5S rDNA. Genetica. 2006;127:133–141.

Maruska KP, Peyton KA. Interspecific spawning between a recent immigrant and an endemic damselfish (Pisces: Pomacentridae) in the Hawaiian Islands. Pac Sci. 2007;61:211–221.

Molina WF, Galetti Jr PM. Karyotypic changes associated to the dispersive potential on Pomacentridae (Pisces, Perciformes). J Exp Mar Biol Ecol. 2004a;309:109–119.

Molina WF, Galetti Jr PM. Multiple pericentric inversions and chromosomal divergence in the reef fishes *Stegastes* (Perciformes, Pomacentridae). Genet Mol Biol. 2004b;27:543–548.

Molina WF, Galetti Jr PM. Robertsonian rearrangements in the reef fish Chromis (Perciformes, Pomacentridae) involving chromosomes bearing 5S rRNA genes. Genet Mol Biol. 2002;25:373–377.

Molina WF, Martinez PA, Bertollo LA, Bidau CJ. Preferential accumulation of sex and Bs chromosomes in biarmed karyotypes by meiotic drive and rates of chromosomal changes in fishes. An Acad Bras Ciênc. 2014b;86:4:1801–1812.

Molina WF. Chromosomal changes and stasis in marine fish groups. In: Pisano E, Ozouf-Costaz C, Foresti F, Kapoor BG. editors. Fish cytogenetics. Enfield: Science Publishers; 2007. pp. 69–110,

Montanari SR, Hobbs JP, Pratchett MS, van Herwerden L. The importance of ecological and behavioural data in studies of hybridisation among marine fishes. Reviews in Fish Biology and Fisheries. 2016;26:181–198.

Nagpure NS, Kumar R, Srivastava SK, Kushwaha B, Gopalakrishnan A, Basheer VS. Cytogenetic characterization of two marine ornamental fishes, *Chaetodon collare* and *Stegastes insularis*. Journal of the Marine Biological Association of India. 2006; 48(2):267-269.

Naish T, Powell R, Levy R, Wilson G, Scherer R, Talarico F, Krissek L, Niessen F, Pompilio M, Wilson T. Obliquity-paced Pliocene West Antarctic ice sheet oscillations. Nature. 2009;458:322–328.

Ojima Y. Fish cytogenetics. In: Sharma AK, Sharma A, editors. Chromosomes in evolution of eukaryotic groups. CRC Press: Boca Raton; 1983.

Ojima Y. Yamamoto K. Cellular DNA contents of fishes determined by flow cytometry. La Kromosomo II. 1990;57:1871–1888.

Planes S, Doherty PJ, Bernardi G. Strong genetic divergence among populations of a marine fish with limited dispersal, *Acanthochromis polyacanthus*, within the Great Barrier reef and the Coral Sea. Evolution. 2001;55:2263–2273.

Rishi KK. A preliminary report on the karyotypes of eighteen marine fishes. Research Bulletin of the Punjab University. 1973;24:161–162.

Rocha LA, Rocha CR, Robertson DR, Bowen BW. Comparative phylogeography of Atlantic reef fishes indicates both origin and accumulation of diversity in the Caribbean. BMC Evolutionary Biology. 2008; 8:157.

Russell ST. Evolution of intrinsic post-zygotic reproductive isolation in fish. Ann Zool Fennici. 2003;40:321–329.

Sorenson L, Allen GR, Erdmann MV, Dai CF, Liu S-YV. Pleistocene diversification of the Pomacentrus coelestis species complex (Pisces: Pomacentridae): historical biogeography and species boundaries. Mar Biol. 2014;161:2495–2507.

Steinke D, Zemlak TS, Hebert PDN. Barcoding Nemo: DNA-based identifications for the ornamental fish trade. PLoS One 2009; 4:e6300.

Sumner AT. A simple technique for demonstrating centromeric heterochromatin. Exp Cell Res. 1972;75:304–306.

Takai A, Ojima Y. Chromosome evolution associated with Robertsonian rearrangements in Pomacentrid fish (Perciformes). Cytobios. 1995;84:103–110.

Takai A, Ojima Y. Comparative studies of karyotypes and distributions of nucleolus organizer regions in pomacentrid fish. Cytobios. 1991;65:199–205.

Takai A, Ojima Y. Constitutive heterochromatin distribution in the chromosomes of Pomacentrid fishes (Perciformes). Cytologia. 1999;64:87–91.

Takai A. Chromosomal distribution of C-band-positive heterochromatin in eight species of Pomacentridae (Perciformes). Chromosome Science. 2012;15:39–42.

Takai A. Karyotype and nucleolar organizer regions in the pomacentrid fish *Neoglyphidodon melas*. Memoirs of Osaka Shin-Ai College. 2010; 45:9–13.

Takai A. Ojima Y. Comparative studies of karyotypes and distributions of nucleolus organizer regions in Pomacentrid fishes. Proceedings of the Japan Academy, Series B. 1986;62(1):17–22.

Takai A. Ojima Y. Comparative studies of karyotypes and distribution of nucleolus organizer regions in Pomacentrid fish. Proc Jpn Acad. 1987;63B: 17–20.

Van Herwerden L, Doherty PJ. Contrasting genetic structures across two hybrid zones of a tropical reef fish, *Acanthochromis polyacanthus* (Bleeker 1855). Journal of Evolutionary Biology. 2006;19:239–252.

Wellington GM, Victor BC. Planktonic larval duration of one hundred species of Pacific and Atlantic damselfishes (Pomacentridae). Marine Biology. 1989;101:557–567.

Yano CF, Bertollo LAC, Cioffi MB. Fish-FISH: Molecular Cytogenetics in Fish Species. In: Liehr T, editors.

Fluorescence *in situ* Hybridization (FISH)-Application Guide. 3rd ed. Springer: Berlin; 2017. pp. 429–444.

Caryologia
International Journal of Cytology,
Cytosystematics and Cytogenetics

Firenze University Press
https://riviste.fupress.net/index.php/caryologia

Genome size and cytogenetic features of the critically endangered *Glehnia littoralis* F. Schmidt ex Miq. (Apiaceae): Implications for conservation and future genomic research

Yi Zhong[#], Hui-min Li[#], Jun Wen, Bao-cheng Wu, Wei Zhou, Nai-wei li[*], Chun-feng Song[*]

Jiangsu Key Laboratory for Conservation and Utilization of Plant Resources, Institute of Botany, Jiangsu Province and Chinese Academy of Sciences (Nanjing Botanical Garden Mem. Sun Yat-Sen), Nanjing 210014, Jiangsu, China
[*]Corresponding author. E-mail: cfsong79@cnbg.net
[#]These authors contributed equally to this work

OPEN ACCESS

Citation: Zhong, Y., Li, H.-M., Wen, J., Wu, B.-C., Zhou, W., Li, N.-W., & Song, C.-F. (2025). Genome size and cytogenetic features of the critically endangered *Glehnia littoralis* F. Schmidt ex Miq. (Apiaceae): Implications for conservation and future genomic research. *Caryologia* 78(4): 31-40. doi: 10.36253/caryologia-3782

Received: October 4, 2025

Accepted: December 28, 2025

Published: Month 11, 2026

Data Availability Statement: All relevant data are within the paper and its Supporting Information files.

Competing Interests: The Author(s) declare(s) no conflict of interest.

ORCID
YZ: 0009-0008-9149-9949
H-ML: 0000-0001-6660-7620
JW: 0000-0002-1926-6517
B-CW: 0009-0006-1719-3517
WZ: 0000-0003-1627-1529
N-WL: 0009-0004-6262-2646
C-FS: 0000-0003-2077-0486

Abstract. *Glehnia littoralis*, a critically endangered coastal plant endemic to sandy beach habitats, plays a unique role in the ecology of fragile coastal ecosystems. Its genome was characterized using an integrated approach combining flow cytometry, high-throughput sequencing, k-mer analysis, Smudgeplot, and cytogenetic validation. Flow cytometry estimated the genome size at ~2,913 Mb, while k-mer analysis under a diploid model ($p = 2$) revealed low heterozygosity (1.15%) and a high repeat content (80.87%), reflecting a relatively homogeneous yet highly repetitive genome shaped by historical whole-genome duplication events and transposon expansion. Smudgeplot patterns and cytogenetic analysis further confirmed the diploid status ($2n = 22$, $x = 11$) with a karyotype of $2n = 2x = 18m + 4sm$ (type 2A). These findings not only illuminate the evolutionary history and genomic architecture of this rare Apiaceae species but also offer critical insights into its adaptation to extreme coastal environments, providing valuable information for conservation strategies aimed at preserving this highly vulnerable, ecologically significant plant.

Keywords: *Glehnia littoralis,* genome size, flow cytometry, K-mer analysis, Ploidy.

1. INTRODUCTION

Glehnia F. Schmidt ex Miq. is a monotypic genus in the family Apiaceae, notable for its unique ecological and evolutionary significance. A single species, *Glehnia littoralis* F. Schmidt ex Miq., is currently comprised (Shan & She, 1979). Traditionally, the genus has been placed in the subfamily Apioideae, tribe Peucedaneae Dumort., subtribe Angelicinae Drude. There are eight genera in the subtribe Angeliceae in China, namely *Angelica* L., *Archangelica* Hoffm., *Czernaevia* Turcz., *Ostericum* Hoffm., *Coelopleurum* Ledeb., *Conioselinum* Fisch. ex Hoffm., *Levisticum* Hill (cultivated), and *Glehnia*. However, recent molecular phylogenetic studies have reassigned it to the tribe Selineae Spreng., where it is closely related to genera such as *Angelica* L., *Archangelica* Wolf., *Melanosciadium* de Boiss. and *Cnidium* Cusson (Wen *et al.* 2021).

G. littoralis is distributed along the coastal sandy beaches of the North Pacific, including East Asia and North America. In China, it mainly grows along the coasts of the Yellow Sea and Bohai Sea, including the Liaodong Peninsula, Qinhuangdao in Hebei, Shandong Peninsula, the Zhoushan Archipelago in Zhejiang, Lianjiang, Mawei, and Changle in Fujian, Taiwan, as well as in Russia, Korea, Japan, and North America. *G. littoralis* was once recorded in Jiangsu (Ganyu and Lianyungang), Guangdong (Shenzhen), and Hainan (Wanning and Wenchang), China (Shan & She, 1979). However, based on the author's previous investigations, these populations are now extinct, primarily due to super typhoons and human-induced disturbances.

As a key species in the East Asia–North America coastal ecosystem, *G. littoralis* was recognized for its important ecological functions. Its well-developed root system was considered effective in stabilizing sand and preventing coastal erosion. *G. littoralis* was also widely utilized as a medicinal and edible herb; its roots, known as "Bei Sha Shen" in traditional Chinese medicine, were commonly used as an antitussive and expectorant. The species experienced a sharp decline in the wild, primarily due to its narrow ecological niche, destruction of dune vegetation, habitat loss, and excessive harvesting (Yang *et al.*, 2011; Zhang *et al.*, 2022). It was subsequently classified as a Class II National Key Protected Plant in China and assessed as Critically Endangered (CR) according to national conservation criteria (Fu, 1992; Ministry of Environmental Protection & Chinese Academy of Sciences, 2013; National Key Protected Wild Plants List, 2021).

From the perspective of genetic resource conservation, the endangered status of *G. littoralis* not only threatened the survival of its populations but also posed the risk of permanently losing its unique genetic information, resulting in irreversible biodiversity loss. As a typical halophyte, *G. littoralis* exhibited strong salt and drought tolerance, yet its underlying molecular mechanisms had not been systematically elucidated.

Although the genomes of several Apiaceae species such as *Daucus carota* L., *Apium graveolens* L., *Angelica sinensis* (Oliv.) Diels, *Coriandrum sativum* L., and *Oenanthe javanica* (Blume) DC. had been sequenced, genomic information for the genus *Glehnia* remained completely lacking (Li *et al.* 2020; Song *et al.* 2020; Liu *et al.* 2021; Han *et al.* 2022; Wang *et al.* 2023). This limited our understanding of its environmental adaptation and evolutionary mechanisms, the biosynthetic pathways of characteristic secondary metabolites (e.g., coumarins and polyacetylenes), and the causes of its endangered status. Therefore, conducting genome sequencing research on *G. littoralis* was expected to provide critical data support for conservation genetics, comparative genomics, and functional gene discovery.

In this study, karyotype analysis, flow cytometry and genome survey sequencing were carried out to investigate the basic genomic characteristics of *G. littoralis*. Similar approaches have been applied in other angiosperm groups, providing valuable comparative insights (Loureiro et al., 2023; David et al., 2024; Radmanesh and Karimzadeh, 2025). As a result, the chromosome number and karyotype were determined, and the genome size, heterozygosity level, and proportion of repetitive sequences were estimated. These findings provided essential data for understanding the genome structure and complexity of *G. littoralis*.

2. MATERIALS AND METHODS

2.1. Plant materials

Samples of *G. littoralis* used in this study were collected from Yusha Bay Park, Hui'an County, Quanzhou City, Fujian Province (27°52′19″N, 118°47′46″E).

2.2. Chromosome karyotype analysis

Seedlings of *G. littoralis* were excavated and transplanted to the experimental nursery of Institute of Botany, Jiangsu province and Chinese Academy of Sciences. Actively growing root tips approximately 1 cm in length were excised and pretreated at room temperature for 3.5 hours in a 1:1 (v/v) mixture of 0.1% (w/v) colchicine and 0.002 mol·L^{-1} 8-hydroxyquinoline. The pretreated root tips were then rinsed three times with distilled water and fixed in Carnoy's solution [absolute ethanol: glacial acetic acid = 3:1 (v/v)] at 4 °C for 6 hours. After fixation, the samples were rinsed again three times with distilled water and macerated in a 1:1 (v/v) mixture of 1 mol·L^{-1} hydrochloric acid and 45% glacial acetic acid in a 37 °C water bath for 45 minutes. Following maceration, the root tips were washed three more times with distilled water, stained with modified carbol fuchsin for 4 hours, and squashed using the conventional squash method (Zhu, 1982).

Chromosomes were observed under a Nikon ECLIPSE Ci-S biological microscope (Nikon Corporation, Japan) and photographed using a Nikon Ds-Fi2 digital imaging system (Nikon Corporation, Japan). For each specimen, at least two root tips were used, and 5 to 10 well-scattered metaphase cells with clearly visible chromosomes were selected for observation, counting, and imaging. Chromosome classification and karyotype analysis were conducted following the standards of Levan et al. (Levan et al., 1964) and Stebbins (Stebbins, 1971) and the asymmetry index was calculated according to the method of Zarco (Zarco, 1986).

2.3. Flow cytometry analysis

Three replicates of fresh, tender leaves (approximately 0.2 g each) from plants were weighed and placed in Petri dishes (Mumbrú et al., 2025). A volume of 500 μL nuclear lysis buffer was added around each sample (Sysmex Partec, Germany). The leaves were then finely and quickly chopped using a sharp razor blade in a vertical motion to fully release intact nuclei, with an extraction time of 60 seconds. The resulting suspension was filtered through a 50 μm mesh into a sample tube. Subsequently, 2000 μL of fluorescent staining solution containing RNase was added to the sample tube, and the mixture was incubated in the dark for 15 minutes. The stained nuclei suspension was then analyzed using a flow cytometer.

An internal reference method was used for genome size estimation via flow cytometry. Prior to measurement, the CyFlow Cube6 flow cytometer (Sysmex Partec GmbH, Germany) was pre-warmed for 30 minutes (Zhang et al., 2025). During the assay, nuclear suspensions of tomato (*Solanum lycopersicum* L.), used as the internal standard, and *G. littoralis* were analyzed separately to preliminarily determine their respective fluorescence intensity ranges (Sun et al., 2021). A 488 nm blue laser was used for excitation, and fluorescence was collected via the FL2 channel. Since propidium iodide (PI) binds stoichiometrically to double-stranded DNA, the fluorescence intensity is directly proportional to the DNA content of the nuclei. For each test sample, at least 10,000 particles were collected at low flow rate during analysis (Doležel et al., 2007; Gong et al., 2011).

The known genome size of the internal standard tomato is 827 Mb. The genome size of the sample was calculated using the following formula: Genome size (Mb) = (Fluorescence intensity of sample / Fluorescence intensity of standard) × 827 (Doležel et al., 2005).

2.4. K-mer analysis and heterozygosity estimation

Genomic DNA was extracted from fresh, tender leaves using a modified CTAB protocol. DNA quality was initially assessed by agarose gel electrophoresis to ensure high integrity. DNA concentration and purity were subsequently determined using a NanoDrop Lite spectrophotometer (Thermo Fisher Scientific, Waltham, USA). High-quality DNA samples were fragmented randomly using a Covaris ultrasonic disruptor. Standard library construction procedures were followed, including end repair, A-tailing, adapter ligation, purification, and PCR amplification. The constructed libraries were first quantified using the Qubit 3.0 Fluorometer. After gradient dilution, insert size distribution was analyzed using the Agilent 2100 Bioanalyzer. Quantitative PCR was used to accurately determine the effective concentration of the libraries, ensuring they met the quality standards required for Illumina sequencing platforms.

Upon passing quality control, the libraries were sequenced using the DNBSEQ-T7 platform. Raw sequencing data underwent quality control filtering to remove adapter contamination, low-quality reads, and PCR duplicates, resulting in clean data suitable for further analysis (Cock et al., 2010).

High-quality Illumina short-read sequencing data were used for whole-genome characterization of *G. littoralis* via K-mer frequency analysis. Based on K-mer analysis principles, the heterozygosity rate was estimated from the ratio of the heterozygous to homozygous peak heights. The proportion of repetitive sequences was inferred from the area difference between the ideal Poisson distribution and the actual data curve beyond the main peak (Marcais et al., 2011; Liu et al., 2013).

For this analysis, the optimal K-mer size was set to k=19. K-mer counting and depth distribution were performed using Jellyfish (version 2.2.10), and genome size and heterozygosity were estimated using GenomeScope (version 2.0) (Vurture et al., 2017). GenomeScope fitting was performed under ploidy assumptions of p = 2 (diploid) and p = 4 (tetraploid), with an appropriate maximum coverage cutoff applied to minimize the influence of sequencing errors and extremely high-frequency k-mers. The following parameters were recorded: haploid genome size, heterozygosity, proportions of unique and repetitive sequences, model fit (R^2), and confidence intervals. The final genome size estimation was based on K-mer depth distribution and the following formula: Genome size = (Total number of K-mers) / (Peak K-mer depth).

To infer genome ploidy, we applied Smudgeplot analysis. The resulting joint k-mer spectrum was analyzed in Smudgeplot, which visualizes the distribution of heterozygous k-mer pairs (e.g., AA, AB, AAB, AABB) to infer the most likely ploidy level of the genome (Ranallo-Benavidez, 2020).

3. RESULTS

3.1. Genome size and ploidy identification analysis of G. littoralis by flow cytometry

Based on the known genome size of tomato, flow cytometry analysis was performed using the internal standard method. Nuclei suspensions prepared from a mixture of tomato and *G. littoralis* tissues were stained with propidium iodide (PI), and fluorescence intensity was measured through the FL2 channel. Six parallel measurements were performed. The recorded fluorescence intensity values for tomato were 2442.94, 2437.22, and 2289.72, while those for *G. littoralis* were 8458.73, 8411.83, and 8376.04. Based on these measurements and using tomato as the reference, the estimated genome size of *G. littoralis* was calculated to be 2913.44 Mb (Fig. 1).

3.2. Quality assessment of G. littoralis sequencing

Statistical analysis of the high-throughput sequencing data revealed that the raw dataset contained approximately 1.398 billion reads, totaling about 2096.55 Gb of bases, with a GC content of 37.35%. The quality scores Q20 and Q30 reached 98.66% and 95.81%, respectively. After quality filtering, the clean data showed a slight reduction, with a total base count of 2084.95 Gb and a marginal decrease in GC content to 37.27%. Notably, the Q20 and Q30 values remained nearly unchanged at 98.66% and 95.80%, respectively (Tab. 1). Overall, the sequencing data exhibited high quality, and the filtering process had minimal impact on data volume.

To assess potential contamination in the sequencing data, the first 50,000 reads were extracted and subjected to nucleotide homology analysis using the NT database (version: 202107). Sequence alignment was performed with the BLASTN tool (version: 2.11.0+) using the parameters: -evalue 1e-5 -max_target_seqs 1. The results showed that 11,162 out of the 50,000 reads matched

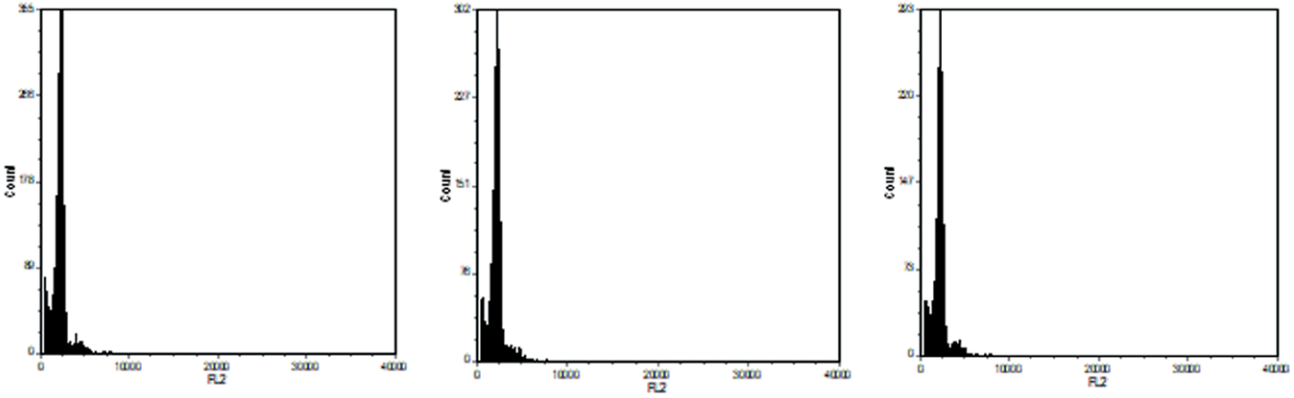

Solanum lycopersicum (a) Solanum lycopersicum (b) Solanum lycopersicum (c)

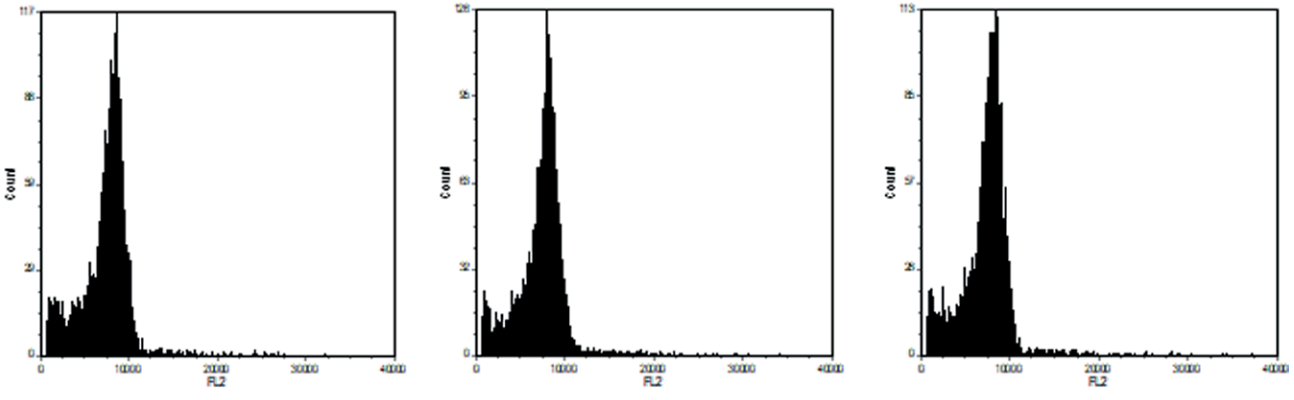

Glehnia littoralis (a) Glehnia littoralis (b) Glehnia littoralis (c)

Figure 1. Flow cytometry analysis of *G. littoralis* genome size.

Table 1. Statistics of sequencing data of *G. littoralis* survey library construction.

Type	Num_seqs	Sum_len	GC_content(%)	Q20(%)	Q30(%)
Raw data	1,397,696,990	209,654,548,500	37.35	98.66	95.81
Clean data	1,397,677,882	208,494,796,176	37.27	98.66	95.80

Table 2. Comparison results with the NT database.

Species	Family	Reads	Percentage (%)
Daucus carota subsp. *sativus*	Apiaceae	5271	10.54
Daucus carota	Apiaceae	1772	3.54
Ligusticum thomsonii	Apiaceae	521	1.04
Glehnia littoralis	Apiaceae	497	0.99
Hydrocotyle vulgaris	Araliaceae	302	0.60
Hedera helix	Araliaceae	191	0.38
Angelica dahurica	Apiaceae	173	0.35
Ligusticopsis scapiformis	Apiaceae	133	0.27
Zizia aurea	Apiaceae	108	0.22

entries in the database. Taxonomic classification revealed that the majority of matched reads (5,271) aligned to *Daucus carota* subsp. *sativus*, and the remaining top hits were also members of Apiaceae or Araliaceae (Tab. 2). Based on these annotations, no significant evidence of exogenous contamination was detected in the analyzed sample (Liu et al., 2013).

3.3. Genome size estimation based on K-mer analysis

To provide a comprehensive evaluation and avoid biases from model assumptions, we fitted both a diploid model (p = 2) and a tetraploid model (p = 4) to the data (Tab. 3, Fig. 4). Based on the k-mer analysis under different ploidy assumptions, the diploid model (p = 2) and the tetraploid model (p = 4) yielded markedly different estimates (Tab. 3). The diploid model predicted a genome size of approximately 2,465 Mb with a very low heterozygosity of 1.15% and a repeat content of 80.87%. In contrast, the tetraploid model produced a much smaller genome size estimate of ~1,231 Mb, together with a higher heterozygosity (8.6%) and a repeat content of 82.5%.

The distinct k-mer peak distributions for the two models were illustrated in Figure 2, with an average k-mer coverage of 28.6×, indicating sufficient sequencing depth for reliable genome characterization. The k-mer spectrum analysis under the diploid model (p = 2) shows a dominant homozygous peak (aa = 98.8%) and a smaller heterozygous peak (ab = 1.15%), reflecting a genome with low heterozygosity. The estimated genome size is approximately 2.47 Gbp, with a unique sequence proportion of 19.1% and repeat content of 80.87%. In contrast, the tetraploid model (p = 4) predicts a smaller genome size of 1.23 Gbp and higher heterozygosity (8.6%), with a slightly higher duplication ratio (82.5%).

Table 3. The K-mer analysis results of *G. littoralis* under diploid (p = 2) and tetraploid (p = 4) models.

P	K-mer	K-mer number	K-mer depth	Genome size(Mb)	Heterozygous ratio(%)	Duplication ratio(%)
2	19	140,160,192,996	57.2	2465.15	1.15	80.87
4	19	140,160,192,996	114.4	1230,71	8.6	82.5

3.4. Analysis of ploidy

To further investigate the ploidy state, a Smudgeplot analysis was generated (Fig. 3). Smudgeplot analysis revealed a series of distinct k-mer patterns, annotated as AAAAABB, AAAABB, AABB, and AB. Quantitative analysis of these patterns showed that the AABB class was the most abundant, representing 59% of the identified k-mers (8,694,820), followed by the AB class at 31% (4,586,615 k-mers). Higher-ploidy patterns (AAAABB and AAAAABB) together accounted for 10% of the total k-mers. The predominance of the balanced AABB pattern, along with the specific proportions of the other classes, supports the interpretation of a complex genome structure consistent with an allopolyploid organization.

3.5. Karyotype analysis

To validate the results from flow cytometry and k-mer analyses, the morphological characteristics of metaphase chromosomes and the karyotype of *G. littoralis* root tip cells are shown in Figure 4, with the corresponding ideogram presented in Figure 5. The chromosome number was determined to be 2n = 22, with a basic chromosome number of x = 11. The karyotype formula is 2n = 2x = 18m + 4sm, indicating that the complement consists of chromosomes with median (m) and submedian (sm) centromeres. Chromosome lengths ranged from 0.79 to 2.15 μm, with a total haploid chro-

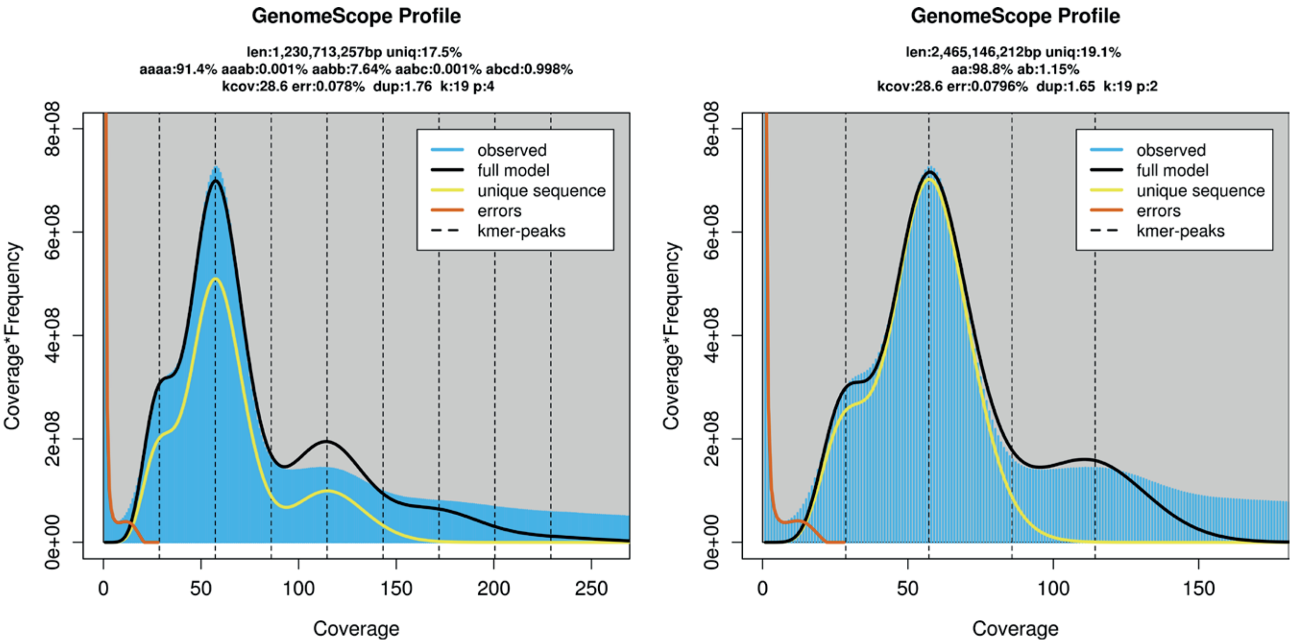

Figure 2. K-mer frequency distributions of *G. littoralis* under diploid (p = 2) and tetraploid (p = 4) models.

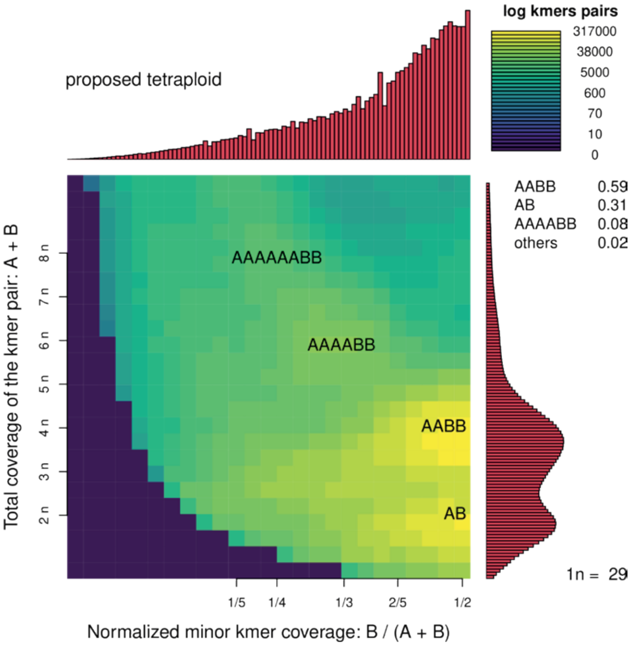

Figure 3. Smudgeplot Analysis of the Sequencing Data.

mosome length of 67.30 μm. The interchromosomal asymmetry index (A_2) was 0.71, and the intrachromosomal asymmetry index (A_1) was 0.33. No distinct bimodality or satellite chromosomes were observed, and the karyotype was classified as type 2A according to Stebbins' system (Stebbins, 1971).

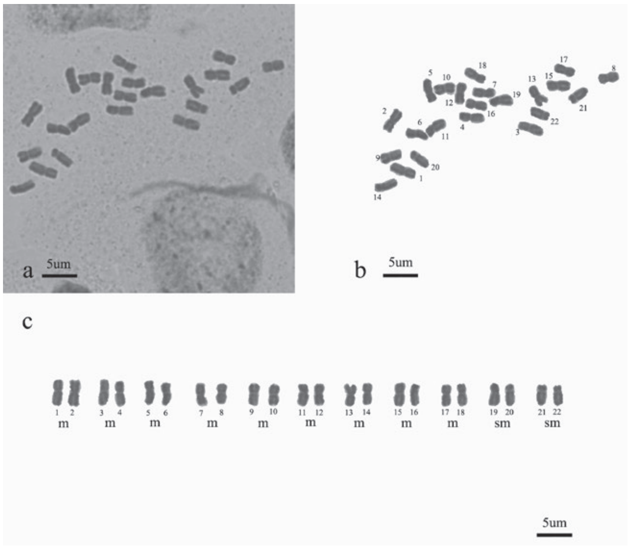

Figure 4. Chromosome morphological characteristics and karyotypes in root tip cells of *G. littoralis.*

4. DISCUSSION

We conducted a comprehensive assessment of the genome of *G. littoralis* using flow cytometry, k-mer frequency analysis, and karyotype observation. Flow cytometry indicated that the genome DNA content aligns with the expected diploid level. K-mer analysis under the diploid model showed a better fit and pro-

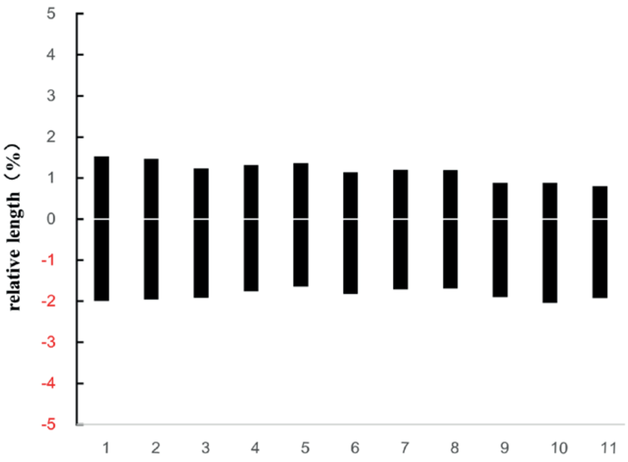

Figure 5. Karyotype diagram of chromosomes in root tip cells of *G. littoralis.*

vided reasonable estimate of heterozygosity (~1.15%) and repeat content. Compared with the tetraploid model, the diploid interpretation is more consistent with the observed peak patterns, genome size estimates, and cytological evidence, making it a more biologically plausible representation of the species' genomic structure. Karyotype analysis likewise showed no signs of homologous chromosome polyploidy. Taken together, these independent lines of evidence consistently indicate that *G. littoralis* is a diploid species (2n = 22, x = 11), with an estimated genome size of approximately 2,913.44 Mb. This result is in agreement with previous cytogenetic studies on *Glehnia* populations from Jiangsu, Shandong and Hebei (Liu et al., 1999; Zhou et al., 2022).

Smudgeplot analysis suggested an apparent allotetraploid genome for *G. littoralis*, which contrasts with cytological and k-mer evidence supporting a diploid state. This discrepancy likely results from the combination of high repetitive content (~80%) and low-level heterozygosity (~1.15%). In such a genome, k-mer pairs from repetitive regions can produce complex frequency patterns resembling the AABB distribution of a tetraploid, causing Smudgeplot to misclassify the ploidy. The method is also sensitive to input parameters, including k-mer size and coverage thresholds, which can contribute to the misinterpretation. Consequently, the apparent tetraploid signal should be viewed as a false positive, reflecting genome complexity rather than true polyploidy, underscoring the importance of multiple lines of evidence in ploidy assessment (Ranallo-Benavidez, 2020).

Genome size, also referred to as the DNA C-value, represents the total amount of DNA contained within a haploid nucleus of a species. It is one of the most fundamental parameters reflecting the genetic diversity of a species, providing critical reference information for whole-genome sequencing strategies, the exploration and utilization of genetic resources, as well as studies on phylogenetics and ecological adaptation. Genome size exhibits remarkable diversity among plants, and this variation is closely associated with plant evolution and adaptability (Bennett et al., 2005; Zavesky et al., 2005; Bainard et al., 2013).

The Apiaceae family comprises approximately 452 genera and 4,000 species. Genome sizes (C-values) exhibit considerable variation within the family, ranging from about 0.44 pg/1C in *Berula erecta* (Huds.) Coville to 6.57 pg/1C in *Portenschlagiella ramosissima* (Port.) Tutin (Leitch et al., 2019). The genome size of *Glehnia littoralis* is estimated at ~2.91 Gbp (approximately 2.98 pg), exceeding that of roughly 70% of the listed Apiaceae species and placing it among the taxa with relatively large genomes within the family.

Generally, an increase in genome size is often linked to events such as gene duplication and transposable element amplification, which may contribute additional genetic material for adaptive evolution during the course of plant diversification (Lee and Kim, 2014). Previous studies have shown that the Apiaceae family underwent two whole-genome duplication (WGD) events: the first occurred in the common ancestor of the family approximately 54–61 Ma ago, and the second was specific to the subfamily Apioideae, around 45–52 Ma ago (Bai et al., 2024; Li et al., 2020; Liu et al., 2021). It has been found that the duplicated genes resulting from these two WGD events exhibit significant imbalances in gene loss and expression levels, as exemplified by the coriander (*Coriandrum sativum*) genome.

Although traditionally considered a relatively primitive taxon, molecular evidence indicates that *Glehnia* is actually a more derived lineage of Selineae within the subfamily Apioideae (Xie et al., 2022), which also includes genera such as *Angelica, Cnidium, Saposhnikovia, Peucedanum,* and *Melanosciadium*. Notably, it occupies an upper branch of the phylogeny, with an estimated origin of approximately 5.94 Ma, representing a relatively recent divergence. In terms of its genome, *G. littoralis* maybe underwent two ancestral whole-genome duplication (WGD) events, which provided a foundation of duplicated genes. As a result, the species exhibits a high duplication ratio (~80.87%), reflecting abundant repetitive elements likely derived from both historical WGD events and transposon accumulation. Meanwhile, its relatively low heterozygosity (Heterozygous Ratio ~1.15%) suggests that the species may have experienced a recent bottleneck or increased selfing, resulting in a fairly homogeneous genome.

Moreover, genome size variation may be associated with ecological adaptability. Variation in genome size and structure in *G. littoralis* may be closely linked to responses to abiotic stresses, such as salinity, drought, and UV radiation (Tamura et al, 2022). Most lineages of Selineae retain the basic chromosome number x = 11, which indicates a relatively conservative pattern of chromosome evolution within the tribe and supports its recognition as a phylogenetically coherent and stable lineage. This cytological feature also provides important evidence for understanding intratribal relationships and evolutionary history within Selineae. Notably, these genomic features align with morphological traits commonly observed in Selineae. Members of the tribe often produce larger yet relatively light fruits, frequently with widely winged marginal ribs, which tend to occur in tall, robust umbellifers. Together, these characteristics may facilitate more effective dispersal and contribute to adaptation to open or windy habitats (Wen et al., 2021).

In summary, comparative studies on chromosome number and genome size not only enhance our understanding of the evolutionary dynamics within Apiaceae but also provide strong evidence supporting the phylogenetically basal position of *Glehnia*. Integration of cytogenetic, genomic, and phylogenetic data allows for a more comprehensive understanding of its evolutionary significance within the family.

CONCLUSION

G. littoralis, a critically endangered coastal plant restricted to sandy beach habitats, is a diploid species (2n = 22, x = 11) with an estimated genome size of ~2,913 Mb, as determined by integrated analyses including flow cytometry, k-mer profiling, Smudgeplot, and cytogenetics. K-mer analysis under a diploid model revealed heterozygosity (1.15%) and a high repeat content (80.87%), indicating a relatively homogeneous yet highly repetitive genome, likely shaped by historical whole-genome duplication events and transposon expansion. Cytogenetic analysis further confirmed a karyotype of 2n = 2x = 18m + 4sm, corroborating the diploid genome organization. The combination of these genomic insights not only advances our understanding of the evolutionary history of this rare Apiaceae lineage but also highlights the genetic basis underlying its adaptation to extreme coastal environments. Given its restricted distribution and critical conservation status, these findings are particularly valuable for informing targeted conservation strategies and elucidating the molecular mechanisms that support survival in highly specialized, vulnerable habitats.

ACKNOWLEDGMENTS

The authors thank Haoran Zhuang and Jingling of Huaiyin Institute of Technology for their enthusiastic assistance and strong support during our field investigations.

FUNDING

This research was funded by National Key R&D Program, grant number 2024YFF1307400 and National Natural Science Foundation of China, grant number 32370220.

CONTRIBUTIONS

All authors contributed to the study conception and design.

Yi Zhong: Methodology, Validation, Software.

Hui-Min Li: Data curation, Formal analysis, Writing – Review & Editing.

Jun Wen, Bao-Cheng Wu, Wei Zhou: Investigation.

Nai-Wei Li, Chun-Feng Song: Conceptualization, Writing – Original Draft, Writing – Review & Editing.

All authors have read and approved the final version of the manuscript.

ETHICS DECLARATIONS

All sampling procedures were conducted in accordance with the principles established by the Convention on Biological Diversity and the Regulations on Wild Plant Protection of the People's Republic of China. In this study, only a small amount of leaf and root tissues was collected, which did not exert any adverse impact on the survival and reproduction of wild populations. Since no human participants were involved, the necessity of obtaining consent for participation was not applicable.

REFERENCES

Assessment Team for China's Biodiversity Red List: Higher Plants. (2013). *China's biodiversity red list: Higher plants*. Beijing: Science Press.

Bai, M. Z., Jiang, S. J., Chu, S. S., et al. (2024). The telomere-to-telomere (T2T) genome of *Peucedanum praeruptorum* Dunn provides insights into genome evolution and coumarin biosynthesis. *GigaScience, 13*, giae025.

Bainard, J. D., & Villarreal, J. C. (2013). Genome size increases in recently diverged hornwort clades. *Genome, 56*(8), 431–435.

Bennett, M. D., & Leitch, I. J. (2005). Plant genome size research: A field in focus. *Annals of Botany, 95*(1), 1–6.

Cock, P. J., Fields, C. J., Goto, N., et al. (2010). The Sanger FASTQ file format for sequences with quality scores, and the Solexa/Illumina FASTQ variants. *Nucleic Acids Research, 38*(6), 1767.

David, F. S., Antonio, R. C. J., de Jesus, P. B. J., Francisco, S. B. U., Jennifer, S. H., Alfredo, C. R., … & Lucina, B. M. (2024). Evaluation of ploidy and the DNA index by flow cytometry in central nervous system tumors: a review. *Molecular Biology Reports*, 51(1), 1141.

Dolezel J (2005) Plant DNA Flow Cytometry and Estimation of Nuclear Genome Size. *Ann Bot* 95:99–110.

Doležel, J., Greilhuber, J., & Suda, J. (2007). Estimation of nuclear DNA content in plants using flow cytometry. *Nature Protocols, 2*(9), 2233–2244.Fu, L. G. (1992). *China plant red data book: Rare and endangered plants* (p. 699). Beijing: Science Press.

Gong, N., Tian, X. M., & Zhou, X. Y. (2011). Applications of flow cytometry in plant research—Analysis of nuclear DNA content and ploidy level in plant cells. *Chinese Agricultural Science Bulletin, 27*(9), 21–27.

Han, X. X., Li, C., Sun, S. C., et al. (2022). The chromosome-level genome of female ginseng (*Angelica sinensis*) provides insights into molecular mechanisms and evolution of coumarin biosynthesis. *Plant Journal, 112*, 1224–1237. https://doi.org/10.1111/tpj.16007

Iorizzo, M., Ellison, S., Senalik, D., et al. (2016). A high-quality carrot genome assembly provides new insights into carotenoid accumulation and asterid genome evolution. *Nature Genetics, 48*(6), 657–666.

Lee, S. I., Kim, N. S. (2014). Transposable elements and genome size variations in plants. *Genomics & informatics*, 12(3), 87.

Leitch, I. J., Johnston, E., Pellicer, J., et al. (2019). Angiosperm DNA C-values database (release 9.0, Apr 2019). https://cvalues.science.kew.org. Accessed 29 July 2025.

Levan, A., Fredga, K., & Sandberg, A. A. (1964). Nomenclature for centromeric position on chromosomes. *Hereditas, 52*, 201–220.

Li, M. Y., Feng, K., Hou, X. L., et al. (2020). The genome sequence of celery (*Apium graveolens* L.), an important leaf vegetable crop rich in apigenin in the Apiaceae family. *Horticulture Research, 7*, 9. https://doi.org/10.1038/s41438-019-0235-2

Liu B H, Shi Y J, Yuan J Y, et al. (2013). Estimation of genomic characteristics by analyzing k-mer frequency in de novo genome projects. *Quantitative Biology, 35*(s1–3), 62–67.

Liu, J.-X., Jiang, Q., Tao, J.-P., et al. (2021). Integrative genome, transcriptome, microRNA, and degradome analysis of water dropwort (*Oenanthe javanica*) in response to water stress. *Horticulture Research, 8*, 262. https://doi.org/10.1038/s41438-021-00707-8

Liu, Q. X., Hui, H., & Liu, M. H. (1999). Chromosomal characteristics and evolutionary status of a rare and endangered plant *Glehnia littoralis*. *Guihaia,* (4), 344–348.

Loureiro, J., Čertner, M., Lučanová, M., Sliwinska, E., Kolář, F., Doležel, J., … & Galbraith, D. W. (2023). The use of flow cytometry for estimating genome sizes and DNA ploidy levels in plants. *Plant cytogenetics and cytogenomics: methods and protocols* (pp. 25-64). New York, NY: Springer US.

Marcais, G., & Kingsford, C. (2011). A fast, lock-free approach for efficient parallel counting of occurrences of k-mers. *Bioinformatics, 27*(6), 764–770.

Ministry of Environmental Protection & Chinese Academy of Sciences. (2013). *China red list of biodiversity: Higher plants* [Internal document].

Mumbrú, M., Garnatje, T., Vallès, J. (2025). Methods of internal standards' preservation for genome size assessments: a comparative study. *Caryologia*, 78(1), 53-58.

National Forestry and Grassland Administration & Ministry of Agriculture and Rural Affairs. (2021, September 7). *National key protected wild plants list* (Announcement No. 15; approved by the State Council on August 7, 2021).

Ranallo-Benavidez, T. R., Jaron, K. S., & Schatz, M. C. (2020). GenomeScope 2.0 and Smudgeplot for reference-free profiling of polyploid genomes. *Nature Communications, 11*, 1432.

Radmanesh, P., Karimzadeh, G. (2025). Chromosome, ploidy analysis, and flow cytometric genome size of caper (Capparis spinosa) medicinal plant. *Caryologia*, 78(2), 3-19.

Shan, R. H., & She, M. L. (1979). *Umbelliferae III: Flora of China* (Vol. 55, p. 316). Beijing: Science Press.

Song, X., Wang, J., Li, N., et al. (2020). Deciphering the high-quality genome sequence of coriander that causes controversial feelings. *Plant Biotechnology Journal, 18*, 1444–1456. https://doi.org/10.1111/pbi.13310

Stebbins, G. L. (1971). *Chromosomal evolution in higher plants*. London: Edward Arnold.

Tamura, Y., Kubo, N., & Ohsako, T. (2022). Genetic diversity among Japanese local populations of an edible and medicinal coastal plant *Glehnia littoralis* F.

Schmidt ex Miq. *Genetic Resources and Crop Evolution, 69*(1), 85–97.

Su X, Wang BA, Geng XL, Du YF, Yang QQ, Liang B et al (2021) A high-continuity and annotated tomato reference genome. BMC Genomics 22:898.

The Angiosperm Phylogeny Group. (2016). An update of the Angiosperm Phylogeny Group classification for the orders and families of flowering plants: APG IV. *Botanical Journal of the Linnean Society, 181*, 1–20.

Vurture, G. W., Sedlazeck, F. J., Nattestad, M., et al. (2017). GenomeScope: Fast reference-free genome profiling from short reads. *Bioinformatics, 33*(14), 2202–2204.

Wang, Y.-H., Liu, P.-Z., Liu, H., et al. (2023). Telomere-to-telomere carrot (*Daucus carota*) genome assembly reveals carotenoid characteristics. *Horticulture Research, 10*, uhad103. https://doi.org/10.1093/hr/uhad103

Wen, J., Xie, D.-F., Price, M., et al. (2021). Backbone phylogeny and evolution of Apioideae (Apiaceae): New insights from phylogenomic analyses of plastome data. *Molecular Phylogenetics and Evolution, 161*, 107183. https://doi.org/10.1016/j.ympev.2021.107183

Xie, D. F., Xie, C., Ren, T., et al. (2022). Plastid phylogenomic insights into relationships, divergence, and evolution of Apiales. *Planta, 256*, 117. https://doi.org/10.1007/s00425-022-04031-w

Yang, H. X., Chu, J. M., & Zhang, J. T. (2011). Wild plants on the fore-edge of coastal sandy beaches in the Shandong Peninsula. *Acta Botanica Boreali-Occidentalia Sinica, 46*(1), 50–58.

Zarco, C. R. (1986). A new method for estimating karyotype asymmetry. *Taxon, 35*(3), 526–530.

Záveský, L., Jarolímová, V., & Štěpánek, J. (2005). Nuclear DNA content variation within the genus *Taraxacum* (Asteraceae). *Folia Geobotanica, 40*(1), 91–104.

Zhang, G. F., Xiong, T. S., Sun, T., et al. (2022). Diversity, distribution, and conservation of rare and endangered plants in Jiangsu. *Biodiversity Science, 30*(2), 21335.

Zhang LM, Yuan JM, Pu TL, Qu WL, Lei X, Ma KH, et al. Chromosome-scale genome assembly of *Phyllanthus emblica* L. 'Yingyu.' DNA Res. 2025;32:dsaf006.

Zhou, C. X., Zhang, J. S., & An, K. (2022). Chromosome karyotype and variation of coral vegetables from different places. *Molecular Plant Breeding*, 1–11.

Zhu, C. (1982). *Plant chromosomes and chromosome techniques* (p. 82). Beijing: Science Press.

Caryologia
International Journal of Cytology,
Cytosystematics and Cytogenetics

Firenze University Press
https://riviste.fupress.net/index.php/caryologia

Citation: Aksu Kalmuk, N. (2025). Phytochemical composition and genotoxic potential of *Sambucus ebulus* L. (Adoxaceae): Insights from *Allium cepa* bioassay and antioxidant profiling. *Caryologia* 78(4): 41-52. doi: 10.36253/caryologia-3709

Received: August 7, 2025

Accepted: December 29, 2025

Published: Month 11, 2026

Data Availability Statement: All relevant data are within the paper and its Supporting Information files.

Competing Interests: The Author(s) declare(s) no conflict of interest.

Phytochemical composition and genotoxic potential of *Sambucus ebulus* L. (Adoxaceae): Insights from *Allium cepa* bioassay and antioxidant profiling

Nursen Aksu Kalmuk

Artvin Coruh University, Medicinal and Aromatic Plants Application and Research Center, 8100, Artvin, Türkiye
E-mail: naksu@artvin.edu.tr

Abstract. *Sambucus ebulus* has long been used in traditional medicine for its anti-inflammatory and immune-modulatory properties; however, the cytogenetic safety of its aqueous extract remains insufficiently studied. This research aimed to evaluate the cytotoxic and genotoxic effects of *S. ebulus* fruit extract on *Allium cepa* root meristem cells. A comprehensive phytochemical characterization was conducted, including total phenolic and flavonoid content, antioxidant capacity (DPPH and FRAP), and HPLC and GC-MS analyses. Treatment groups were exposed to extract concentrations of 1%, 5%, 10%, 20%, and 50% for 48 hours. Cytogenetic parameters such as mitotic index (MI), chromosomal aberrations (CA), and micronucleus (MN) formation were evaluated. Tap water served as the negative control, while a 680 mg/L zinc oxide (ZnO) solution was used as the positive control. HPLC analysis identified epicatechin, catechin, gallic acid, chlorogenic acid, and rutin as the major phenolic constituents of the extract. GC-MS results revealed a volatile profile dominated by isovaleric acid ethyl ester, methyl isovalerate, and trans-β-ocimene. Antioxidant assays showed a total flavonoid content of 1.008 ± 0.02 mg QE/g, a FRAP value of 7.045 ± 0.08 mg TE/g, and a DPPH scavenging activity of 0.008 ± 0.30 mg/mL. The results indicated that low concentrations (1–10%) did not significantly suppress mitotic activity, whereas higher concentrations (20% and 50%) led to a marked decrease in MI, along with increased CA and MN frequencies. The extract exhibited dose-dependent effects on cell division. The observed biological responses may be partly attributed to its phenolic and volatile constituents. Overall, the findings highlight the dual nature of *S. ebulus* extract – potentially beneficial at low doses but harmful at higher concentrations – underscoring the importance of a scientifically grounded approach to its traditional use.

Keywords: *Sambucus ebulus*, *Allium cepa* assay, cytogenotoxicity, mitotic index, phenolic compounds, micronucleus test.

INTRODUCTION

Medicinal plants have long served as a valuable resource for the prevention and treatment of various diseases throughout human history. Despite advancements in modern medical systems, the World Health Organization (WHO) reports that approximately 85% of the population in developing countries still relies on traditional herbal products to meet their basic healthcare needs (Brasil 2006). However, the continued use of certain plant species based solely on empirical knowledge – without adequate scientific investigation into their chemical composition and biological effects – raises significant toxicological concerns. Thus, evaluating commonly used ethnomedicinal plants through scientific methodologies is essential to define safe usage thresholds (Martins et al. 2003).

Assessing the potential genotoxic and proliferative effects of medicinal plants is critical to substantiate the safety of their traditional use. In this context, cytogenetic bioassays play an essential role in detecting chromosomal alterations induced by chemically complex plant extracts. Among them, the *Allium cepa* test stands out as a globally recognized, sensitive, and cost-effective bioassay capable of directly visualizing chromosomal changes caused by mutagenic or potentially carcinogenic agents (Tedesco and Laughinghouse 2012; Bonciu et al. 2018; Sarac et al. 2019). Numerous studies have successfully applied this test to evaluate the cytotoxicity of plant-derived substances (Tedesco et al. 2015; Hister et al. 2017; Sousa et al. 2018; Trapp et al. 2020; Tuna-Gülören et al. 2021; Mohan and Joseph 2024). Furthermore, Rank and Nielsen (1994) reported an 82% correlation between the *A. cepa* assay and rodent carcinogenicity tests, suggesting its higher sensitivity compared to the Ames test. Teixeira et al. (2003) corroborated these findings by demonstrating consistency across *A. cepa* root meristem cells, rat bone marrow cells, and human lymphocytes, thereby confirming the reliability of this model for cytogenetic evaluations.

Sambucus ebulus L. (dwarf elder) is a perennial herbaceous species native to Türkiye, widely used in folk medicine for its anti-rheumatic, diuretic, and wound-healing properties (Yeşilada et al. 2014; Barak et al. 2020). However, pharmacological research on this species has predominantly focused on methanol- or ethanol-based extracts, while aqueous fruit extracts – commonly used in traditional applications – remain underexplored with regard to their impact on cell division and genetic material. Additionally, the relationship between the levels of phenolic and volatile constituents in *S. ebulus* fruits and their potential cytogenotoxic effects has not been sufficiently investigated. Evaluating these effects alongside antioxidant parameters such as total flavonoid content (TFC), DPPH radical scavenging capacity, and ferric reducing antioxidant power (FRAP) could offer a more integrative understanding of the plant's functional potential.

The present study aimed to evaluate the possible genotoxic and proliferative effects of an aqueous fruit extract of *S. ebulus* using the *Allium cepa* assay. Simultaneously, the chemical profile of the extract was comprehensively characterized: volatile constituents were analyzed via gas chromatography–mass spectrometry (GC-MS), phenolic composition was determined using high-performance liquid chromatography (HPLC), and antioxidant activity was assessed through TFC, DPPH, and FRAP assays. The aqueous extract was applied to *A. cepa* root meristematic cells at concentrations of 1%, 5%, 10%, 20%, and 50% (v/v). Tap water served as the negative control, while a 680 mg/L zinc oxide (ZnO) solution was used as the positive control. Genotoxicity markers such as mitotic index (MI), chromosomal aberrations (CA), and micronucleus (MN) formation were evaluated in all treatment groups and statistically analyzed. Overall, this study seeks to provide scientific validation for the traditional medicinal use of *S. ebulus* and to elucidate the biological relevance of its functional constituents through a multidisciplinary approach.

MATERIALS AND METHODS

Plant material and aqueous extract preparation

The fruits of *Sambucus ebulus* L. used in this study were collected from their natural habitat in the Hatila

Figure 1. *Sambucus ebulus* fruit and its natural habitat. A. Fruiting body of *Sambucus ebulus* growing in its native environment (Hatila Valley, Artvin, Türkiye). B. Fresh fruits of *Sambucus ebulus* collected for aqueous extract preparation prior to phytochemical and cytogenetic analysis.

Valley of Artvin province, located in northeastern Türkiye (41°09’18.0”N 41°44’16.0”E; 1300 m) (Figure 1). The botanical identification was conducted based on the *Flora of Turkey* (Davis 1970), and voucher specimens were deposited under the reference number Aksu 378B at the Artvin Çoruh University Medical and Aromatic Plants Application and Research Center.

For the preparation of the aqueous extract, a traditional method commonly used in folk practices was adopted. Accordingly, freshly collected fruits were carefully washed with tap water and left to drain overnight to remove excess moisture. Then, 40 grams of fresh fruit were ground with 2000 mL of tap water using a laboratory mill until a homogeneous mixture was obtained. The resulting crude extract was first filtered through muslin cloth, followed by filtration using Whatman No. 1 filter paper to obtain a clear aqueous extract.

Antioxidant activity

DPPH radical scavenging activity

The free radical scavenging capacity of the aqueous extract of *Sambucus ebulus* fruits was evaluated using the DPPH (2,2-diphenyl-1-picrylhydrazyl) assay, based on the procedure described by Molyneux (2004) with minor modifications. Briefly, 0.75 mL of the extract at various concentrations was mixed with 0.75 mL of 0.1 mM DPPH solution prepared in methanol. The mixture was vortexed and then incubated in the dark at room temperature for 50 minutes. After incubation, the absorbance was measured at 517 nm using a UV-Vis spectrophotometer. Trolox was used as the standard antioxidant. The scavenging activity was expressed as IC_{50} (mg/mL), which denotes the concentration of extract required to inhibit 50% of the DPPH radicals.

Ferric reducing antioxidant power (FRAP)

The ferric ion reducing capacity of the aqueous extract obtained from *Sambucus ebulus* fruits was determined based on the method originally described by Benzie and Strain (1996) and further refined by Prior et al. (2005). This assay is based on the principle that, under acidic conditions, antioxidants present in the extract reduce the ferric-tripyridyltriazine (Fe^{3+}-TPTZ) complex to its ferrous form (Fe^{2+}-TPTZ), resulting in the formation of an intense blue-colored complex. The intensity of the blue color, which directly correlates with the sample’s antioxidant reducing power, was measured spectrophotometrically at 593 nm. The FRAP values were expressed as milligrams of quercetin equivalent per gram of sample (mg QE/g), indicating the extract’s potential to reduce ferric ions.

Total flavonoid content (TFC)

The total flavonoid content in the aqueous extract of *Sambucus ebulus* fruits was quantified using a modified protocol adapted from Zhishen et al. (1999). This colorimetric method is based on the formation of flavonoid–aluminum chloride complexes. In particular, aluminum ions interact with the C-4 carbonyl and C-3 or C-5 hydroxyl groups of flavones and flavonols, forming stable complexes. Additionally, aluminum chloride may bind to ortho-dihydroxyl substitutions on the A or B rings, though these interactions are generally weaker. Quercetin was used as the reference compound for calibration, with standard solutions ranging from 0.03125 to 1.0 mg/mL. The absorbance of the resulting complexes was measured spectrophotometrically, and the total flavonoid content was expressed as milligrams of quercetin equivalent per gram of sample (mg QE/g).

High-performance liquid chromatography (HPLC) profiling of phenolic compounds

To achieve a comprehensive analysis of structurally diverse phenolic compounds, two different HPLC protocols were utilized, both employing the ACE 5 C18 column (250 × 4.6 mm, i.d.) to maintain consistency in stationary phase selectivity.

Method 1 was tailored to detect common phenolic acids and flavonols. The chromatographic separation employed a binary mobile phase system comprising (A) acetonitrile and (B) 1.5% aqueous acetic acid. The gradient began at 15% A and 85% B, progressively reaching 40% A and 60% B within 29 minutes. The chromatographic system included a 1260 DAD WR detector set at 250, 270, and 320 nm; a 1260 Quaternary Pump operating at a flow rate of 0.7 mL/min; a 1260 Vialsampler administering 10 μL injections; and a G7116A column oven maintained at 35 °C (Table 1).

Method 2 was configured to enhance the separation of phenolic compounds with extended conjugated systems or differing absorption profiles. It utilized a mobile phase composed of (A) methanol and (B) 1.5% aqueous acetic acid. The gradient began at 10% A and 90% B, shifted to 40% A and 60% B by 29 minutes, continued with 60% A and 40% B from 29 to 40 minutes, and ended with 90% A and 10% B from 40 to 53 minutes. Detection wavelengths were set at 280, 290, 320, 370, and 535

Table 1. Comparison of HPLC Method 1 and Method 2

Parameter	Method 1	Method 2
Mobile Phase A	Acetonitrile	Methanol
Mobile Phase B	1.5% Acetic Acid	1.5% Acetic Acid
Gradient Start	15% A / 85% B	10% A / 90% B
Gradient End	40% A / 60% B (at 29 min)	90% A / 10% B (40–53 min)
Run Time (min)	29	53
Detection Wavelengths (nm)	250, 270, 320	280, 290, 320, 370, 535
Flow Rate (mL/min)	0.7	0.7
Injection Volume (μL)	10	10
Column Temperature (°C)	35	35

nm. Flow rate, injection volume, and column temperature were kept identical to Method 1 (Table 1).

This two-method approach improved analytical reliability and allowed for a broader characterization of the phenolic profile by addressing the chemical heterogeneity of the target compounds.

HS-SPME-GC-MS analysis of volatile compounds

Volatile compound analysis was performed on the aqueous extract prepared from the plant material, which was transferred into headspace vials and tightly sealed with silicone/PTFE septa prior to HS-SPME. The analysis utilized the headspace-solid phase microextraction (HS-SPME) technique, employing an autosampler (PAL RSI, PAL System, Switzerland) equipped with a fiber coated with a composite sorbent layer of divinylbenzene/carbon wide range/polydimethylsiloxane (DVB/C-WR/PDMS, 80 μm).

Samples were pre-equilibrated by incubation at 50 °C for 10 minutes prior to fiber exposure to the headspace, followed by a 10-minute extraction period. Thermal desorption of analytes was achieved by directly inserting the fiber into the GC injection port under splitless mode and maintaining it for 10 minutes. This solvent-free approach allowed efficient capture and transfer of volatile molecules for chromatographic separation.

Gas chromatography was performed using an HP-5MS capillary column (30 m × 0.25 mm, 0.25 μm; Agilent Technologies) with helium as the carrier gas (1 mL/min). The injector operated in splitless mode. The oven temperature was programmed to begin at 50 °C (held for 5 min), then ramped at 3 °C/min to 220 °C, followed by a final isothermal step of 5 minutes. Ionization was conducted via electron impact (EI) at 70 eV, and the mass spectrometer acquired data over an m/z range of 30–500, with a scan rate of 3.1 scans per second.

Compound identification was based on comparison with entries in the NIST 14 (2014) spectral library (National Institute of Standards and Technology, Gaithersburg, MD, USA), with a match quality threshold of ≥85%. Retention indices (RI) were calculated and compared against established literature values for confirmation. Data acquisition and peak deconvolution were processed using Agilent's MassHunter Qualitative Analysis Workflows. Quantification of volatiles was performed by calculating the percentage of each peak area relative to the total ion chromatogram. Compound identifications were additionally verified by matching retention indices and spectral patterns with those of n-alkane standards.

Experimental design and application procedure

The meristematic cells of *Allium cepa* (onion, 2n = 16) roots were employed as a biological test system to evaluate morphological and structural alterations in the genetic material and to calculate mitotic indices. Prior to the experiment, the outer scales of the bulbs were carefully removed without damaging the root primordia. The bulbs were then placed in tap water at 22 °C in a dark environment to induce root germination.

For each treatment group, 10 bulbs were initially germinated. Once the root length reached 2–3 cm, five healthy bulbs exhibiting uniform root growth were randomly selected per group. These bulbs were exposed to aqueous extract solutions at different concentrations for 48 hours: 1%, 5%, 10%, 20%, and 50% (v/v, extract/tap water). In addition to the treatment groups, tap water was used as a negative control and a 680 mg/L zinc oxide (ZnO) solution served as the positive control. The ZnO concentration was selected based on previous studies demonstrating its cytotoxic and genotoxic effects in the *A. cepa* model (Kumari et al. 2011; Ghosh et al. 2016; Debnath et al. 2020). The 48-hour exposure period was determined based on the duration of the mitotic cycle in *A. cepa* (Boros and Ostafe 2020; Gupta and Kumar 2025). Following this exposure period, both morphological assessments for root growth inhibition and cytogenetic analyses were conducted to investigate genotoxicity indicators in detail.

Assessment of root growth inhibition

To determine the potential inhibitory effects of *Sambucus ebulus* fruit extract on the primary root development of *Allium cepa*, root length measurements were carried out after 48 hours of treatment. From each group – including the negative control (tap water), the positive control (680 mg/L ZnO solution), and the extract treatments (1%, 5%, 10%, 20%, and 50% v/v) – a total of 50 roots were randomly selected, with 10 roots taken from each of five bulbs. The root lengths were measured in millimeters and expressed as mean ± standard deviation (SD).

The percentage of root growth inhibition was calculated using the following formula:

Root Growth Inhibition (%) = (Mean root length of control group – Mean root length of treatment group) / Mean root length of control group × 100

This approach enabled a quantitative comparison of inhibitory effects across all treatment groups and revealed the dose-dependent biological response of *A. cepa* roots to the aqueous extract.

Cytogenetic evaluation

At the end of the treatment period, one root tip was randomly selected from each of the five bulbs in each group, resulting in five slides per treatment group. Root tips approximately 0.5–1 cm in length were excised and fixed in a 3:1 solution of 3% ethanol and 1% acetic acid for 24 hours. The fixed material was then hydrolyzed in 1 N HCl at 60 °C for 5 minutes and subsequently stained with Schiff's reagent to prepare it for cytogenetic analysis.

Microscopic examination was performed to evaluate three major cytogenetic parameters for each group: mitotic index (MI), micronucleus (MN) frequency in interphase cells, and chromosomal aberrations (CA) observed in dividing cells. These parameters were quantitatively assessed to determine the potential cytotoxic and genotoxic effects of the extract on cell division and genetic material, enabling comparative evaluation across the different concentration groups.

Statistical analysis

All antioxidant assays and *Allium cepa*-based cytogenetic evaluations were carried out in three independent replicates (n = 3). Results are expressed as mean ± standard deviation (SD). Statistical analyses were performed using SPSS software (version 22.0; IBM Corp., Armonk, NY, USA). To determine statistically significant differences among treatment groups, one-way analysis of variance (ANOVA) was applied. When significant differences were observed, Dunnett's post hoc test was used to identify the groups differing from the control. Prior to the ANOVA, data were assessed for normality using the Kolmogorov–Smirnov test and for homogeneity of variances using Levene's test. These tests verified that the assumptions for parametric analysis were met. Statistical significance was accepted at $p < 0.05$.

RESULTS AND DISCUSSION

Allium species are widely recognized as reliable biological model systems commonly used to evaluate the cytotoxic and genotoxic effects of plant-derived substances (Tedesco and Laughinghouse 2012, Bonciu et al. 2018; Sarac et al. 2019). In traditional medicine, plants are generally utilized in their entirety or with specific parts (such as leaves, roots, stems) without separation. Therefore, it is of great importance to evaluate the toxicological profiles of herbal products in a holistic manner. Moreover, it has been shown that the bioactive compounds in plants can exert stronger and synergistic effects when interacting with each other rather than acting individually (Tallarida 2011). This suggests that the biological efficacy of plant-based treatments often arises from compound–compound interactions (Rajčević et al. 2022).

In this study, the total flavonoid content (1.008 ± 0.02 mg QE/g), FRAP value (7.045 ± 0.08 mg TE/g), and DPPH radical scavenging activity (0.008 ± 0.30 mg/mL) of the fruit extract of *Sambucus ebulus* were measured (Table 2). Although the DPPH value was lower than the Trolox standard (0.0033 ± 0.00 mg/mL), the obtained IC_{50} value is consistent with those reported for aqueous *Sambucus* species in the literature (Pietta et al. 1998; Rodino et al. 2015). Considering that the aqueous extract is aligned with traditional methods of use (infusion, decoction), the values obtained can be considered biologically relevant. However, studies have reported that methanolic and ethanolic extracts of *S. ebulus* exhibit higher antioxidant activity in DPPH and FRAP assays (Pietta et al. 1998; Meriç et al. 2014; Rodino et al. 2015). In the studies conducted by ; Pietta et al. (1998) and

Table 2. Antioxidant activity and flavonoid content of *Sambucus ebulus* extract

Parameter	Value (Mean ± SD)
Total Flavonoid Content (mg QE/g)	1.008 ± 0.02
Ferric Reducing Antioxidant Power (FRAP) (mg QE/g)	7.045 ± 0.08
DPPH Radical Scavenging Activity (IC_{50} Inhibition-mg/ml)	0.008 ± 0.30
Standard (IC50 DPPH Inhibition (mg/ml)	0.0033±0.00

Table 3. HPLC profile of phenolic constituents in the aqueous extract of *Sambucus ebulus.*

No	Compounds	(mg/L)
Vitamin		
1	L-Ascorbic acid	94.98
Phenolics		
2	Gallic acid	135.4
3	3,4-Dihydroxy benzoic acid	53.1
4	Vanillic acid	N/D
5	Syringic acid	N/D
6	p-Coumarıc Acid	N/D
7	Trans-Caffeic acid	46.69
8	Ferulic acid	
9	Rosmarinic acid	3.89
10	Pyrogallol	6.48
11	Chlorogenic acid	89.58
12	Resveratrol	N/D
13	Oleuropein	N/D
Flavonoids		
14	(+)-Catechin	142.86
15	(-)-Epicatechin	398.29
16	Rutin	0.5
17	Myricetin	N/D
18	Quercetin	N/D
19	Apigenin	N/D
20	Cyanidin chloride	N/D
21	Hesperitin	N/D
22	Kaempferol	N/D
23	Baicalien	N/D
24	Chrysin	N/D

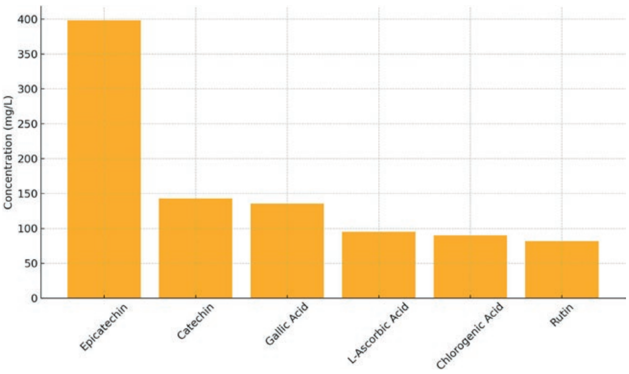

Figure 2. Bar chart illustrating the major phenolic compounds detected in the aqueous extract of *Sambucus ebulus* via HPLC analysis.

Rodino et al. (2015), DPPH inhibition levels of methanolic extracts were found to reach 80–90%, while aqueous extracts generally ranged between 40–60%. This has been attributed to the better solubility of polyphenols and flavonoids in organic solvents. Similar trends have also been reported for *S. nigra* and *S. canadensis* species (Sidor and Gramza-Michałowska 2015; Januškevičė et al. 2025). Ethanolic and acetonic extracts obtained from the fruits and flowers of *S. nigra* were shown to be associated with high phenolic content and strong antioxidant activity (Sidor and Gramza-Michałowska 2015; Januškevičė et al. 2025). Although interspecies differences are to be considered, the current findings support that *S. ebulus* is a strong natural antioxidant source.

It is well established that antioxidants not only have chemical potential but also exert cytogenetic effects at the cellular level. Reactive oxygen species (ROS) can lead to DNA damage, chromosomal abnormalities, and mitotic disturbances, while antioxidants may prevent such harmful effects (Meriç et al., 2014; Sidor and Gramza-Michałowska 2015; Kayıran et al. 2022; Januškevičė et al. 2025). Therefore, it is presumed that the antioxidant capacity of the aqueous extract used in this study may be effective in reducing chromosomal damage or preserving mitotic activity. Supporting this assumption, Meriç et al. (2014) reported that the high phenolic content and DPPH activity in the methanolic extract of *S. ebulus* were associated with non-cytotoxic but potentially anticarcinogenic effects. Similarly, Rodino et al. (2015) demonstrated strong anti-oxidative stress effects with high FRAP (1725.5 ± 9.8 µmol Fe^{2+}/g) and DPPH (85.3 ± 0.2%) values in *S. ebulus* fruit extract.

HPLC analyses revealed that the extract contains significant phenolic compounds such as epicatechin (398.29 mg/L), catechin (142.86 mg/L), gallic acid (135.4 mg/L), chlorogenic acid (89.58 mg/L), L-ascorbic acid (94.98 mg/L), and rutin (81.43 mg/L) (Table 3, Figure 2). According to the literature, flavonoids such as epicatechin and catechin are known to be involved in processes related to cell cycle regulation and the enhancement of mitotic activity (Alimullah et al. 2025; Aljuhaimi et al. 2025; Sancer et al. 2025; Uslu et al. 2025;). Therefore, it is plausible that these compounds may exert beneficial effects on cytogenetic parameters. Phenolic acids like

Table 4. Volatile compounds identified in the aqueous extract of *Sambucus ebulus* fruits by HS-SPME-GC-MS technique.

No	RT (min)	RI	Name of the compound	Content [%]
1	3.891	650	Butanal, 3-methyl-	4.162
2	4.329	716	Pentanal	1.285
3	5.899	790	Methyl isovalerate	24.848
4	6.501	812	Hexanal	3.611
5	6.775	821	Butanoic acid, 3-methyl-, ethyl ester	10.544
6	7.095	830	Butanoic acid, 3-methyl-	4.775
7	8.209	827	Isovaleric acid, ethyl ester	25.277
8	14.344	1016	o-Cymene	7.486
9	14.575	1021	trans-.beta.-Ocimene	14.421
10	16.329	1059	gamma.-Terpinene	3.591

Table 5. Effect of *Sambucus ebulus* aqueous extract on root growth in *Allium cepa*.

Treatments	Examined root number	Root length (mm) (Mean±SD)	Inhibition (%)
Negative control	50	61.84±7.96	-
Positive control	50	10.02±5.53*	83.78
1%	50	41.93±6.00	32.18
5%	50	46.76±6.09	27.61
10%	50	49.31±5.89	20.27
20%	50	31.29±6.34*	23.23
50%	50	23.92±5.26*	61.32

*Significant at $p<0.05$.

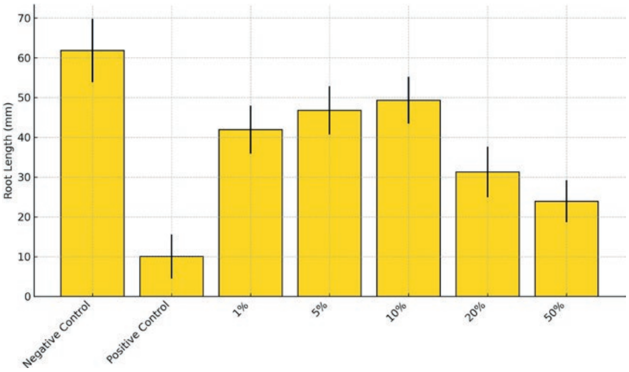

Figure 3. Effect of *Sambucus ebulus* fruit extract on root elongation in *Allium cepa* after 48 hours of treatment. Root lengths (mean ± SD) are shown for negative control (tap water), positive control (ZnO, 680 mg/L), and extract-treated groups at 1%, 5%, 10%, 20%, and 50% concentrations (v/v).

gallic acid and chlorogenic acid have also been identified as bioactive molecules with potential roles in reducing DNA damage and maintaining chromosomal integrity. In this context, Amić et al. (2025) and Signorini et al. (2025) have reported that these compounds might contribute to the preservation of genetic material by mitigating oxidative DNA damage. Furthermore, L-ascorbic acid is not only a potent antioxidant but also has been associated with regulatory functions in the cell cycle Shams (Shams El Dine et al. 2025). The presence of this compound in the extract may help explain the observed regulatory effects on mitotic activity. The coexistence of these compounds is likely to enhance the overall antioxidant capacity of the extract and may promote synergistic interactions, further supporting its biological efficacy (Tallarida 2011).

According to GC-MS analysis, more than 95% of the volatile profile consisted of compounds such as ethyl isovalerate, methyl isovalerate, and trans-β-ocimene (Table 4). These volatiles have been linked in the literature to antioxidant, anti-inflammatory, and membrane-regulating properties (Calva et al. 2025; Jaishi et al. 2025; Otto et al. 2025). In addition, o-cymene and butanoic acid derivatives have been reported to enhance bioactivity through interactions with cellular membranes (Dorman and Deans 2000). This chemical diversity suggests that the extract may possess a biological potential capable of supporting cytogenetic activity (Rajčević et al. 2022).

The dose-dependent cytogenetic effects of the extract were revealed through analyses of root elongation, mitotic index (MI), chromosomal abnormalities, and micronucleus formation. The effect of the aqueous extract of Sambucus ebulus on root elongation was observed in the negative control group, where the highest mean root length (61.84 ± 7.96 mm) was recorded. This result indicates that mitotic activity proceeded normally and that there was no impairment in cellular proliferation. In contrast, in the positive control group (ZnO treatment), a significant reduction in root length (10.02 ± 5.53 mm) was detected, confirming the test's sensitivity to toxic agents with an inhibition rate of 83.78% (Table 5, Figure 3).

Among the extract-treated groups, a dose-dependent inhibition of root growth was observed as extract concentration increased. Notably, 50% (23.92 ± 5.26 mm) and 20% (31.29 ± 6.34 mm) concentrations resulted in significant reductions in root length with inhibition rates of 61.32% and 23.23%, respectively (Table 5, Figure 3). These effects were statistically significant compared to the negative control, suggesting that the extract contains bioactive compounds capable of affecting cell division and elongation processes (Chauhan et al. 1999; Murthy et al. 2011).

However, the relatively low inhibition rates observed at moderate concentrations (1% to 10%) and the nonlin-

Table 6. Effects of *Sambucus ebulus* aqueous extract on mitotic index and distribution of dividing cells at different stages in *Allium cepa* root meristem cells.

Treatments	Examined Cell Number	MI±SD	Total number of cells at prophase	Total number of cells at metaphase	Total number of cells at anaphase	Total number of cells at telophase
Negative control	5000	7.71±1.07	440	200	60	110
Positive control	5000	2.24±0.04*	170	120	50	40
1%	5000	4.98±0.50	360	70	60	30
5%	5000	5.26±0.90	430	60	70	30
10%	5000	6.55±3.16	330	180	70	80
20%	5000	2.56±0.39*	200	90	60	20
50%	5000	2.57±0.10*	170	140	70	2

*Significant at *p*<0.05.

ear response between 10% and 20% suggest that some compounds may exhibit hormetic effects at low doses or may activate non-cytotoxic mechanisms (Chauhan et al., 1999; Murthy et al. 2011). Previous studies have also reported that plant extracts rich in polyphenols and terpenoids may inhibit root growth in *A. cepa* by disrupting mitotic spindle formation and interfering with cell wall synthesis (Leme and Marin-Morales 2009; Celik 2012).

The effect on mitotic activity was assessed by considering MI values and the distribution of cells at different mitotic stages in *A. cepa* root meristem tissue. The high MI value observed in the negative control group (7.71 ± 1.07%) indicates that the mitotic process functioned physiologically without disruption. In contrast, the MI in the ZnO-treated positive control group decreased significantly to 2.24 ± 0.04% ($p < 0.05$), confirming that ZnO inhibits mitosis and that the Allium test is a reliable model for detecting cytotoxic effects (Table 6).

In the extract-treated groups, MI values varied depending on the applied concentration. At low concentrations (1%, 5%, and 10%), MI was determined as 4.98 ± 0.50%, 5.26 ± 0.90%, and 6.55 ± 3.16%, respectively (Table 6). These values were significantly higher than those of the positive control group, suggesting that these doses did not suppress mitotic activity and may even support limited proliferation. This aligns with the concept of hormesis, which posits that certain natural compounds can stimulate cellular responses at low doses (Calabrese and Baldwin 2003). However, at higher concentrations (20%: 2.56 ± 0.39%; 50%: 2.57 ± 0.10%), MI values dropped to levels comparable to the positive control, indicating that these doses markedly suppressed cell division.

MI values changed inversely with concentration, with lower doses supporting mitotic activity, while significant reductions in MI were observed in the 20% and 50% groups. This decline may be explained by the ability of phenolic acids and volatile terpenes to inhibit mitosis at the G2/M phase (Akaneme and Amaefule 2012; Yıldız et al. 2025).

Chromosomal abnormalities, particularly C-mitosis, chromosome stickiness, and bridge formation, increased markedly at higher doses. Similarly, micronucleus frequencies showed significant increases at 20% and 50% concentrations, while these effects remained minimal in the 1–10% groups. These findings indicate that genotoxic effects are dose-threshold dependent and that cell division is not impaired at low concentrations (Calabrese and Baldwin, 2003; Ždralović et al. 2019; Smirnova and Korovkina 2021).

Structural anomalies commonly observed in the positive control group – particularly C-mitosis, chromosome stickiness, and chromatid bridges – were also detected in the high-dose extract treatment groups. For example, in the 50% extract group, the frequency of C-mitosis (7.33 ± 0.00), bridge formation (4.00 ± 1.41), and chromosome stickiness (3.17 ± 0.32) were considerably high (Table 7, Figure 4). These anomalies are associated with disruptions in the formation of mitotic spindle fibers during the metaphase–anaphase transition (Yüzbaşıoğlu et al. 2003; Smirnova and Korovkina 2021).

In contrast, a lower number of abnormal cells were observed in the extract treatments administered at low and moderate concentrations, and structural abnormalities generally remained at a mild level. This dose-dependent trend suggests that increasing extract concentration enhances genotoxic stress and exacerbates chromosomal damage. Particularly in the 20% and 50% groups, the total numbers of abnormal cells were recorded as 11.50 ± 0.71 and 21.00 ± 1.02, respectively (Table 7).

The formation of C-mitosis indicates the presence of agents that disrupt spindle fiber development, whereas chromosome stickiness may hinder the proper segregation of chromosomes, potentially leading to mitotic arrest (Asita et al. 2021; Pharmawati et al. 2022). Bridges and lagging chromosomes are mitotic anomalies result-

Table 7. Types of the chromosomal aberrations in *Allium cepa* root tip after application of *Sambucus ebulus* extract at different concentrations.

Treatments	Disturbed prophase	Chromosome stickness	C-mitosis	Chromatid bridge	Laggard chromosome	Vagrant chromosome	Total abberant cells
Negative control	-	0.33±0.52	-	0.67±0.02	-	-	1.00±0.21
Positive control	4.00±0.41	4.83±1.06	9.00±0.00	6.67±0.05	0.50±0.06	2.50±0.71	27.50±0.71*
1%	-	0.50±0.14	1.00±0.03	0.50±0.51	-	1.00±0.31	3.00±1.1
5%	0.67±0.01	0.33±0.02	-	0.50±0.01	-	1.50±0.11	3.00±0.7
10%	-	0.78±1.20	0.33±0.58	1.56±0.02	-	-	2.67±0.1
20%	-	4.00±0.43	2.50±0.71	3.50±0.60	-	1.50±0.41	11.50±0.71*
50%	2.50±0.71	3.17±0.32	7.33±0.00	4.00±1.41	-	4.00±1.01	21.00±1.02*

*Significant at p<0.05.

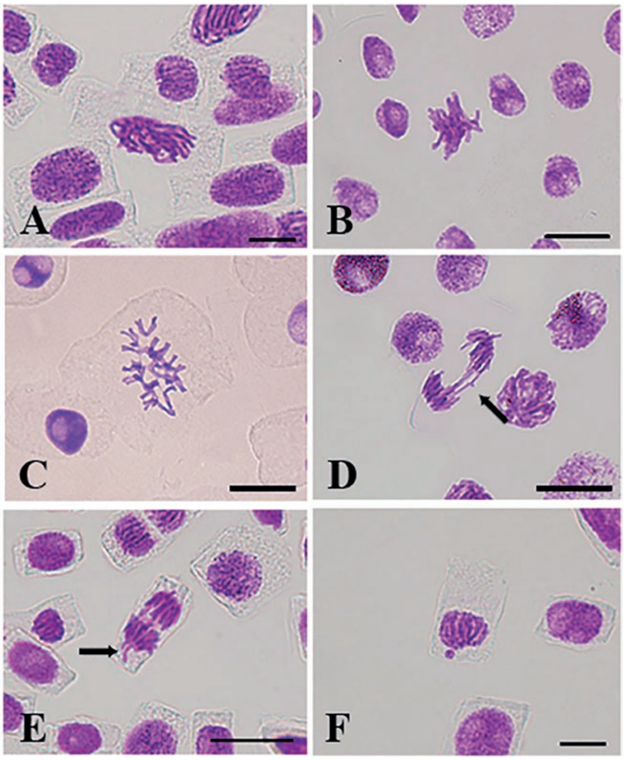

Figure 4. Representative mitotic abnormalities observed in *Allium cepa* root meristem cells with aqueous *Sambucus ebulus* extract. A. Irregular prophase configuration; B. Chromosome adhesion (stickiness); C. C-mitosis indicative of spindle apparatus disruption; D. Chromatin bridge during anaphase; E. Vagrant chromosome; F. Micronucleus formation. All images include scale bars corresponding to 20 µm.

Table 8. Frequency of micronucleus formation in *Allium cepa* root tip cells after application of *Sambucus ebulus* extract at different concentrations.

Treatments	Examined Cell Number	Micronucleus (%)
Negative control	5000	-
Positive control	5000	1.35±0.02*
1%	5000	0.05±0.01
5%	5000	0.05±0.01
10%	5000	-
20%	5000	0.45±0.07*
50%	5000	1.05±0.02*

*Significant at p<0.05.

ing from improper chromosome separation toward the poles and are commonly associated with DNA strand breaks or replication errors (Leme and Marin-Morales 2009; Asita et al. 2021).

The obtained micronucleus (MN) data indicate that the *Sambucus ebulus* fruit extract may exhibit genotoxic potential at high concentrations, whereas its effects remain minimal at lower concentrations (Table 8). Statistically significant increases in MN frequency were observed particularly in the 20% and 50% treatment groups, indicating that these doses may induce DNA damage and genomic instability. However, in the 1% and 5% extract groups, MN frequencies remained similar to those of the negative control, and no micronucleus formation was detected at the 10% concentration (Table 8). These findings point to the possibility of a hormetic response, suggesting that the extract does not impair cytogenetic stability below a certain threshold concentration (Calabrese and Baldwin, 2003).

CONCLUSION

This study demonstrates that the aqueous extract obtained from the fruits of *Sambucus ebulus* exhibits notable antioxidant and cytogenetic effects through its bioactive compounds. While applications at low concentrations displayed supportive effects on cellular antioxidant defense and preservative effects on mitotic activity, higher concentrations led to suppression of the cell cycle and structural damage to the genetic material. These findings indicate that compounds such as phenolic acids and volatile terpenes may elicit different biological responses depending on their concentration and interaction level (Sultan and Çelik 2009; Smirnova and Korovkina 2021; Pharmawati et al. 2022). Considering that *S. ebulus* is widely used in traditional medicine for immunomodulatory, anti-inflammatory, and antiviral purposes, the aim of this study is not to label the plant as harmful, but rather to draw attention to the potential cytogenetic risks associated with concentrations exceeding certain threshold doses. In particular, concentrations at or below 10%, where no micronucleus formation was observed, provide preliminary data that could serve in defining safe usage ranges for the aqueous extract of *Sambucus ebulus*. The results reveal that *S. ebulus*, with its rich profile of bioactive compounds, has the potential to modulate cell proliferation and genetic stability; they also emphasize the necessity of carefully determining dose ranges for safe and effective use.

REFERENCES

Akaneme FI, Amaefule CC. 2012. Evaluation of the cytotoxicity and genotoxicity of aqueous leaf extracts of *Azadirachta indica* A. Juss using the *Allium* test. *Journal of Medicinal Plants Research.* 6(22):3898–3907.

Alimullah M, Jahan I, Rahman MM, Khan F, Ahmed KS, Hossain MH, Subhan N. 2025. *Camellia sinensis* powder rich in epicatechin and polyphenols attenuates isoprenaline-induced cardiac injury by activating the Nrf2–HO1 antioxidant pathway in rats. *Scientific Reports.* 15:20859. https://doi.org/10.1038/s41598-025-08720-w

Aljuhaimi F, Uslu N, Özcan MM, Ahmed IAM, Walayat N. 2025. Investigation of changes in the bioactive properties and phenolic compositions of different layers of the leek plant. *Acta Scientiarum Polonorum Technologia Alimentaria.* 24:447–456.

Amić A, Milanović Ž, Cagardová DM. 2025. Protective roles of α-tocopherol, α-CEHC, and gallic acid against $CO_3^{\bullet -}$-induced DNA damage and their effect on OGG1 and pro-oxidant enzymes. *Journal of Molecular Liquids.* 438:128847. https://doi.org/10.1016/j.molliq.2025.128847

Asita AO, Maga-ma S, Moahloli TM, Baholo S. 2021. Evaluation of extracts of wild *Cannabis sativa* L. for genotoxicity and phytochemical composition. *Caryologia.* 74(1):135–150.

Barak TH, Celep E, İnan Y, Yeşilada E. 2020. *In vitro* human digestion simulation of the bioavailability and antioxidant activity of phenolics from *Sambucus ebulus* L. fruit extracts. *Food Bioscience.* 37:100711. https://doi.org/10.1016/j.fbio.2020.100711

Benzie IFF, Strain JJ. 1996. The ferric reducing ability of plasma (FRAP) as a measure of “antioxidant power”: the FRAP assay. Analytical Biochemistry. 239:70–76. https://doi.org/10.1006/abio.1996.0292

Boros BV, Ostafe V. 2020. Evaluation of ecotoxicology assessment methods of nanomaterials and their effects. *Nanomaterials.* 10:610. https://doi.org/10.3390/nano10040610

Brasil. Ministério da Saúde. Secretaria de Ciência, Tecnologia e Insumos Estratégicos. 2006. Política Nacional de Plantas Medicinais e Fitoterápicos. Brasília (Brazil): Editora MS.

Bonciu E, Firbas P, Fontanetti CS, Wusheng J, Karaismailoğlu MC, Liu D, et al. 2018. An evaluation for the standardization of the *Allium cepa* test as cytotoxicity and genotoxicity assay. *Caryologia.* 71(3):191–209. https://doi.org/10.1080/00087114.2018.1503496

Calabrese EJ, Baldwin LA. 2003. Hormesis: the dose-response revolution. *Annual Review of Pharmacology and Toxicology.* 43(1):175–197. https://doi.org/10.1146/annurev.pharmtox.43.100901.140223

Calva J, Cuenca MB, León A, Benítez Á. 2025. Chemical composition, acetylcholinesterase-inhibitory potential and antioxidant activity of essential oils from three populations of *Parthenium hysterophorus* L. in Ecuador. *Molecules.* 30:2712. https://doi.org/10.3390/molecules30132712

Chauhan LKS, Saxena PN, Gupta SK. 1999. Cytogenetic effects of cypermethrin and fenvalerate on the root meristem cells of *Allium cepa*. *Environmental and Experimental Botany.* 42:181–189. https://doi.org/10.1016/S0098-8472(99)00033-7

Celik TA. 2012. Potential genotoxic and cytotoxic effects of plant extracts. In: *A compendium of essays on alternative therapy.* p. 233–250.

Davis PH. 1970. *Flora of Turkey and the East Aegean Islands.* Edinburgh (UK): Edinburgh University Press.

Debnath P, Mondal A, Sen K, Mishra D, Mondal NK. 2020. Genotoxicity study of nano Al_2O_3, TiO_2 and ZnO along with UV-B exposure: an *Allium cepa* root tip assay. *Science of the Total Environment.* 713:136592. https://doi.org/10.1016/j.scitotenv.2020.136592

Dorman HD, Deans SG. 2000. Antimicrobial agents from plants: antibacterial activity of plant volatile oils. *Journal of Applied Microbiology.* 88(2):308–316.

Shams El Dine RS, Youseef HT, Awaad AK, Hammoury SI, Mohamed EI. 2025. The potentially therapeutic effects of ascorbic acid in different cell lines in an attempt to reduce the risk of radiation therapy. *Scientific Reports.* 15:15077. https://doi.org/10.1038/s41598-025-96697-x

Ghosh M, Jana A, Sinha S, Jothiramajayam M, Nag A, Chakraborty A, et al. 2016. Effects of ZnO nanoparticles in plants: cytotoxicity, genotoxicity, deregulation of antioxidant defenses, and cell-cycle arrest. *Mutation Research/Genetic Toxicology and Environmental Mutagenesis.* 807:25–32. https://doi.org/10.1016/j.mrgentox.2016.07.006

Gupta S, Kumar A. 2025. Cytogenetic analysis of mitotic cell cycle phases in *Allium cepa* root meristem: a model for chromosomal behaviour and environmental toxicity assessment. *International Internal Medicine Journal.* 3:1–5.

Hister CAL, Boligon AA, Laughinghouse HD IV, Tedesco SB. 2017. Determination of phenolic compounds and assessment of the genotoxic and proliferative potential of *Psidium cattleianum* Sabine (Myrtaceae) fruits. *Caryologia.* 70:350–356. https://doi.org/10.1080/00087114.2017.1360571

Jaishi DR, Ojha I, Ojha SR, Pal P, Thalal B, Chaudhary PN. 2025. Extraction, chemical composition, antioxidant, and antibacterial activities of essential oil using aerial parts of *Artemisia indica. Journal of the Nepal Chemical Society.* 45:34–44. https://doi.org/10.3126/jncs.v45i2.82974

Januškevičė V, Saunoriūtė S, Ondrášek I, Petrikaitė V, Štreimikytė P, Liaudanskas M, Česonienė L. 2025. Biochemical diversity and anticancer potential of phenolic compounds in *Sambucus nigra* L. cultivars. *Applied Food Research.* 5:101404. https://doi.org/10.1016/j.afres.2025.101404

Kayıran SD, Özkan EE, Kara EM, Tarı Ö, Nenni M. 2022. Determination of the chemical composition and antioxidant potential of *Sambucus ebulus* L. (dwarf elder) fruit extracts and investigation of antimicrobial activity on *Trichophyton rubrum* (Castell.) Sabour and some microorganisms. *Istanbul Journal of Pharmacy.* 52(2):148–155. https://doi.org/10.26650/IstanbulJPharm.2022.929762

Kumari M, Khan SS, Pakrashi S, Mukherjee A, Chandrasekaran N. 2011. Cytogenetic and genotoxic effects of zinc oxide nanoparticles on root cells of *Allium cepa. Journal of Hazardous Materials.* 190(1–3):613–621. https://doi.org/10.1016/j.jhazmat.2011.03.095

Leme DM, Marin-Morales MA. 2009. Allium test in monitoring. *Mutation Research.* 682:71–81. https://doi.org/10.1016/j.mrrev.2009.06.002

Martins ER, Castro DM, Castellani DC, Dias JE. 2003. Plantas medicinais. Viçosa (Brazil): Editora UFV.

Meriç Z, Bitiş L, Tan SB, Turan SÖ, Akbuğa J. 2014. Antioxidant, antimicrobial and anticarcinogenic activities of *Sambucus ebulus* L. flowers, fruits and leaves. *Marmara Pharmaceutical Journal.* 18(1):22–25.

Mohan AR, Joseph N. 2024. Cytotoxic assessment of aqueous extracts of *Heliotropium keralense* Sivar. & Manilal on *Allium cepa* root tip cells. *Caryologia.* 77(2):29–36. https://doi.org/10.36253/caryologia-2436

Molyneux P. 2004. The use of the stable free radical diphenylpicrylhydrazyl (DPPH) for estimating antioxidant activity. *Songklanakarin Journal of Science and Technology.* 26:211–219.

Murthy GS, Francis TP, Singh CR, Nagendra HG, Naik C. 2011. An assay for screening anti-mitotic activity of herbal extracts. *Current Science.* 100:1399–1404. https://www.jstor.org/stable/24076606

National Institute of Standards and Technology (NIST). 2014. *NIST/EPA/NIH mass spectral library.* Version 14. Gaithersburg (MD, USA): National Institute of Standards and Technology.

Otto P, Ninkovic V, Meiners T, Pashalidou FG, Fortuna TM, Louis J, Cusumano A. 2025. Multifunctionality of plant VOCs in agroecological systems: perspectives for biological pest control. *Entomologia Generalis.* https://doi.org/10.1127/entomologia/3506

Pharmawati M, Wirasiti NN, Wrasiati LP. 2022. Genotoxic and antigenotoxic potential of encapsulated *Enhalus acoroides* (L. f.) Royle leaves extract against nickel nitrate. *Caryologia.* 75(2):89–99.

Pietta P, Simonetti P, Mauri P. 1998. Antioxidant activity of selected medicinal plants. *Journal of Agricultural and Food Chemistry.* 46:4487–4490. https://doi.org/10.1021/jf980310p

Prior RL, Wu X, Schaich K. 2005. Standardized methods for the determination of antioxidant capacity. *Journal of Agricultural and Food Chemistry.* 53:4290–4302. https://doi.org/10.1021/jf0502698

Rajčević N, Bukvički D, Dodoš T, Marin PD. 2022. Interactions between natural products – a review. *Metabolites.* 12:1256. https://doi.org/10.3390/metabo12121256

Rank J, Nielsen MH. 1994. Evaluation of the *Allium* anaphase–telophase test in relation to genotoxicity screening of industrial wastewater. *Mutation Research.* 312:17–24. https://doi.org/10.1016/0165-1161(94)90004-3

Rodino S, Butu A, Petrache P, Butu M, Dinu-Pîrvu CE, Cornea CP. 2015. Evaluation of the antimicrobial and antioxidant activity of *Sambucus ebulus* extract. *Farmacia.* 63:751–754.

Sancer O, Tepebaşı MY, Şahin U, İlhan İ. 2025. Uncovering the benefits of epicatechin for oxidative stress in human health. *Süleyman Demirel University Journal of Health Sciences.* 16:75–81. https://doi.org/10.22312/sdusbed.1539732

Sarac I, Bonciu E, Butnariu M, Petrescu I, Madosa E. 2019. Evaluation of the cytotoxic and genotoxic potential of some heavy metals by use of *Allium* test. *Caryologia.* 72(2):37–43.

Shams El Dine RS, Youseef HT, Awaad AK, Hammoury SI, Mohamed EI. 2025. The potentially therapeutic effects of ascorbic acid in different cell lines in an attempt to reduce the risk of radiation therapy. *Scientific Reports.* 15:15077. https://doi.org/10.1038/s41598-025-96697-x

Sidor A, Gramza-Michałowska A. 2015. Advanced research on the antioxidant and health benefit of elderberry (*Sambucus nigra*) in food – a review. *Journal of Functional Foods.* 18:941–958. https://doi.org/10.1016/j.jff.2014.07.012

Signorini C, Corsaro R, Collodel G, Maettner R, Sterzik K, Strehler E, Moretti E. 2025. Addition of chlorogenic acid to human semen: effects on sperm motility, DNA integrity, oxidative stress, and Nrf2 expression. *Antioxidants.* 14:382. https://doi.org/10.3390/antiox14040382

Smirnova MV, Korovkina AV. 2021. Toxic and genotoxic effects of aqueous extracts of *Polygonum weyrichii* Fr. Schmidt on the *Allium* test taken as an example. *Caryologia.* 74(2):79–88.

Sousa C, Silva R, Costa J, Figueiredo N, Oliveira A, Santos D, Almeida M. 2018. *In vivo* assessment of cyto/genotoxic, antigenotoxic and antifungal potential of *Costus spiralis* (Jacq.) Roscoe leaves and stems. *Biocatalysis and Agricultural Biotechnology.* 14:135–143. https://doi.org/10.1016/j.bcab.2018.02.007

Sultan AÖ, Çelik TA. 2009. Genotoxic and antimutagenic effects of *Capparis spinosa* L. on the *Allium cepa* L. root tip meristem cells. *Caryologia.* 62(2):114–123.

Tallarida RJ. 2011. Quantitative methods for assessing drug synergism. *Genes & Cancer.* 2(11):1003–1008. https://doi.org/10.1177/194760191244057.

Tedesco SB, Laughinghouse HD IV. 2012. Bioindicator of genotoxicity: the *Allium cepa* test. In: Srivastava JK, editor. *Environmental contamination*. Rijeka (Croatia): InTech. p. 137–156. https://doi.org/10.5772/35355

Tedesco M, Kuhn AW, Boligon AA, Laughinghouse HD IV, Athayde ML, Silva ACS, Tedesco SB. 2015. Chromatographic analysis, antiproliferative effect and genotoxicity of aqueous extracts of *Citrus sinensis* (L.) Osbeck on the *Allium cepa* L. test system. *Bioscience Journal.* 31:1213–1221.

Teixeira RO, Camparoto ML, Mantovani MS, Vicentini VEP. 2003. Assessment of two medicinal plants, *Psidium guajava* L. and *Achillea millefolium* L., *in vitro* and *in vivo* assays. *Genetics and Molecular Biology.* 26:551–555. https://doi.org/10.1590/S1415-47572003000400021

Trapp KC, Hister CAL, Laughinghouse HD IV, Boligon AA, Tedesco SB. 2020. Determination of phenolic compounds and evaluation of cytotoxicity in *Plectranthus barbatus* using the *Allium cepa* test. *Caryologia.* 73(2):145–153.

Tuna-Gülören Ö, Korkmaz F, Erdir M, Ataşlar E. 2021. Cytotoxic and genotoxic effects of methanol extracts of vegetative parts of some *Gypsophila* L. species using *Allium cepa* assay. *Caryologia.* 74(2):141–148.

Uslu K, Çavuşoğlu K, Yalçın E. 2025. Quantitative phenolic profiling and protective effects of grape seed extract on mancozeb-induced cellular and genetic toxicity. *Scientific Reports.* 15:36249. https://doi.org/10.1038/s41598-025-20204-5

Yeşilada E, Gürbüz İ, Toker G. 2014. Anti-ulcerogenic activity and isolation of the active principles from *Sambucus ebulus* L. leaves. *Journal of Ethnopharmacology.* 153:478–483. https://doi.org/10.1016/j.jep.2014.03.004

Yıldız E, Meredova G, Aksoy H. 2025. The genoprotective role of *Laurocerasus officinalis*: study on genotoxic/antigenotoxic and cytotoxic/anticytotoxic effects in human lymphocytes. *Journal of Food Biochemistry.* 2025:7455954. https://doi.org/10.1155/jfbc/7455954

Yüzbaşıoğlu D, Ünal F, Sancak C, Kasap R. 2003. Cytological effects of the herbicide racer "flurochloridone" on *Allium cepa*. *Caryologia.* 56(1):97–105.

Ždralović A, Mešić A, Eminović I, Parić A. 2019. Cytotoxic and genotoxic activity of *Plantago major* L. extracts. *Caryologia.* 72(3):35–40.

Zhishen J, Mengcheng T, Jianming W. 1999. The determination of flavonoid contents in mulberry and their scavenging effects on superoxide radicals. *Food Chemistry.* 64:555–559. https://doi.org/10.1016/S0308-8146(98)00102-2

OPEN ACCESS POLICY

Caryologia provides immediate open access to its content. Our publisher, Firenze University Press at the University of Florence, complies with the Budapest Open Access Initiative definition of Open Access: By “open access” , we mean the free availability on the public internet, the permission for all users to read, download, copy, distribute, print, search, or link to the full text of the articles, crawl them for indexing, pass them as data to software, or use them for any other lawful purpose, without financial, legal, or technical barriers other than those inseparable from gaining access to the internet itself. The only constraint on reproduction and distribution, and the only role for copyright in this domain is to guarantee the original authors with control over the integrity of their work and the right to be properly acknowledged and cited. We support a greater global exchange of knowledge by making the research published in our journal open to the public and reusable under the terms of a Creative Commons Attribution 4.0 International Public License (CC-BY-4.0). Furthermore, we encourage authors to post their pre-publication manuscript in institutional repositories or on their websites prior to and during the submission process and to post the Publisher’s final formatted PDF version after publication without embargo. These practices benefit authors with productive exchanges as well as earlier and greater citation of published work.

PUBLICATION FREQUENCY

Papers will be published online as soon as they are accepted, and tagged with a DOI code. The final full bibliographic record for each article (initial-final page) will be released with the hard copies of *Caryologia*. Manuscripts are accepted at any time through the online submission system.

COPYRIGHT NOTICE

Authors who publish with *Caryologia* agree to the following terms:

- Authors retain the copyright and grant the journal right of first publication with the work simultaneously licensed under a Creative Commons Attribution 4.0 International Public License (CC-BY-4.0) that allows others to share the work with an acknowledgment of the work's authorship and initial publication in Caryologia.
- Authors are able to enter into separate, additional contractual arrangements for the non-exclusive distribution of the journal's published version of the work (e.g., post it to an institutional repository or publish it in a book), with an acknowledgment of its initial publication in this journal.
- Authors are permitted and encouraged to post their work online (e.g., in institutional repositories or on their website) prior to and during the submission process, as it can lead to productive exchanges, as well as earlier and greater citation of published work (See The Effect of Open Access).

PUBLICATION FEES

Open access publishing is not without costs. *Caryologia* therefore levies an article-processing charge of € 150.00 for each article accepted for publication, plus VAT or local taxes where applicable.

We routinely waive charges for authors from low-income countries. For other countries, article-processing charge waivers or discounts are granted on a case-by-case basis to authors with insufficient funds. Authors can request a waiver or discount during the submission process.

PUBLICATION ETHICS

Responsibilities of *Caryologia*'s editors, reviewers, and authors concerning publication ethics and publication malpractice are described in *Caryologia*’s Guidelines on Publication Ethics.

CORRECTIONS AND RETRACTIONS

In accordance with the generally accepted standards of scholarly publishing, *Caryologia* does not alter articles after publication: "Articles that have been published should remain extant, exact and unaltered to the maximum extent possible".

In cases of serious errors or (suspected) misconduct *Caryologia* publishes corrections and retractions (expressions of concern).

Corrections

In cases of serious errors that affect or significantly impair the reader’s understanding or evaluation of the article, *Caryologia* publishes a correction note that is linked to the published article. The published article will be left unchanged.

Retractions

In accordance with the "Retraction Guidelines" by the Committee on Publication Ethics (COPE) *Caryologia* will retract a published article if:

- there is clear evidence that the findings are unreliable, either as a result of misconduct (e.g. data fabrication) or honest error (e.g. miscalculation)
- the findings have previously been published elsewhere without proper crossreferencing, permission or justification (i.e. cases of redundant publication)
- it turns out to be an act of plagiarism
- it reports unethical research.

An article is retracted by publishing a retraction notice that is linked to or replaces the retracted article. *Caryologia* will make any effort to clearly identify a retracted article as such.

If an investigation is underway that might result in the retraction of an article *Caryologia* may choose to alert readers by publishing an expression of concern.

COMPLYNG WITH ETHICS OF EXPERIMENTATION

Please ensure that all research reported in submitted papers has been conducted in an ethical and responsible manner, and is in full compliance with all relevant codes of experimentation and legislation. All papers which report in vivo experiments or clinical trials on humans or animals must include a written statement in the Methods section. This should explain that all work was conducted with the formal approval of the local human subject or animal care committees (institutional and national), and that clinical trials have been registered as legislation requires. Authors who do not have formal ethics review committees should include a statement that their study follows the principles of the Declaration of Helsinki

ARCHIVING

Caryologia and Firenze University Press are experimenting a National legal deposition and long-term digital preservation service.

ARTICLE PROCESSING CHARGES

All articles published in *Caryologia* are open access and freely available online, immediately upon publication. This is made possible by an article-processing charge (APC) that covers the range of publishing services we provide. This includes provision of online tools for editors and authors, article production and hosting, liaison with abstracting and indexing services, and customer services. The APC, payable when your manuscript is editorially accepted and before publication, is charged to either you, or your funder, institution or employer.

Open access publishing is not without costs. *Caryologia* therefore levies an article-processing charge of € 150.00 for each article accepted for publication, plus VAT or local taxes where applicable.

FREQUENTLY-ASKED QUESTIONS (FAQ)

Who is responsible for making or arranging the payment?

As the corresponding author of the manuscript you are responsible for making or arranging the payment (for instance, via your institution) upon editorial acceptance of the manuscript.

At which stage is the amount I will need to pay fixed?

The APC payable for an article is agreed as part of the manuscript submission process. The agreed charge will not change, regardless of any change to the journal’s APC.

When and how do I pay?

Upon editorial acceptance of an article, the corresponding author (you) will be notified that payment is due.

We advise prompt payment as we are unable to publish accepted articles until payment has been received. Payment can be made by Invoice. Payment is due within 30 days of the manuscript receiving editorial acceptance. Receipts are available on request.

No taxes are included in this charge. If you are resident in any European Union country you have to add Value-Added Tax (VAT) at the rate applicable in the respective country. Institutions that are not based in the EU and are paying your fee on your behalf can have the VAT charge recorded under the EU reverse charge method, this means VAT does not need to be added to the invoice. Such institutions are required to supply us with their VAT registration number. If you are resident in Japan you have to add Japanese Consumption Tax (JCT) at the rate set by the Japanese government.

Can charges be waived if I lack funds?

We consider individual waiver requests for articles in Caryologia on a case-by-case basis and they may be granted in cases of lack of funds. To apply for a waiver please request one during the submission process. A decision on the waiver will normally be made within two working days. Requests made during the review process or after acceptance will not be considered.

I am from a low-income country, do I have to pay an APC?

We will provide a waiver or discount if you are based in a country which is classified by the World Bank as a low-income or a lower-middle-income economy with a gross domestic product (GDP) of less than $200bn. Please request this waiver of discount during submission.

What funding sources are available?

Many funding agencies allow the use of grants to cover APCs. An increasing number of funders and agencies strongly encourage open access publication. For more detailed information and to learn about our support service for authors.

APC waivers for substantial critiques of articles published in OA journals

Where authors are submitting a manuscript that represents a substantial critique of an article previously published in the same fully open access journal, they may apply for a waiver of the article processing charge (APC).

In order to apply for an APC waiver on these grounds, please contact the journal editorial team at the point of submission. Requests will not be considered until a manuscript has been submitted, and will be awarded at the discretion of the editor. Contact details for the journal editorial offices may be found on the journal website.

What is your APC refund policy?

Firenze University Press will refund an article processing charge (APC) if an error on our part has resulted in a failure to publish an article under the open access terms selected by the authors. This may include the failure to make an article openly available on the journal platform, or publication of an article under a different Creative Commons licence from that selected by the author(s). A refund will only be offered if these errors have not been corrected within 30 days of publication.

2025
Vol. 78 – n. 4

Caryologia

International Journal of Cytology, Cytosystematics and Cytogenetics

Table of contents